

A STUDY OF THE EFFECTS OF EXPERIMENTAL TECHNIQUES ON POOL  
BOILING OF NANOFUIDS

A STUDY OF THE EFFECTS OF EXPERIMENTAL TECHNIQUES ON POOL  
BOILING OF NANOFLUIDS

By

Osama Ahmed, B. Sc.

A Thesis

Submitted to the School of Graduate Studies

in Partial Fulfilment of the Requirements

for the Degree

Master of Applied Sciences

McMaster University

Hamilton, Ontario, Canada

© Copyright by Osama Ahmed, November 2010

MASTERS OF APPLIED SCIENCES (2010)

McMaster University

(Mechanical Engineering)

Hamilton, Ontario, Canada

TITLE: A Study of the Effects of Experimental Techniques on  
Pool Boiling of Nanofluids

AUTHOR: Osama Ahmed, B. Sc. (Ain Shams University)

SUPERVISOR: Dr. Mohamed S. Hamed

NUMBER OF PAGES: 116

## Abstract

Pool boiling of nanofluids has been studied in the past decade and contradicting results have been found. Several parameters have been investigated, the most popular being the nanofluid concentration. The investigations in the literature have been carried out under different conditions. The effects of method of nanofluid preparation, pH value and boiling duration on the Heat Transfer Coefficient (HTC) and nanoparticle deposition have not been thoroughly investigated.

An experimental investigation has been carried out to investigate such effects and the effect of nanofluids concentration on the HTC and nanoparticle deposition. A flat copper surface with a mirror-finish ( $Ra = 50 - 150$  nm) has been used as the boiling surface. Using a nanofluid prepared from a ready-made suspension showed to have a similar HTC to a nanofluid prepared from dry nanoparticles at a neutral pH value. Reducing the pH value of the nanofluids prepared from dry particles gave different responses in HTC at different concentrations. At 0.01 vol. % concentration the HTC decreased due to change in base fluid properties, at 0.1 vol. % the HTC increased due to enhanced electrostatic stabilisation, and no change took place at 0.5 vol. % due to a high intensity of nanoparticle deposition. Increasing the concentration of the nanofluids resulted in a reduction in HTC, higher nanoparticle deposition as well as a faster rate of deposition on the surface.

The effect of concentration on nanoparticle deposition has been studied by boiling water on nanoparticle deposited surfaces after boiling nanofluids. This approach has shown that nanoparticle deposition from boiling a higher concentration nanofluid gives a higher HTC, which is opposite to expectations. This approach has also shown that the surface condition depends on the intensity of the deposition as well as its uniformity.

An analysis has been carried out using the Rohsenow correlation to quantify the effect of nanoparticle deposition on the heat transfer. Prediction of the boiling heat transfer of nanofluids may be used by adopting a transient surface factor in the Rohsenow correlation.

## **Acknowledgements**

I would I like to thank my supervisor Dr. M. Hamed for his guidance, support and encouragement.

I would also like to thank the department technicians for their advice and expertise. Joe, Ron, Jim, JP and Mark, thanks a lot for your help.

I would like to thank all my colleagues who made this Masters a memorable experience. Hossam, Kevin, Wajih, Hassan, Hazem, Tawfik, Khalifa, Tawhid, Abu Gabal, you guys have been awesome.

Last but not least, special thanks to all my family members and friends back home for their continuous support. Without them I would not have made it this far.

## Table of Contents

<i>Chapter 1: Introduction</i>	1
<i>Chapter 2: Literature Review</i>	4
2.1 Pool Boiling	4
2.2 Nanofluids	7
2.3 Thermal Conductivity of Nanofluids	8
2.4 Stability of Nanofluids	11
2.5 Parameters Affecting Pool Boiling of Nanofluids	13
2.6 Investigations Carried out on Pool Boiling of Nanofluids	15
2.7 Deposition of Nanoparticles on the Heater Surface under Pool Boiling Conditions	25
2.8 Summary	31
2.9 Research Objectives and Research Plan	35
2.10 Thesis Structure	36
<i>Chapter 3: Experimental Setup and Methodology</i>	37
3.1 Experimental Setup	37
3.1.1 Heaters Control	40
3.1.2 Data Acquisition	41
3.1.3 Thermocouple Calibration	42
3.1.4 High-Speed Imaging	43
3.1.5 3D Profiling of the Surface	43
3.2 Determination of Heat Flux ( $q''$ ) and Surface Temperature ( $T_s$ ) of the Copper Block	44
3.3 Uncertainty Analysis	46
3.3.1 Uncertainty in Heat Flux ( $q''$ )	48
3.3.2 Uncertainty in Surface Temperature ( $T_s$ )	48
3.3.3 Uncertainty in Bulk Fluid / Liquid Saturation Temperature ( $T_{sat}$ )	48
3.3.4 Uncertainty in Surface Superheat ( $T_s - T_{sat}$ )	49
3.4 Parameters Investigated and Conditions of Experiments	50

3.4.1	Stage 1: Effect of Preparation Method and Stability	50
3.4.2	Stage 2: Effect of Concentration and Stability	51
3.4.3	Stage 3: Effect of Concentration and Prolonged Boiling Duration on Nanoparticle Deposition	52
3.5	Nanofluid Preparation	54
3.6	Surface Preparation	57
3.7	Test Procedure	58
3.8	Post-Experiment Procedure	60
3.8.1	Experiments to Assess Nanoparticle Deposition not due to Boiling	61
3.9	Validation of Water Boiling Curve	62
<i>Chapter 4: Results and Discussion</i>		64
4.1	Effects of Stability and Preparation Method (Stage 1)	64
4.1.1	Effect of Stability	66
4.1.2	Effect of Preparation Method	69
4.2	Combined Effects of Concentration and Stability (Stage 2)	71
4.2.1	Effect of Concentration	75
4.2.2	Effect of Stability	76
4.2.3	Nanoparticle Deposition Pattern	79
4.3	Effect of Concentration and Prolonged Boiling Duration on Nanoparticle Deposition (Stage 3)	81
4.3.1	Assessment of Surface Factor Change and Nanofluid Properties using the Rohsenow Correlation	89
4.3.2	Examination of Nanoparticle Deposition	91
4.3.3	Effect of Prolonged Boiling Duration on Nanoparticle Deposition and Surface Temperature	94
4.3.4	Transient Surface-Factor	99
4.4	Comparison of HTC Ratio with Literature	103
<i>Chapter 5: Summary and Conclusions</i>		105
<i>Chapter 6: Recommendations for Future Work</i>		108
<i>Appendix A</i>		111
<i>References</i>		113

## List of Figures

Figure 1.1: Number of publications containing keyword "nanofluid" on www.sciencedirect.com as of March 2010	2
Figure 2.1: The pool boiling curve	5
Figure 2.2: Variation of thermal conductivity enhancement with concentration and pH value of alumina-water nanofluids at a particle size of 60.4 nm [10]	12
Figure 2.3: Nanoparticles size distribution reported in [4]	17
Figure 2.4: Variation of HTC ratio with SIP, [7]	24
Figure 2.5: Summary of variation of HTC ratio against concentration reported in the literature	32
Figure 3.1: The boiling vessel	38
Figure 3.2: Heaters control circuit	41
Figure 3.3: Locations of thermocouples placed in the copper blocks for experiments in (a) Stage 1 and (b) Stages 2 & 3	45
Figure 3.4: Temperature profiles in copper block for Stage 1 experiments at different heat fluxes	47
Figure 3.5: Temperature profiles in copper block for Stages 2 & 3 experiments at different heat fluxes	47
Figure 3.6: Locations of surface-roughness measurements of the boiling surface taken in Stage 1 experiments	51
Figure 3.7: Locations of surface-roughness measurements of the boiling surface taken in Stage 3 experiments	53
Figure 3.8: SEM image of the nanoparticles sample	55
Figure 3.9: Variation of particle size with ultrasonic vibration time using DLS	56
Figure 3.10: 3D profiles of the polished surface before Stage 1, 2 and 3 experiments	59
Figure 3.11: Rohsenow correlation validation	63
Figure 4.1: Boiling curves obtained during experiments of Stage 1	65
Figure 4.2: 3D images of surfaces after Stage 1 experiments	68

Figure 4.3: Particle size distribution for nanofluids used in Stage 1 experiments	69
Figure 4.4: Boiling curves for neutral nanofluids (pH = 6.5)	72
Figure 4.5: Boiling curves for acidic nanofluids (pH = 5)	73
Figure 4.6: Surface-roughness measurements for Stage 2 experiments	73
Figure 4.7: 3D images of surfaces after Stage 2 experiments	74
Figure 4.8: Boiling curves for Stage 2 experiments at 0.01 vol. % concentration	77
Figure 4.9: Boiling curves for Stage 2 experiments at 0.1 vol. % concentration	77
Figure 4.10: Boiling curves for Stage 2 experiments at 0.5 vol. % concentration	78
Figure 4.11: Nanoparticle deposition pattern at a heavy deposition spot on the surface after 0.01 vol. %, pH = 6.5 nanofluid ( $Ra = 1332$ nm)	80
Figure 4.12: Nanofluids boiling curves for a clean surface in Stage 3 experiments	82
Figure 4.13: Water boiling curves for a nanoparticle-deposited (NPD) surface in Stage 3 experiments	83
Figure 4.14: Comparison between boiling water on a clean surface, 0.5 vol. % nanofluid on a clean surface and water on a 0.5 vol. % NPD surface in Stage 3 experiments	84
Figure 4.15: Results of repeated water boiling experiments on a clean surface	86
Figure 4.16: Images 1 ms apart of water boiling from (a) clean surface (b) 0.01 vol. % (c) 0.1 vol. % and (d) 0.5 vol. % nanoparticle-deposited surface	88
Figure 4.17: Surface-roughness measurements for Stage 3 experiments	92
Figure 4.18: Photographs of the boiling surface for Stage 3 experiments:	93
Figure 4.19: 3D images of surfaces after Stage 3 experiments	95
Figure 4.20: Surface superheat and heat flux vs. time during water boiling experiment	96
Figure 4.21: Surface superheat and heat flux vs. time during 0.01 vol. % nanofluid boiling experiment	96
Figure 4.22: Surface superheat and heat flux vs. time during 0.1 vol. % nanofluid boiling experiment	97

Figure 4.23: Surface superheat and heat flux vs. time during 0.5 vol. % nanofluid boiling experiment	97
Figure 4.24: Surface temperature change during steady-state periods	98
Figure 4.25: Change in $C_{sf}$ for the water and nanofluid boiling experiments	100
Figure 4.26: $C_{sf}$ for water and nanofluid experiments showing associated errors	102
Figure 4.27: HTC ratio found in literature and determined in this investigation	104
Figure A.1: Repeatability of water boiling in Stage 2 experiments	112
Figure A.2: Repeatability of 0.01 vol. % nanofluid boiling at pH = 5 from Stage 2 experiments	112

## **List of Tables**

Table 2.1: Summary of conditions and HTC findings from previous pool boiling investigations of nanofluids. [NR = Not Reported]	34
Table 3.1: Parameters investigated in this study	53
Table 4.1: Results of experiments carried out during Stage 1	65
Table 4.2: Results of experiments carried out during Stage 2	75
Table 4.3: Results of experiments carried out during Stage 3	83
Table 4.4: Surface factor and fluid properties analysis using the Rohsenow correlation	91

## Nomenclature

<u>SYMBOL</u>	<u>DESCRIPTION</u>	<u>UNITS</u>
$C_p$	<i>Specific heat</i>	$J/kg^{\circ}C$
$C_{sf}$	<i>Surface factor</i>	-
$d_p$	<i>Particle diameter</i>	$m$
$g$	<i>Gravitational acceleration</i>	$m/s^2$
$h$	<i>Heat transfer coefficient (HTC)</i>	$W/m^2^{\circ}C$
$h_{lv}$	<i>Latent heat of vaporisation</i>	$J/kg$
$k$	<i>Thermal conductivity</i>	$W/m^{\circ}C$
$L$	<i>Length</i>	$m$
$Pr$	<i>Prandtl number</i>	-
$q''$	<i>Heat Flux</i>	$W/m^2$
$R_a$	<i>Average surface-roughness</i>	$m$
$SIP$	<i>Surface interaction parameter</i>	-
$T$	<i>Temperature</i>	$^{\circ}C$
$x$	<i>Displacement</i>	$m$
$Z$	<i>Orthogonal position</i>	$nm$

### Greek Symbols

$\delta k$	<i>Change in thermal conductivity</i>	$W/m^{\circ}C$
$\mu$	<i>Viscosity</i>	$Ns/m^2$

$\rho_l$	<i>Liquid density</i>	$kg/m^3$
$\rho_v$	<i>Vapour density</i>	$kg/m^3$
$\sigma$	<i>Surface tension</i>	$N/m$
<u>SYMBOL</u>	<u>DESCRIPTION</u>	<u>UNITS</u>
$\phi_v$	<i>Volumetric concentration</i>	%
$\phi_m$	<i>Mass concentration</i>	%

#### Subscripts

$f$	<i>Fluid</i>
$NF$	<i>Nanofluid</i>
$p$	<i>Particle</i>
$s$	<i>Surface</i>
$sat$	<i>Saturation</i>
$W$	<i>Water</i>

## Chapter 1

### Introduction

Boiling heat transfer is an important process that takes place in many industrial applications such electronics cooling, metal processing and power generation. Boiling is a complex phenomenon and so it has been investigated for many decades in order to understand and utilise it in the best way possible.

In the past, scientists attempted to use fluids with suspended particles to enhance their thermal properties. However, they experienced problems of erosion, sedimentation, fouling and pressure drop. The technology in the past permitted particles to be of milli- and micro- meter size scale. However, with the recent development of nanotechnology, engineers and scientists have been able to use particles of nanometer size, referred to as *nanoparticles*. Problems arising from suspending particles in fluids have been greatly reduced with the use of nanoparticles.

A *nanofluid* is dispersed nanoparticles in a base fluid. The term “Nanofluid” was used for the first time by U. S. Choi in 1995. The most commonly used nanofluids are made of water and alumina nanoparticles. While alcohol, ethyl glycol or oils have been used as other base fluids, copper oxide, copper, titania, zinc oxide and other materials have been also used as nanoparticles.

Most working fluids used in industry have thermal conductivities that are one or two orders of magnitude lower than metals used in heat exchange equipment. As such, working fluids are considered the bottleneck in heat exchange effectiveness. The key property that makes nanofluids attractive as heat transfer fluids is their enhanced thermal conductivity compared with their base fluids. Nanofluids have attracted significant attention during the last decade as the possible next generation of working heat transfer fluids. Figure 1.1 shows the rate of increase in research in nanofluids over the past decade.

Past research on pool boiling of nanofluids shows contradicting trends in the findings regarding heat transfer coefficient (HTC), as will be discussed in Chapter 2. The main objective of this study is to better understand pool boiling of nanofluids, by investigating the effects of nanofluid preparation method, electrostatic stabilisation,

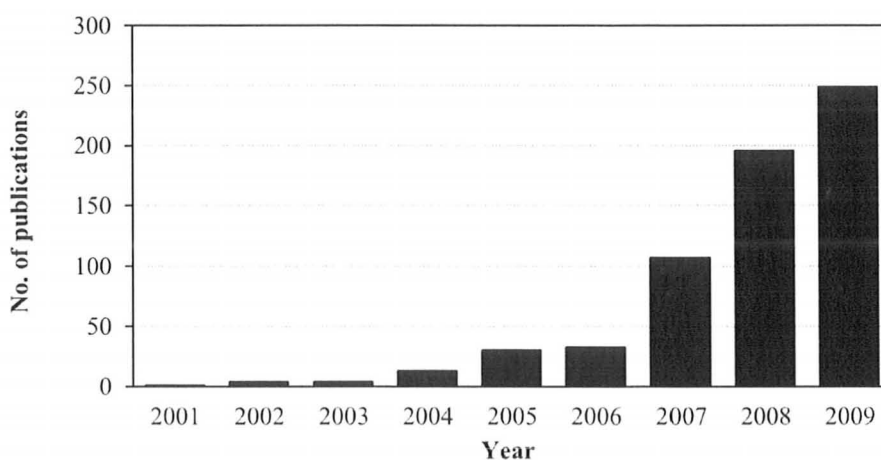


*Figure 1.1: Number of publications containing keyword "nanofluid" on www.sciencedirect.com as of March 2010*

concentration and boiling duration on HTC of nanofluids and nanoparticle deposition. It is favourable to find the appropriate conditions under which an enhancement in HTC would be achieved, as industrial applications favour enhancing heat transfer mechanisms.

Although most industrial applications involve flow boiling as the main heat transfer mechanism, it is recommended to carry out fundamental boiling research under pool boiling. The behaviour of nanofluids under flow boiling will be influenced by the boiling phenomenon, as well as the characteristics of the fluid flow. The scope of this research is to study the behaviour of nanofluids undergoing boiling only.

## Chapter 2

### Literature Review

This chapter presents the previous works that have been carried out on pool boiling of nanofluids. The regimes of pool boiling and synthesis of nanofluids are explained briefly in sections 2.1 and 2.2, respectively. Thermal conductivity of nanofluids is discussed in section 2.3. Section 2.4 explains the stability of nanofluids, and section 2.5 discusses the parameters affecting pool boiling of nanofluids. Studies investigating pool boiling of nanofluids are then presented in detail in section 2.6 followed by studies that focus on the deposition of nanoparticles on the boiling surface in section 2.7. Section 2.8 presents a summary of the main findings in the literature. The research objectives and plan for the present research is discussed in section 2.9 and a description of the thesis structure will conclude this chapter in section 2.10.

#### 2.1 Pool Boiling

Boiling of a stagnant liquid in direct contact with a heated surface is referred to as *pool boiling*. Pool boiling takes place in many industrial applications such as quenching of metals or electronics cooling, as well as in domestic uses, such as boiling water in a kettle. The regimes of pool boiling are identified by the classic pool boiling curve [1] shown in Figure 2.1.

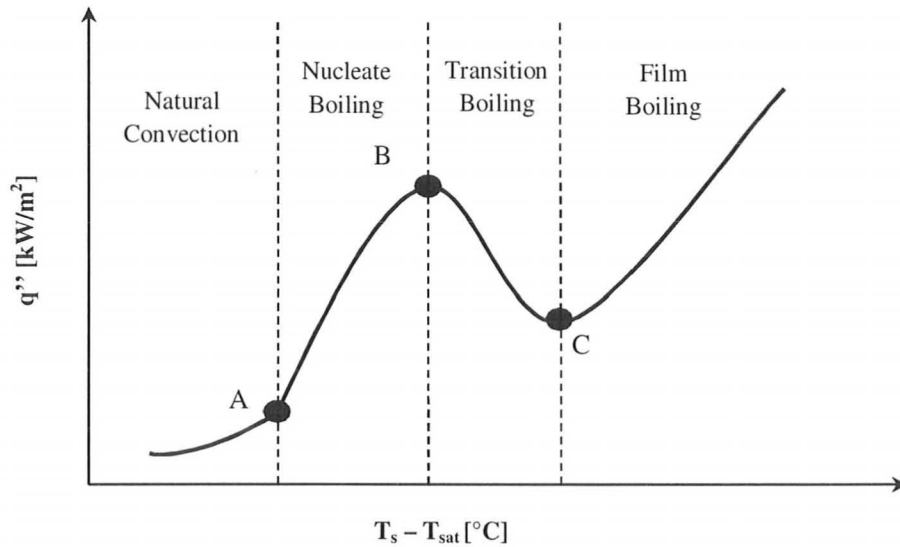


Figure 2.1: The pool boiling curve

The boiling curve shows the variation in the heat flux at different levels of surface superheat temperature, which is expressed as  $T_s - T_{sat}$ . At low surface superheat, the heat is transferred to the surface via *natural convection*. As the surface temperature increases beyond the temperature for the *onset of nucleate boiling* (Point A), bubbles start to form on the surface and grow and depart from the surface rapidly. This is called the *nucleate boiling* regime, identified in Figure 2.1 as part AB of the curve. Much higher heat fluxes are delivered at this temperature range due to a much higher heat transfer coefficient,  $h$ .

$$h = \frac{q''}{T_s - T_{sat}} \quad (2.1)$$

The heat transfer coefficient (HTC) increases due to the rapid generation and release of vapour bubbles at the heater surface which cause a high disturbance of the liquid near the surface. This increased HTC is what makes nucleate boiling a favourable mechanism of heat transfer in industrial applications. The sites at which bubbles form are called *nucleation sites*. As the surface superheat is further increased, more nucleation sites are activated and more bubble generation takes place. The heat flux increases with surface temperature up to the point of the Critical Heat Flux (CHF), point B. At this point, the large amount of vapour generated covers portions of the surface and restricts liquid access to the surface. As the surface temperature is increased beyond the point of CHF, a severe reduction in heat transfer takes place due to more regions of the surface covered by vapour. This is portion BC of the boiling curve and is referred to as *transition boiling*.

The surface eventually becomes totally covered by a vapour film as the surface temperature is increased further beyond point C. The heat transfer increases with increasing the surface superheat. In this region, the heat is transferred to the bulk liquid mainly via radiation and conduction. This is called *film boiling*.

Industrial applications mainly operate in the nucleate boiling regime. It is generally unfavourable to exceed the heat flux or surface superheat beyond CHF, as this would be associated with deteriorated heat transfer rates and much higher surface temperatures. This study is focused on pool boiling of nanofluids in the nucleate boiling regime.

## 2.2 Nanofluids

Nanofluids are produced by dispersing nanoparticles in a base fluid. Nanoparticles are produced using various techniques making nanoparticles ranging from 10 to 250 nm in size. Techniques of producing nanoparticles include inert gas condensation, mechanical grinding, chemical vapour deposition, chemical precipitation, micro emulsions, thermal spray, and spray pyrolysis [2].

*Nanophase Technologies*, which is the most popular provider of nanoparticles and nanofluids used by many researchers, employ a *Physical Vapour Synthesis* method to manufacture their nanoparticles. In this method, arc energy is supplied to a metal at temperatures above the evaporating point causing the metal to evaporate. Exposing the vapour to a reactive gas produces a metal oxide, which is then cooled at a controlled rate producing the required nanoparticles.

The success of dispersing the nanoparticles in the base fluid is key in producing nanofluids. Nanoparticles have a high tendency to agglomerate together due to a strong Van der Waals attraction force between the particles [3]. Particles might agglomerate to up to 10 micrometers in size [4]. There are several ways to break down these agglomerates. Common ways of breaking up the agglomerates are ultrasonic vibration and high speed homogenisers.

Another issue that arises when preparing nanofluids is the time nanoparticles remain dispersed, which is a measure of the nanofluid *stability*. Two methods are usually

used to enhance the stability of nanofluids; adding surfactants such as laureate salts [5-6] and changing the pH value of the nanofluid [3, 7-8].

### 2.3 Thermal Conductivity of Nanofluids

Nanofluids have a higher thermal conductivity,  $k$ , than their base fluids. Xuan & Li [5] performed a study to measure thermal conductivity of nanofluids using a transient hot-wire method, where a wire with a very large length to diameter ratio is used to conduct heat to the liquid for a short period of time (5 seconds) before convection starts to take place. They used copper nanoparticles of 100 nm size. They used two base fluids: water and transformer oil. Laureate salt was used as a dispersing agent with water, and oleic acid with transformer oil. The water-based and oil-based nanofluids were stable for 30 hours and one week, respectively. The concentrations of the nanoparticles were varied from 2.5 to 7.5 vol. %. They reported enhancement of  $k$  by 12 % to 43 % for the transformer oil-based nanofluid and by 24 % to 78 % for the water-based nanofluid when changing the concentrations from 2.5 to 7.5 vol. %.

Das et al. [9] measured thermal conductivity of nanofluids at elevated temperatures and reported some interesting results. They used a temperature oscillation method for their thermal conductivity measurements where the temperature of the nanofluid container wall was oscillated by 1.5 °C using a Peltier element. The phase and amplitude of the fluid temperature was measured at specific locations within the fluid, which was used to evaluate the fluid thermal diffusivity. The specific heat capacity and

density of the fluid were calculated and used to determine the value of the thermal conductivity. They used water as the base fluid of alumina (38.4 nm) and copper oxide (28.6 nm) nanofluids with concentrations varying from 1 to 4 vol. %. They did not use any stabilising agent. The nanofluids at 3 and 4 vol. % concentrations were found to sediment after 12 hours. They measured the nanofluids' thermal conductivity at temperatures of 21 °C and 51 °C. They found that the enhancement in thermal conductivity increases with concentration and temperature. For example, they found 2 % enhancement for the 1 vol. % alumina nanofluid at room temperature and 10.8 % at 51 °C. A higher enhancement of 36 % was found for the 4 vol. % copper oxide nanofluids at 51°C. These findings indicate that nanofluids are more attractive for high temperature applications.

Das et al. compared their results with the Hamilton and Crosser (HC) model [2], which was developed to predict thermal conductivity of solid-liquid mixtures. The HC model under predicted the thermal conductivity of their nanofluids. The model was developed to predict thermal conductivity of slurries with larger particles. Das et al. concluded that, with smaller particles, thermal conductivity is enhanced through nanoparticles stochastic or Brownian motion in the fluid. They used this mechanism to explain how thermal conductivity is enhanced at elevated temperatures. They also indicated that for each particle size there is a threshold temperature at which the effective thermal conductivity of nanofluids starts deviating from that of usual slurries and the enhancement is primarily due to stochastic motion of particles. They explained the higher thermal conductivity of the copper oxide nanoparticles due to their smaller size which

makes them more mobile in the fluid and their larger area to volume ratio compared to the alumina nanoparticles.

Xie et al. [10] investigated the effect of particle size and base fluid on nanofluids effective thermal conductivity. They used 12 – 300 nm alumina nanoparticles dispersed in water, ethyl glycol and pump oil at concentrations of 1.8 – 5 vol. %. A hot-wire method was used to measure the thermal conductivity. They found 28 % to 38 % enhancement in  $k$  as particle size was decreased from 300 to 60 nm when using alumina nanoparticles and pump oil at a concentration of 5 vol. %. The thermal conductivity decreased with particle size below 60 nm. They explained such drop in  $k$  occurred due to the fact that 60 nm is close to the phonon mean free path of alumina, which is 35 nm. This closeness in size causes “scattering of the primary carriers of energy (photons) at the particle boundary”. Xie et al. also found that the enhancement in thermal conductivity was more profound for the base fluids with lower thermal conductivity; pump oil showed an enhancement of 38 % while ethyl glycol showed 30 % and water showed 24 % at 5 vol. % concentrations and particle size of 60 nm. Pump oil has the lowest thermal conductivity followed by ethyl glycol, and water. More of their results are discussed in section 2.4.

Jang & Choi [11] developed a model that predicts thermal conductivity of nanofluids. They did not assume that the particles are motionless as other traditional models did. The following four modes of energy transport were included in their model:

1. Collision between the base fluid molecules
2. Thermal diffusion of nanoparticles in the fluid

3. Collision between the nanoparticles due to Brownian motion
4. Thermal interactions of dynamic nanoparticles with the base fluid molecules.

The third mode is a very slow process; an order of magnitude slower than the other three and was therefore neglected. Their model showed good agreement with experimental results, taking into account the change in nanofluids temperature and the particle size. They concluded that as the particles become smaller, they become more mobile and convection-like effects due to Brownian motion become dominant, leading to a higher thermal conductivity enhancement.

Other models have been developed by other scientists to predict the anomalously increased thermal conductivity of nanofluids. Mechanisms such as particle motion, surface action, electro kinetic effects, increased surface area of nanoparticles, particle-particle collisions, dispersion of nanoparticles, Brownian motion and nanoparticles clustering have all been identified [2].

## **2.4 Stability of Nanofluids**

The *stability* of nanofluids has recently attracted attention from the nanofluid research community. Once particles are dispersed in the base fluid, an electric double layer is formed around each particle, which creates a charge that repels them from one another. It is this charge that keeps the particles stable in suspension, which is called

*Electrostatic Stabilisation.* At a critical pH value, known as the *Iso-Electric Point* (IEP), these charges disappear and particles sediment very rapidly or crash-out of suspension. i.e., become unstable. The further away the pH value is from the IEP, the stronger the charges and, the better the stability of the nanofluid. The IEP of alumina is at a pH of 9.1, [2-3, 7, 10].

Xie at al. [10] investigated the effect of concentration and the pH value of nanofluids on their effective thermal conductivity. They varied the concentration from 1.8 to 5 vol. % as well as the pH value from 2 to 11. Their results are shown in Figure 2.2. It is clear that thermal conductivity is enhanced with increasing concentration and decreasing pH value. A maximum enhancement of 24 % above that of water was recorded at pH = 2 and 5 vol. % concentration. These results confirm that the enhanced stability has a positive effect on thermal conductivity of nanofluids.

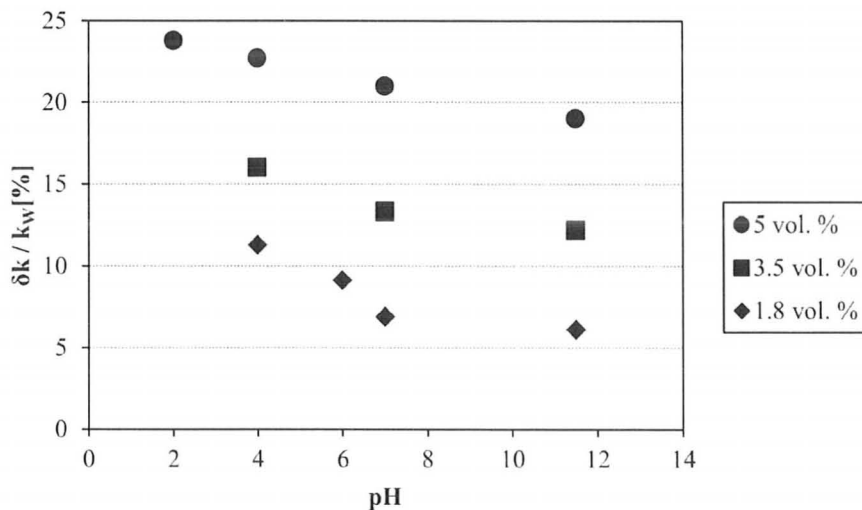


Figure 2.2: Variation of thermal conductivity enhancement with concentration and pH value of alumina-water nanofluids at a particle size of 60.4 nm [10]

## 2.5 Parameters Affecting Pool Boiling of Nanofluids

There are several factors that affect pool boiling of any fluid. These factors are related to the boiling surface and the fluid. The surface-roughness of the boiling surface has a significant effect. Surface-roughness is most commonly expressed as the average surface-roughness,  $Ra$ , shown in Equation (2.2) [4].

$$Ra = \frac{1}{L} \int_0^L |Z(x)| dx \quad (2.2)$$

Rougher surfaces have a higher number of cavities acting as nucleation sites and will, therefore, give higher heat fluxes for a given surface superheat. Also the size of the cavities affects the interaction with the particles that settle on the surface. Surface material is another factor that affects the wettability of the surface. Different surfaces have different wetting properties, different behaviour of bubbles and different deposition of nanoparticles on the surface.

Surface geometry also has an influence on pool boiling. The mechanism of bubble growth and departure taking place during boiling on a horizontal tube will also be associated with a bubble sliding mechanism due to buoyancy forces. The diameter of the tubes will influence the bubble sliding mechanism. However, bubble sliding is less likely to take place on a flat surface.

The orientation of the surface is another factor. With a vertical surface there will be a temperature gradient along surface height due to convection. Bubble sliding is more likely to take place for a vertical surface than for a horizontal surface. The difference in

physical mechanisms taking place on the surface has an effect on the boiling phenomenon taking place on the surface.

As mentioned before, in addition to the surface conditions discussed above, pool boiling is also affected by parameters related to the fluid. In the case of nanofluids, concentration will affect properties of the nanofluid such as thermal conductivity and surface tension. The degree of deposition of nanoparticles taking place on the surface during boiling will also be affected by the concentration. The pH value of the nanofluid will also affect the properties of the nanofluid by changing its stability and thermal conductivity. The acid used to change the pH value affects properties of the base fluid.

The method of preparation of nanofluids is another factor that might have a significant effect on their properties and interaction with the boiling surface. All the researchers mentioned in this thesis have used nanofluids prepared from dry particles, with the exception of one [12] who prepared nanofluids from a ready-made suspension. The size of nanoparticles will also have an effect on their properties, mainly their thermal conductivity. It also affects the size and number of nucleation sites due to particles deposition on the surface during boiling. The size of the particles depends on the nominal particle size, the method used to break up the nanoparticle agglomerates, the method of preparation and the nanoparticles stability.

The type of base fluid has a major effect on pool boiling performance of nanofluids. Different base fluids have different properties and surface wettability. The type of nanoparticles used is another factor to consider. Different materials have different

physical properties which will affect the stability and physical properties of the nanofluids. Nanoparticle materials of a higher density are more likely to crash out of suspension and are less stable. Materials of higher thermal conductivities result in nanoparticles and nanofluids of higher thermal conductivity.

Finally, duration of the boiling experiments might have an effect on their boiling performance. The boiling of pure fluids is known to change with experiment duration due to the flooding and deactivation of nucleation sites [1]. With nanofluids, the duration of the boiling experiment will also influence the level of deposition of nanoparticles on the surface.

## **2.6 Investigations Carried out on Pool Boiling of Nanofluids**

The first study on pool boiling of nanofluids was carried out by Yang and Maa [13]. They used a horizontal stainless steel, 3.2 mm diameter tube as a heater surface. A magnetic stirrer was employed to prevent particles from sedimentation. Measuring the heater surface temperature was carried out by filling the heater tube with silicon carbide powder and inserting thermocouples at the centre of the heater. The temperature gradients in the axial and radial directions were neglected. They used dry alumina nanoparticles of 50, 300 and 1000 nm in size dispersed in water at concentrations of 0.03 and 0.14 vol. %. The surface-roughness of their heater was not reported, neither was the pH value of the nanofluids.

Their results showed an enhancement in pool boiling heat transfer with the addition of nanoparticles, which increased at higher particle concentration. They also showed that the heat transfer is enhanced with decreasing particle size. A maximum enhancement of about 400 % in HTC was recorded at a concentration of 0.14 vol. % and 50 nm particle size. Their work did not provide any explanation for such enhancements. However, they implied that the thermal boundary layer was altered due to the existence of the nanoparticles. Such boundary layer alteration is expected to change the boiling behaviour. They also noted that the existence of nanoparticles reduced heater surface temperature fluctuations during bubble growth and departure.

Das et al. [4] carried out pool boiling experiments of nanofluids using two horizontal tubular stainless steel heaters both of 20 mm diameter, and  $Ra$  of  $0.4\mu\text{m}$  and  $1.15\mu\text{m}$ . To measure the surface temperature, thermocouples were welded to the heater surface, and the power input to the heater was measured using a wattmeter. Nanofluids prepared from dry alumina nanoparticles dispersed in water were used with concentrations ranging from 0.1 to 4 vol. %. They found that surfactants change surface tension of the base fluid and as such will alter their boiling characteristics. They therefore, did not use surfactants to stabilise their nanofluids. There was no mention of any method used to enhance the stability of their nanofluids neither did they mention their pH value. The nanofluids were degassed for 30 minutes prior to each experiment. They used ultrasonic vibration for 4 hours to break down the agglomerates. The particle size distribution of the nanofluids was examined using a Transmission Electron Microscope (TEM). The particles size normal distribution is shown in Figure 2.3. A volume weighted

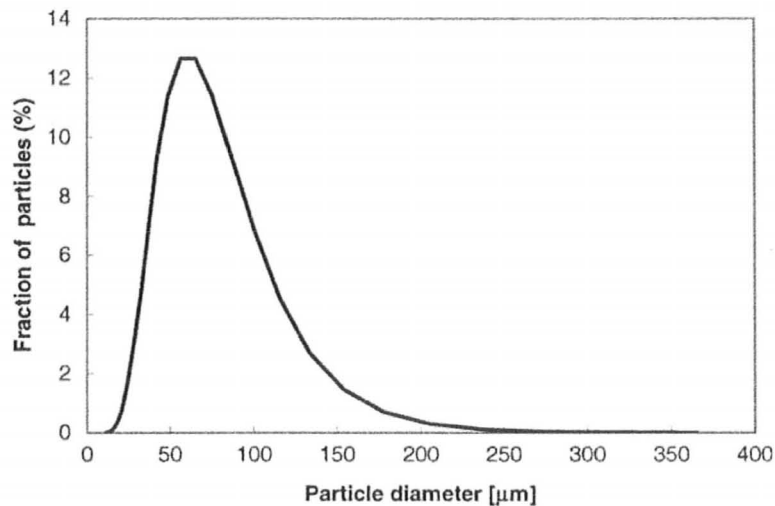


Figure 2.3: Nanoparticles size distribution reported in [4]

average of the particle size was calculated at 38 nm, which was identical to the size indicated by the nanoparticles supplier. Little sedimentation was observed at 3 and 4 vol. % concentrations after 6 hours of preparation. Surface tension of the nanofluids was the same as that of pure water, regardless of concentration. The viscosity increased with the concentration, however, the nanofluids remained Newtonian.

Their experiments revealed that the HTC was reduced to 40% to 80 % of pure water. A considerable deterioration of heat transfer was found with concentrations as low as 0.1 vol. %. The deterioration increased with increasing concentration, but not proportionally. At a concentration of 4 vol. %, the smoother surface ( $Ra = 0.4 \mu\text{m}$ ) showed a deterioration in HTC of 43 % that of water, while the rougher surface ( $Ra = 1.15 \mu\text{m}$ ) showed a 55 % deterioration at the same concentration. They found a layer of nanoparticles settled on the surface. Their measurements of surface-roughness revealed

that both surfaces became smoother due to nanoparticles deposition. The deterioration in heat transfer was attributed to the fact that their nanoparticles were an order or two orders of magnitude smaller than that of the average surface-roughness. They hypothesized that nanoparticles settle inside the surface voids and made the heater surface smoother. Initial expectations were that HTC would be enhanced due to the higher thermal conductivity and the impact of that on the rate of heat transfer due to transient conduction as bubble sliding takes place. However, the enhancement in  $k$  was overshadowed by the effect of particles settling on the surface, making it smoother and changing its boiling characteristics.

The same authors carried out another study [14] where they used smaller diameter tubes as heater surfaces; 6 and 4.5 mm in diameter. The experimental setup and procedure was virtually identical to their previous study. The surface-roughness of the heaters was between 0.37 and 0.45  $\mu\text{m}$  and the nanoparticles average size was 58 nm. The boiling phenomenon with the narrower tubes was qualitatively different. This is because the bubble sliding mechanism was less important with the smaller tubes due to the closeness of the size of the bubbles and the size of the tubes. Similar to the findings in their previous study, the heat transfer was deteriorated with the addition of nanoparticles, where the HTC was deteriorated to 10 % that of pure water at 4 vol. % concentration.

Bang and Chang [15] investigated pool boiling of nanofluids using a horizontal and vertical flat heaters. Results of the vertical heaters were focused on CHF comparison and are not discussed below. They used a very smooth heater with  $Ra$  of 37 nm. Their surface  $Ra$  value was almost equal to the size of the nanoparticles they used, which was

47 nm, on average. They did not report the heater surface material. They used alumina nanoparticles and water to make nanofluids with concentrations of 0.5 – 4 vol. %. Their nanofluids were prepared from dry nanoparticles. Ultrasonic vibration was used for 8 hours to break down the nanoparticles agglomerates. Their boiling facility has visualisation windows to allow visual observation of the boiling phenomenon taking place. However, due to the opaqueness of nanofluids this was only possible at low concentrations (0.5 vol. %) and at high heat fluxes. A mechanical mixer was used to enhance the nanofluids stability, however, its use did not have any effect on their results. There was no mention of the pH value of their nanofluids or the use of any additives to enhance their stability.

The HTC deteriorated to 25 – 50 % that of pool boiling of pure water. The deterioration of the heat transfer increased with particle concentration. Also, the nucleate boiling regime started at about 5 °C wall superheat higher than that in the case of pure water. A comparison of their results with the Rohsenow correlation showed agreement with their pure water results and deviation with nanofluids results. Similar to the findings reported in [4], a layer of nanoparticles formed on the boiling surface during the experiments, which was easily, but not completely, washable by using a water jet. They argued that the settling of nanoparticles altered the surface characteristics which explained the deviation of their results from the Rohsenow correlation. Furthermore, they indicated that the results might match the correlation using an appropriate “modified liquid-surface combination” factor. They observed less bubbles generated with nanofluids than with water, indicating that the number of nucleation sites was reduced. Experiments

were carried out to examine how the surface-roughness would change with a different initial surface-roughness. The surface with initial roughness smaller and larger than that of the particles size became rougher and smoother after the experiments, respectively. They also investigated the effect of nanoparticles on CHF. They found an increase in the CHF by 32%. They finally attributed the CHF enhancement to the reduction in the number of active nucleation sites as well as to the trapping of liquid near the surface due to the porous characteristics of the nanoparticles layer. This layer caused a reduction in the number of bubbles and, hence, reduced the chances for bubbles to coalesce and form a vapour blanket above the surface.

A study focused on the CHF of nanofluids was carried out by Vassallo et al. [12]. They used a 0.4mm NiCr wire as a heater surface horizontally suspended in a 0.5 vol. % silica-water nanofluid placed in a Pyrex dish. The nanoparticles were 15, 50 and 3000 nm in size. Their nanofluids were prepared by diluting a more concentrated, ready-made, nanofluid with deionised water. The pH of the nanofluids was not mentioned, nor was the surface-roughness of the wire. The heat flux was obtained from voltage and current measurements input to the wire. The temperature was obtained from the temperature-electrical resistance characteristics of the wire. They found a minor enhancement in nucleate boiling heat transfer and a 0.05 – 0.25 mm thick layer formed on the wire. They reported CHF 60 % higher than that of pure water.

Kim et al. [16] investigated the CHF of pool boiling of nanofluids using an experimental procedure very similar to that used in [12]. Alumina and titania nanoparticles in water were used with logarithmic concentrations ranging from  $10^{-5}$  –  $10^{-1}$

vol. %. NiCr and titanium wires of diameters 0.2 and 0.25 mm, respectively, were used as heating surfaces. The wire was placed horizontally in the nanofluids. Again, they found an enhancement in the CHF as compared to pure water, which increased sharply with small concentrations and remained constant at concentrations above  $10^{-2}$  vol. %. What was interesting to observe is the deposition pattern of nanoparticles on the wires after the experiments. Upon visual inspection of the wires under a microscope, the thickness of the deposited coating increased with increasing the concentration of the nanofluids. Also, more particles were deposited on the bottom of the wires than the top. The coating formed very quickly with time and did not break down when the wires were used in pure water experiments. This clearly explained that the deposition of nanoparticles phenomenon did not occur due to gravitational settling of nanoparticles, but due to the nucleation of bubbles on the heating surface which is more rapid at the bottom side of the wire than at the top, due to bubble sliding.

Very similar results were also observed by You and Kim [17] who also studied boiling heat transfer of nanofluids, but at low pressures (about 0.2 atm). They used alumina – water nanofluids at low concentrations of  $2.8 \times 10^{-5}$  –  $1.4 \times 10^{-3}$  vol. %. The HTC was almost the same as water at all concentrations. It was possible to observe the boiling phenomenon at low concentrations using a high speed camera at 240 frames per second. They observed lower bubble departure frequency and higher bubble diameter when using nanofluids. This reduction in the bubble departure frequency was attributed to change in surface tension due to addition of nanoparticles to water. They tried to predict the enhancement in CHF due to changes in the surface tension using the Zuber correlation

[1]. Zuber's correlation incorporates liquid properties to predict the CHF of fluids. Their attempt in predicting the CHF for nanofluids was not successful.

Wen and Ding [3] were the first to carry out pool boiling experiments of nanofluids using the electrostatic stabilisation method. They used a 150 mm diameter horizontal flat stainless steel disc as the heating surface. A ring heater was installed below the disc and thermocouples were embedded at the back of the disc to record its surface temperature. The heater surface had a roughness of micro-meter scale. They prepared alumina-water nanofluids from dry nanoparticles with concentrations of 0.09 – 0.35 vol. % and no stabilising agent. To prepare their nanofluids, they used shearing action using a homogeniser, followed by ultrasonic vibration for only 30 minutes. Their particle size distribution analysis revealed that little change took place to the particles' size after 30 minutes of ultrasonic vibration, and the average particle size was measured at 167 nm using Dynamic Light Scattering (DLS). They adjusted the pH value of the solutions to 7. They did not observe any deposition of nanoparticles on the heating surface and no sedimentation of the prepared solutions for several days.

They reported an enhancement in the HTC of nanofluids which increased with increasing concentration, reaching a maximum of 40 % at 0.35 vol. %. They used the Rohsenow correlation to compare their experimental results and found an agreement for the pure water results, but their nanofluid results deviated from the correlation. The deviation increased with increasing concentration. They implied that deterioration in the rate of heat transfer reported by other researchers might have been due to poor stabilisation techniques which caused nanoparticles to deposit on the heating surface and

create an insulating layer. They did not comment on the fact that a pH of 7 is a neutral pH, which is likely to be the same as that used by several other researchers [4, 6, 12-14, 16-19].

Narayan et al. [7] carried out an experimental investigation of pool boiling of nanofluids and proposed a new parameter to explain the contradicting results reported by previous researchers. They conducted experiments varying several parameters; nanofluid concentration from 0.14 to 0.57 vol. %; heater  $Ra$  of 48, 54 and 524 nm and alumina nanoparticles of 47 and 150 nm in size were used. The nanofluids were prepared by dispersing dry nanoparticles in water. As used in [3], electrostatic stabilisation was used to stabilise the nanofluids as well as ultrasonic vibration to break up the agglomerates. The pH value of the nanofluid was adjusted to 5.5 to enhance the stability. The nanoparticles remained in suspension for weeks. They used a vertical stainless steel tube as the heater surface to minimise the effect of sedimentation of nanoparticles on the surface. Thermocouples were brazed within the tube to record the surface temperature, and a cartridge heater was installed inside the tube to supply the heat.

Their results showed a mix of enhancement and deterioration in heat transfer for different combinations of concentration, surface-roughness and particle size. At all concentrations considered in the study, when the particles and surface-roughness were of the same order, the heat transfer reached its minimum value. Therefore, they introduced a new parameter defined as the *Surface Interaction Parameter* (SIP), in Equation (2.3).

$$SIP = \frac{\text{average surface roughness}}{\text{average particle size}} = \frac{R_a}{d_p} \quad (2.3)$$

Figure 2.4 shows the ratio of their nanofluids HTC to that of pure water as a function of  $SIP$ . It can be seen that when  $SIP$  is unity the heat transfer coefficient is minimum. The HTC is higher when  $SIP$  is far from unity. They indicated that when particles are smaller than the average surface-roughness, particles reside within the surface voids causing an increase in the number of active nucleation sites. They confirmed this by taking an image of the surface before and after the experiments using an imaging processing technique and found that the number of peaks in the surface profile was increased. Further, they indicated that when  $SIP$  is near unity, the nanoparticles block the nucleation sites and deactivate them, which reduces boiling heat transfer.

Regarding the effect of concentration, they found that the heat transfer was reduced with increasing concentration of the nanofluids. They explained that as the

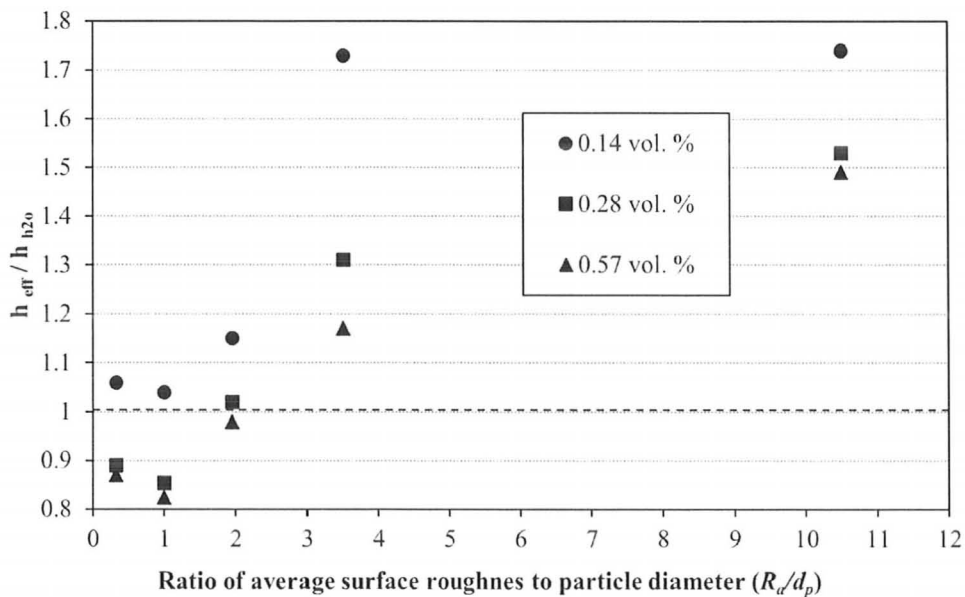


Figure 2.4: Variation of HTC ratio with  $SIP$ , [7]

concentration increases there will be more particles of similar size to the surface-roughness, which increases the chance of blocking the nucleation sites with particles of the same size, resulting in a reduction in the rate of heat transfer.

It should be noted at this point that the size of nucleation sites is independent of the value of the average surface-roughness. The size of the active nucleation sites are a function of the wall temperature and liquid properties only [1]. Therefore, relating the size of active nucleation sites to average surface-roughness is questionable.

## **2.7 Deposition of Nanoparticles on the Heater Surface under Pool Boiling Conditions**

Liu and Liao [6] carried out an experimental investigation to study the deposition of nanoparticles on boiling surfaces that many researchers observed and reported. They described the deposition as sorption or agglutination. Sorption relates to the simultaneous absorption and desorption of nanoparticles, while agglutination relates to the clumping of nanoparticles together. They used 35 nm dry silica and 50 nm copper oxide nanoparticles with concentrations varying from 0.057 to 0.57 vol. %. Water and alcohol were used as base fluids and sodium dodecyl benzene sulphate (SDBS) as a surfactant. When they added a surfactant they named the solution a *nanofluid* and a *nanoparticle suspension* when no surfactant was used. Their fluids were placed in an ultrasonic vibrator for 12 hours prior to the experiments. The pH of the solutions was not reported. When a surfactant was added, the nanoparticles remained in suspension for about a month, whereas the suspension's stability was much poorer without the surfactant. Their heater

was a horizontal copper 20 mm diameter flat surface of average surface-roughness 194 nm. Three thermocouples were installed below the surface to determine the heat flux and the surface temperature.

Their experimental results revealed that for the water-based solutions the HTC was higher than pure water, when using copper oxide nanoparticles, and lower when using silica nanoparticles. The CHF increased in all cases. The more noticeable result is that steady state could not be reached above a surface temperature of 112 °C when using the *nanofluids* due to a high undulation in surface temperature. Upon examination of the heater surface after the *nanoparticle suspensions* experiments, they found a few ten micrometers thick sorption layer of nanoparticles on the surface. This layer was easily, but not totally washable with water. A much thicker agglutination layer of several hundred micrometers thickness was found after boiling the *nanofluids* which could not be washed with water. It was this thick layer which caused the instability in the surface temperature above 112 °C. They concluded that the SDBS broke down at temperatures above 112 °C and caused this thick layer of nanoparticles to adhere to the surface. The surface-roughness was measured before and after the experiments. The surface became smoother after the experiments.

For the alcohol-based *nanofluids* no agglutination layer was formed on the surface because the surface temperature never reached a value above 112 °C. However, a sorption layer was formed on the surface. The HTC deteriorated for all alcohol *nanofluids* and *nanoparticle suspensions* while the CHF was enhanced. The use of SDBS had a minimal effect on the results when using alcohol-based solutions.

Jeong et al. [18] carried out a study to examine the wettability of surfaces under nanofluid boiling. Stainless steel 30 x 30 mm strips were heated using an alcohol lamp to a temperature of 400°C, then quenched in the nanofluids or surfactant solutions and removed at 150 °C, while nucleate pool boiling was taking place on the surface. The excess fluid was removed from the surface, which was then left to cool down. Sessile drop tests were carried out using water and nanofluid droplets. The contact angles of water and nanofluids droplets on the quenched surfaces were measured. The contact angle was used as a measure of surface wettability. Nanofluids were prepared from dry alumina nanoparticles and water of concentrations 0.5 – 4 vol. %. No agent was used to stabilise the nanofluids, and the pH value of the nanofluids was not reported. Trisodium phosphate was used as surfactant solutions. The following review of Jeong et al.'s study is focused towards the nanofluids quenched surfaces.

The experiments showed that the contact angle of a water droplet decreased dramatically on the nanofluid-quenched strips. The contact angle decreased with higher nanofluid concentrations, ranging from 5 to 25 °, which is much smaller than that of the water quenched surfaces, which was about 70°. These results indicated that the wettability of the strips was enhanced when quenched in nanofluids. Moreover, the contact angle was further reduced when using nanofluid droplets on the nanofluid-quenched strips, implying that surface wettability does not depend only on the surface condition, but also on the type of fluid.

They also measured surface tension of alumina nanofluids by measuring the contact angle of the nanofluids at different concentrations on a Teflon FEP Strip. They

found that surface tension of nanofluids decreases with increasing nanofluids concentrations, contrary to previous findings reported in [4].

Kwark et al. [8] carried out pool boiling experiments of nanofluids. They used very low concentrations of  $2.8 \times 10^{-5}$  –  $2.8 \times 10^{-2}$  vol. %. Dry alumina nanoparticles, 139 nm in size, were used with water as the base fluid. The nanofluid was placed in an ultrasonic bath for 2 hours prior to the experiments. The pH of the nanofluids was measured and found to be 6.3, which indicated that the suspension is a stable colloid. A  $1 \text{ cm}^2$  horizontal copper block was used as the heater surface. The roughness of the boiling surface was not reported. A thermocouple was installed below the block for surface temperature measurement. A  $20 \Omega$  resistance was installed below the block to supply the heat, and the heat flux was measured through voltage and current measurements across the resistance. In all their experiments, the heat flux was ramped at regular intervals until CHF was reached. They validated their experimental setup by comparing their water boiling curve against the Rohsenow correlation, and good agreement was found.

At concentrations below  $7 \times 10^{-4}$  vol. %, the HTC was almost the same as water. A minor deterioration in the HTC was found at concentrations higher than  $7 \times 10^{-4}$  vol. %. The CHF was enhanced for all concentrations. They repeated the boiling experiment at  $2.8 \times 10^{-2}$  vol. % concentration three times using the same heater and the same nanofluid. The deterioration was more significant when the experiment was repeated, which made them conclude that nanoparticle deposition was responsible for the deterioration in the HTC, and that the experiments had a transient characteristic due to continuous deposition of nanoparticles on the surface.

They also examined the effect of experiment duration by running some experiments for 2 hours at heat fluxes of 500, 1000 and 1500 kW/m<sup>2</sup> with a nanofluid at 7x10<sup>-4</sup> vol. % concentration. An increase in surface temperature was recorded during the prolonged boiling experiments, which increased at higher heat fluxes. A 2 °C and 8 °C rise in surface temperature were recorded at the lowest and highest heat flux, respectively.

The boiling characteristic of nanoparticle-coated surfaces was investigated using water boiling experiments. Surfaces were first coated with nanoparticles during nanofluid boiling with experiments at low and high concentrations of 7x10<sup>-4</sup> (LC) and 2.7x10<sup>-2</sup> vol. % (HC). The surfaces were immediately used in pure water boiling experiments. The HTC deteriorated in the case of the LC surface at heat fluxes above 500 kW/m<sup>2</sup>. A slightly higher deterioration was observed for the HC surface, for the entire range of heat fluxes.

Kwark et al. used a Scanning Electron Microscope (SEM) to examine the surface. They exposed four different surfaces to nanofluids subjected to: (1) gravity (no heating), (2) natural convection (single phase heating), (3) an electric field and (4) nanofluids boiling at different concentrations. The only noticeable deposition was found when the surface was exposed to boiling. Upon examining the surfaces after boiling experiments, they found the deposition was more profound at higher concentrations. To further examine nanoparticle deposition they carried out a boiling experiment where the applied heat was carefully increased until a single nucleation site was activated. A clear pattern of deposition was observed only at the nucleation site not at the rest of the heater surface.

They concluded that micro-layer evaporation during nucleate boiling of nanofluids is the main mechanism responsible for the deposition of nanoparticles on the surface.

Taylor and Phelan [19] carried out simple nanofluid boiling experiments using a horizontal nickel-cobalt-copper wire placed in a 50 ml beaker. The wire was 0.255 mm in diameter and 5 cm long. The surface temperature was measured through the wire temperature-resistance relation and the heat flux was determined through voltage and current measurements. Dry alumina nanoparticles of 20 nm size were used with water as the base fluid. The concentrations used were 0.2, 0.5 and 1 vol. %. The nanofluid was placed in an ultrasonic vibrator for 45 minutes before each experiment. DLS experiments showed that particle agglomerates after the ultrasonic vibration were 150 – 160 nm in size.

The HTC enhanced by 25 and 40 % for the 0.5 and 1 vol. % concentrations, respectively. The HTC did not change at the low concentration of 0.2 vol. %. They fitted their nanofluid boiling results using the Rohsenow correlation shown in Equation (2.4).

$$q'' = \mu h_{lv} \left[ \frac{\sigma}{g(\rho_l - \rho_v)} \right]^{-1/2} Pr^{-s/r} \left[ \frac{C_p}{h_{lv}} \frac{1}{C_{sf}} (T_s - T_{sat}) \right]^{1/r} \quad (2.4)$$

$s$  and  $r$  are constants given by Rohsenow [1] and are discussed in section 3.9. Taylor and Phelan modified the surface factor,  $C_{sf}$ , to fit their data where it was modified for each data point so that each curve had multiple values of  $C_{sf}$ . The justification for such modification was that continuous deposition of nanoparticles occurred during the

experiment and the surface condition was therefore, changing continuously. They concluded that the Rohsenow correlation could be used to predict the boiling heat transfer of nanofluids through the modification of  $C_{sf}$ .

They also investigated the effect of sub-cooled boiling and found deterioration in HTC below that of pure water. Less deposition took place during sub-cooled boiling experiments. The deterioration was attributed to the deposition of nanoparticles on the wire. They explained the less deposition during sub-cooled boiling experiments due to the thermo-phoretic action, as there is a larger temperature gradient between the wire and the nanofluid than in the case of saturated boiling.

## 2.8 Summary

Figure 2.5 shows a summary of the results of HTC of pool boiling of nanofluids reported in the different investigations discussed above. One can easily note the clear contradiction in the findings. Some investigations reported enhancements in the HTC with nanofluids [3, 12-13, 19], others found the deterioration [4, 8, 14-15] and two investigations reported both enhancement and deterioration [6, 20]. Another observation is that some researchers found a positive effect of concentration on the HTC, such as in [3, 13, 19], while others found the opposite, such as in [4, 7-8, 14-15].

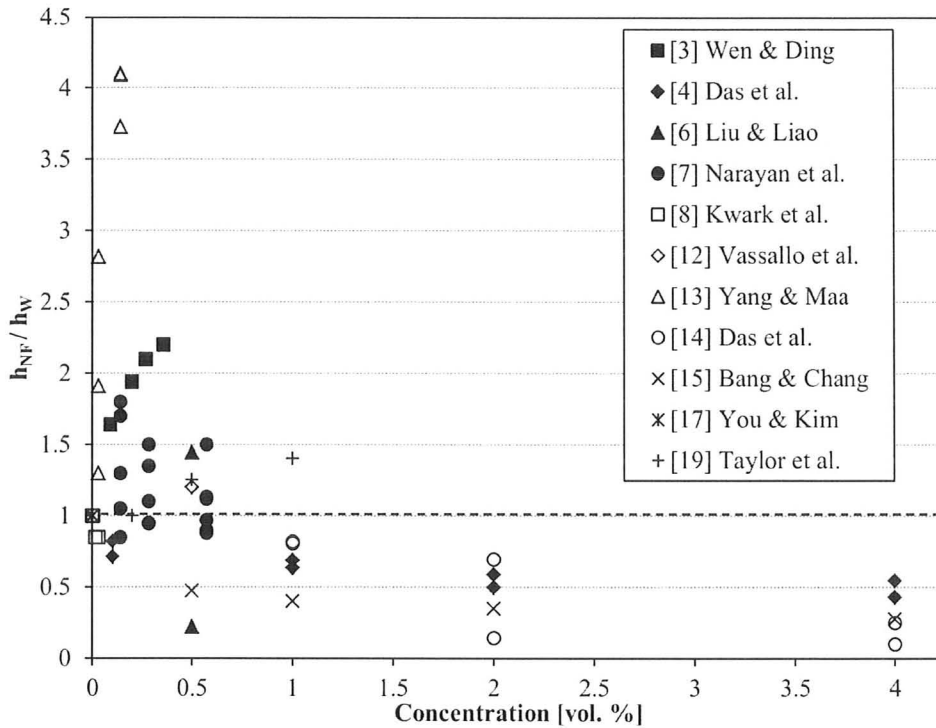


Figure 2.5: Summary of variation of HTC ratio against concentration reported in the literature

Some researchers explained the enhancement in the HTC due to the following mechanisms:

- Particles settling in the voids and increasing the number of nucleation sites,
- Enhanced thermal properties of the nanofluid due to the addition of nanoparticles,
- Enhanced stabilisation method prevents excessive deposition of particles on the boiling surface.

However, the deterioration in the HTC was attributed to the following effects:

- Particles settling in the voids and blocking the nucleation sites
- Nanoparticles settling on the surface creating a thermal insulating layer.

Very different experimental setups have been used among the researchers. Table 2.1 shows the conditions at which experiments were carried out and reported by different researchers. The geometry of the boiling surfaces used was a flat surface, a round tube or a wire. Different surface materials may have different boiling characteristics. Heater surfaces were made from copper, stainless steel or other alloys. Two studies used vertical heaters while all others used horizontal surfaces. The pH value of the nanofluids in most of these studies was not reported or investigated. Most nanofluids were prepared from dry nanoparticles while only one study used ready-made suspensions. These differences in the experimental conditions could explain or shed some light on the reason(s) of the contradicting findings.

Different nanofluids preparation techniques have been used. The use of a surfactant such as SDBS may be necessary for the nanoparticles to remain in suspension for long periods of time. However, its use caused a change in the properties of the base fluid [4] and severe nanoparticle deposition on the heater surface was reported in [6]. Electrostatic stabilisation using certain pH values resulted in less deposition [3, 7], however, there was no mention of the effect of the agent used to adjust the pH value on

*Table 2.1: Summary of conditions and HTC findings from previous pool boiling investigations of nanofluids. [NR = Not Reported]*

Reference	Surface-roughness [nm] Ra	Surface material	Surface geometry	Surface orientation	Nanoparticle type	Base fluid	Concentration [vol. %]	pH	Preparation method	Particle size [nm]	HTC
[13] Yang & Maa	NR	Stainless steel	3.2 mm tube	Horizontal	Alumina	Water	0.03 – 0.014	NR	Dry particles	50 – 1000	Enhancement
[4] Das et al.	400 – 1150	Stainless steel	20 mm tube	Horizontal	Alumina	Water	0.1 – 4	NR	Dry particles	38	Deterioration
[14] Das et al.	400	Stainless steel	4, 6.5 mm tube	Horizontal	Alumina	Water	1 – 4	NR	Dry particles	58	Deterioration
[17] You & Kim	NR	Copper	Flat	Horizontal	Alumina	Water	$2.8 \times 10^{-5}$ – $1.4 \times 10^{-3}$	NR	NR	NR	No change
[12] Vassallo et al.	NR	Nickel Chromium	0.4 mm wire	Horizontal	Silica	Water	0.5	NR	Ready-made suspensions	15 – 3000	Enhancement
[15] Bang & Chang	37	NR	Flat	Horizontal	Alumina	Water	0.5 – 4	NR	Dry particles	47	Deterioration
[3] Wen & Ding	NR	Stainless steel	Flat	Horizontal	Alumina	Water	0.09 – 0.35	7	Dry particles	167	Enhancement
[7] Narayan et al.	48 – 524	Stainless steel	Tube	Vertical	Alumina	Water	0.14 – 0.57	5.5	Dry particles	47 – 150	Enhancement / Deterioration
[6] Liu & Liao	194	Copper	Flat	Horizontal	Silica, copper oxide	Water, alcohol	0.057 – 0.57	NR	Dry particles	35 – 50	Enhancement / Deterioration
[19] Taylor et al.	NR	Nickel-cobalt-iron	0.255 mm wire	Horizontal	Alumina	Water	0.2 – 1	NR	Dry particles	150 – 160	Enhancement
[8] Kwark et al.	NR	Copper	Flat	Horizontal	Alumina	Water	$2.8 \times 10^{-5}$ – $2.8 \times 10^{-2}$	6.3	Dry particles	139	Deterioration

the boiling characteristics of the base fluid. Furthermore, the effect of the electrostatic stabilisation on the boiling performance has not been investigated.

In most of the pervious investigations there was no mention of the effect of the duration of the experiments. Nanoparticle deposition takes place throughout the duration of the experiment, therefore, the experiment duration is an important factor to consider when studying pool boiling of nanofluids.

## **2.9 Research Objectives and Research Plan**

The objective of this study is to investigate parameters which are suspected to explain the contrary findings in the literature, and gain a better understanding of pool boiling of nanofluids. The method of nanofluid preparation and electrostatic stabilisation are two factors which are suspected to change the boiling performance of nanofluids and have not been investigated before. Nanofluid concentration is a popular parameter investigated among the nanofluid community and is, therefore, studied as well. The deposition of nanoparticles has been recently found out to be a transient phenomenon [8] and will be affected by the duration of the experiments. Nanoparticle deposition on the boiling surface under prolonged boiling durations has been investigated to better understand the deposition phenomenon.

The experiments were carried out in three stages:

- Stage 1: Investigate the effects of electrostatic stabilisation and nanofluid preparation method
- Stage 2: Investigate the effects of electrostatic stabilisation and concentration
- Stage 3: Investigate the nanoparticle deposition phenomenon on the boiling surface under prolonged durations of boiling

Nanofluids prepared from alumina nanoparticles and water were used among most researchers, therefore, they are used in this study. All the investigations in this study were carried out experimentally. The boiling surface used in this investigation is a flat copper surface. Horizontal, flat surfaces are recommended to use when carrying out fundamental pool boiling experiments [1, 8]. This is to avoid bubble sliding that will occur when using tubes, wires or vertical surfaces. Also the characteristic length, or size, of the surface should be at least an order of magnitude larger than the bubbles being formed on the surface [1]. Therefore, the surface was 25.4 mm diameter, which is considerably larger than the bubbles.

## **2.10 Thesis Structure**

Chapter 3 provides details of the experimental facility, methodology and validation of the experimental setup using the Rohsenow correlation. Chapter 4 presents all experimental results. Chapter 5 includes the summary and main conclusions. Recommendations for future work are presented in Chapter 6.

## Chapter 3

### Experimental Setup and Methodology

This chapter presents the experimental setup and methodology used for the experimental investigation. The details and specification of the hardware are provided in detail in section 3.1. The instrumentation and measurement of surface temperature and surface heat flux are discussed in section 3.2 followed by a detailed section on uncertainty analysis in section 3.3. Section 3.4 presents the parameters investigated throughout the experiments. The procedure of preparing the nanofluid, the boiling surface and carrying out the experiments is then described in sections 3.5 to 3.8. The chapter is concluded with the details of the validation procedure of the experimental setup in section 3.9.

#### 3.1 Experimental Setup

The boiling vessel used in this study is shown in Figure 3.1. The main body of the vessel is a 20 cm diameter stainless steel pipe (13). A stainless steel skirt is fixed (16) to support the liquid within the pipe. A 2.54 mm diameter and 71 mm length copper block (18) is installed at the centre of the skirt to serve as the boiling surface. Three ¼ inch diameter and 1 ½ inch length cartridge heaters are fixed inside the bottom of the copper block to provide the heat flux to the liquid, referred to as the *Main Heaters* (8). The

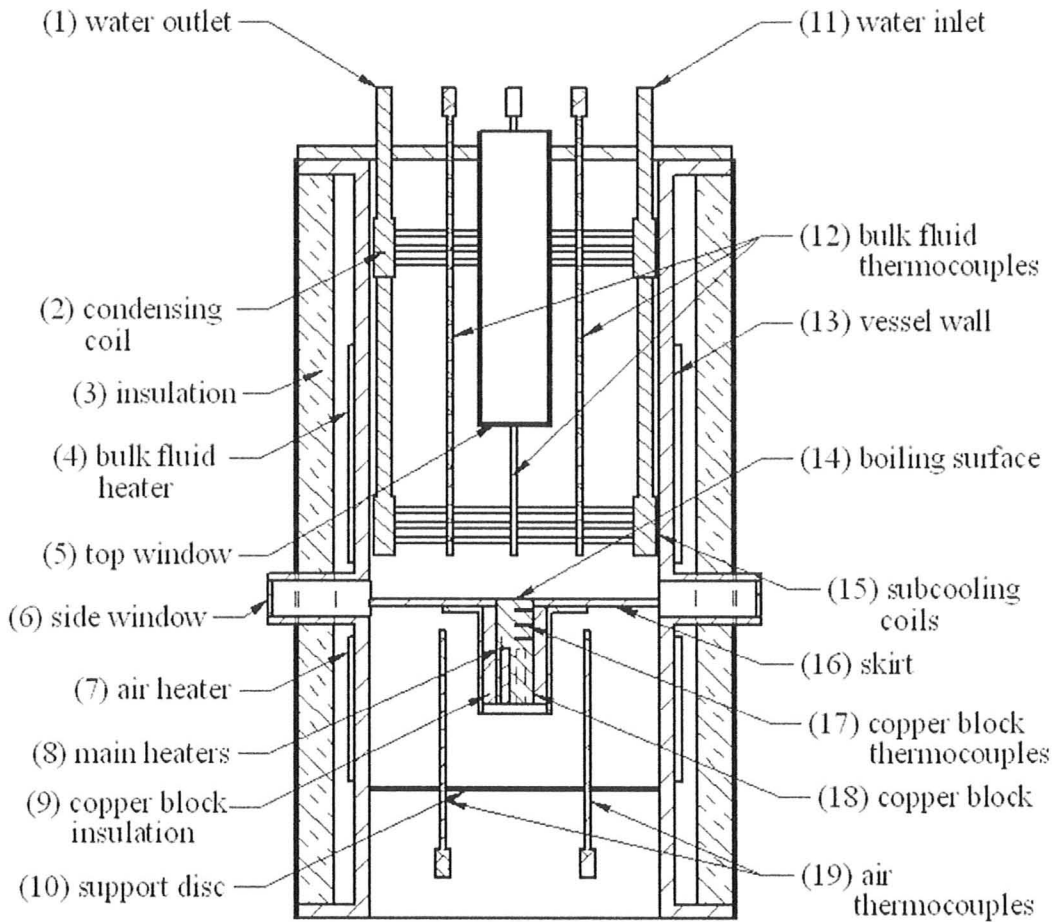


Figure 3.1: The boiling vessel

maximum power of the main heaters is 750 W which is capable of providing a maximum heat flux of  $1.48 \text{ kW/m}^2$ .

Three 1.0 mm diameter type-E thermocouples (17) are installed in the copper block at different axial distances from the top of the block to determine the axial temperature profile of the copper block. One copper block was used for Stage 1 experiments and another copper block for Stages 2 and 3. The locations of the

thermocouples in the copper blocks are shown in Figure 3.3. The copper block is wrapped in insulation (9) to reduce radial heat losses.

Two heaters are installed around the outside of the vessel wall with a combined power of 3000 W to heat up the liquid to saturation temperature, referred to as *Bulk Fluid Heaters* (4). Two 3.2 mm diameter type-E thermocouples were immersed in the bulk fluid to record its temperature (12).

Another heater is installed around the vessel wall below the skirt to heat the air surrounding the copper block, referred to as *Air Heater* (7). The air heater maintains the air around the copper block at a temperature close to that of the copper block to reduce radial heat losses from the copper block. Heating the air around the copper block also reduces the heat losses of the fluid through the skirt which prevents liquid subcooling. A support disc (10) is used to trap the air around the copper block to minimise mixing with the air in the room. A thermocouple (19) is installed to monitor the air temperature around the copper block.

A condensing coil (2) is used to minimise the loss of fluid during the experiments. This important feature helped maintain a constant concentration throughout the experiment time when boiling nanofluids. The water flow rate through the condensing coil is regulated through a needle valve. The inlet condensing water is too cold during the winter season, and causes some liquid subcooling during the experiment because the condensed droplets are too cold. A heater is installed in the inlet condensing water pipe to heat up the inlet condensing water and prevent this subcooling from taking place. A

thermocouple is installed to monitor the temperature of the inlet condensing water, as well as a flow meter to measure its flow rate. A sub-cooling coil (15) is used to lower the liquid temperature before it was drained out of the vessel.

Two opposing glass side windows (6) allow visual observation of the boiling phenomenon on the surface from the side. A top window (5) also allows visual observation of the boiling surface from above. The diameters of the side windows are 2.5 cm and the top window is 4.5 cm.

The whole vessel is wrapped with an aluminium cover to protect the user from contacting the heaters. Insulation (3) is attached between the cover and the vessel to reduce heat losses from the vessel and conserve power.

### 3.1.1 Heaters Control

The bulk fluid, air and main heaters are controlled separately. A simplified schematic diagram of the heater control circuit is shown in Figure 3.2. The heaters are all controlled through a series of ON/OFF solid-state relays. The relays are controlled using three Watlow PID Controllers. The PID controllers control the temperature by varying the power supplied to the heaters through the solid-state relays. A bulk fluid thermocouple and an air thermocouple are installed to feed the water and air temperatures back to the controllers. The controller would vary the ON/OFF switching intervals to match the temperature read by the thermocouple to a set temperature.

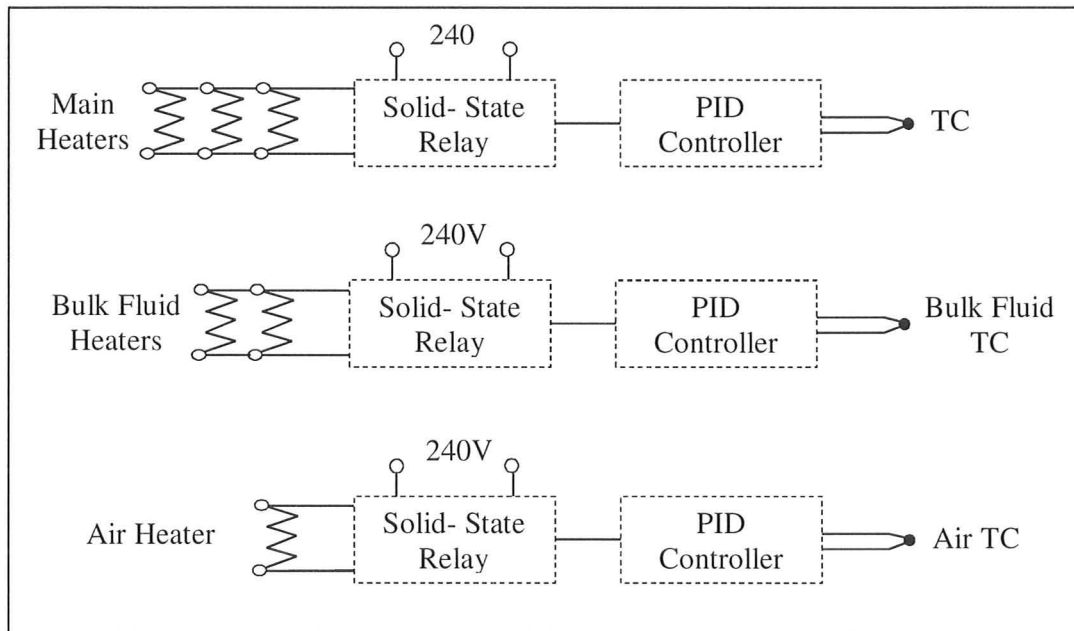


*Figure 3.2: Heaters control circuit*

The main heaters have to supply a constant heat flux to the copper block in order for steady-state to be reached. This is established by setting the PID controller to control heat flux rather than temperature. A dead thermocouple had to be connected to the main heaters controller in order for it to operate, otherwise an error would be displayed and the controller would not work.

### 3.1.2 Data Acquisition

The thermocouples are connected to a Kiethley Data Acquisition System Model 2700. The data acquisition is connected to a personal computer. ExceLinx software is installed into Microsoft Excel on the computer to sample and record the temperatures

from the thermocouples. The temperatures were scanned once every 5 seconds. The readings of total nine thermocouples were scanned and recorded as follows:

- Three axial locations in the copper block
- two bulk liquid locations
- air around copper block
- water heater
- air heater
- inlet condensing water

### 3.1.3 Thermocouple Calibration

The thermocouples were found to deviate by about 0.25 °C. The thermocouples were calibrated against a Resistance Temperature Detector (RTD) which is calibrated to 0.01 °C. The calibration was carried using a solid copper cylinder which was insulated from the surroundings. There copper cylinder had drilled holes to accommodate a RTD, four thermocouples and a cartridge heater. The copper cylinder's temperature was raised using the cartridge heater until the temperature of the RTD reached steady-state. It was assumed that the temperature was uniform in the copper block. The RTD and thermocouples temperatures were recorded using the same wires and data acquisition system used in the actual experiments to account for the deviation in the readings from the wiring and connections. A linear best fit was used to correlate the thermocouple readings to the RTD. To check that the fit was accurate, the  $R^2$  values were calculated and

were found to be 0.999. This calibration ensured that all thermocouple readings were comparable and minimised their deviation.

#### 3.1.4 High-Speed Imaging

The boiling phenomenon was captured by means of a Fastec Imaging high-speed camera model TSHRMS. The images were recorded at a rate of 1000 frames per second, which is the maximum record rate of the camera. The resolution used was optimised to 640 x 480 pixels, which was found to be adequate to observe the bubbles clearly and save disk space. A Lower Pro light source was used to provide the illumination for the camera.

The light source and camera were placed at the opposing side windows. Observation of the boiling phenomenon from the top window was not possible. The bubbles would rise and come into contact with the top window during boiling. The bubbles would then slide along the window which would severely hinder sighting the boiling surface.

#### 3.1.5 3D Profiling of the Surface

The boiling surface 3D profile was examined using a Zygo White Light Interferometer. The surface was positioned under the interferometer to scan an area of 1.09 x 1.45 mm. The resolution used was 640 x 480 pixels for the scanned area. The interferometer was used with MetroPro 8.1.5 software to capture the image on a personal

computer. The software generated a 3D image of the surface, and determined the average surface-roughness of the scanned area. The software evaluated the average surface-roughness of the scanned area in both the x and y directions.

### 3.2 Determination of Heat Flux ( $q''$ ) and Surface Temperature ( $T_s$ ) of the Copper Block

The temperature profile in the copper block was established in order to determine the surface temperature and the heat flux through the surface. Three thermocouples were installed at the radial centre of the copper block and at different axial distances from the surface of the copper block. A linear best fit was carried out on the temperatures recorded, assuming that radial heat losses are negligible and the temperature profile is linear. The equations used to apply the linear best fit and obtain heat flux ( $q''$ ) and surface temperature ( $T_s$ ) are shown in Equations (3.1) and (3.2), respectively.

$$q'' = k \frac{\sum x_i T_i - \sum x_i \sum T_i}{N \sum (x_i^2) - (\sum x_i)^2} \quad (3.1)$$

$$T_s = \frac{N \sum x_i^2 \sum T_i - \sum x_i \sum x_i T_i}{N \sum (x_i^2) - (\sum x_i)^2} \quad (3.2)$$

where:  $N$  = number of temperature readings,  $i = i^{\text{th}}$  reading.

One copper block was used for Stage 1 experiments, and another for Stages 2 and 3 experiments. The locations of the thermocouple holes in the copper blocks used in the

different stages are shown in Figure 3.3. The temperature profiles obtained from the linear best fits for the full range of heat fluxes used during the different stages are shown in Figures 3.4 and 3.5. A different copper block was used after Stage 1 experiments to allow a thermocouple that is placed further away from the surface. The closest thermocouple to the surface in Stage 1 experiments was only 1 mm away from the surface. This distance was regarded as too close to the surface. As the copper block is polished over and over before every experiment, the surface may eventually wear down and expose the thermocouple to the liquid. Therefore, the top thermocouple was moved to a distance of 8 mm from the surface for Stages 2 and 3 experiments. Placing the thermocouple at this distance ensured the surface would never wear down to expose the thermocouple, and also made the assembly of the block much easier.

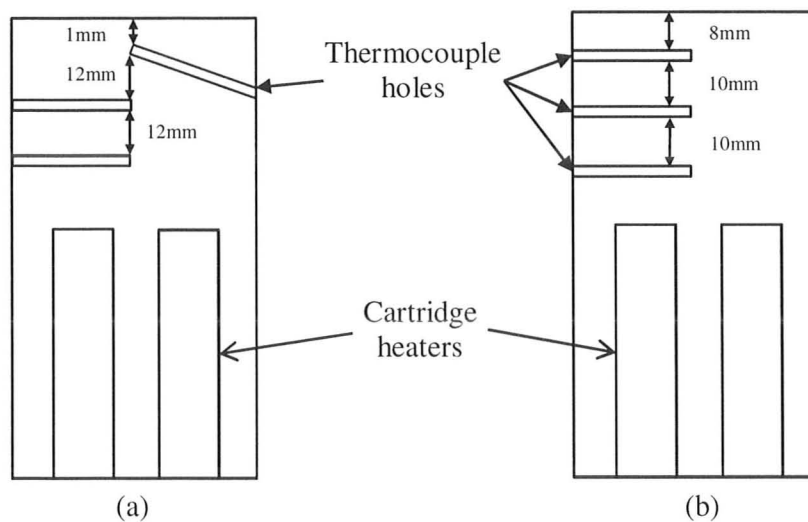


Figure 3.3: Locations of thermocouples placed in the copper blocks for experiments in (a) Stage 1 and (b) Stages 2 & 3

The wear in the copper block due to polishing the surface was quantified by measuring the overall height of the copper block using a Vernier calliper every time the block was polished. The surface was found to wear down by a total of about 0.4 mm after all the experiments were carried out. The reduction in the height of the copper block was calculated for each experiment and subtracted from the distances of the thermocouples from the copper block surface.

The uncertainty in the temperatures recorded was  $\pm 0.85$  °C as provided by the thermocouples supplier. The thermocouples were 1.0 mm in diameter, and the holes drilled in the copper block were 1.1 mm diameter. This gives an uncertainty in the thermocouple location of  $\pm 0.05$  mm. Errors bars are displayed in Figures 3.4 and 3.5. The calculated temperature profiles fit within the experimental error bars. This gives confidence in the linearity of the temperature profile and a linear best fit is appropriate to use in order to obtain the temperature profile in the copper block.

### 3.3 Uncertainty Analysis

The uncertainty analysis was carried out according to Equation (3.3).

$$u(R) = \left[ \left( u(W_1) \frac{\partial R}{\partial W_1} \right)^2 + \left( u(W_2) \frac{\partial R}{\partial W_2} \right)^2 + \dots + \left( u(W_n) \frac{\partial R}{\partial W_n} \right)^2 \right]^{1/2} \quad (3.3)$$

where:  $u(\dots)$  = uncertainty in ( ),  $R$  = calculated result, and  $W_n$  =  $n^{\text{th}}$  variable.

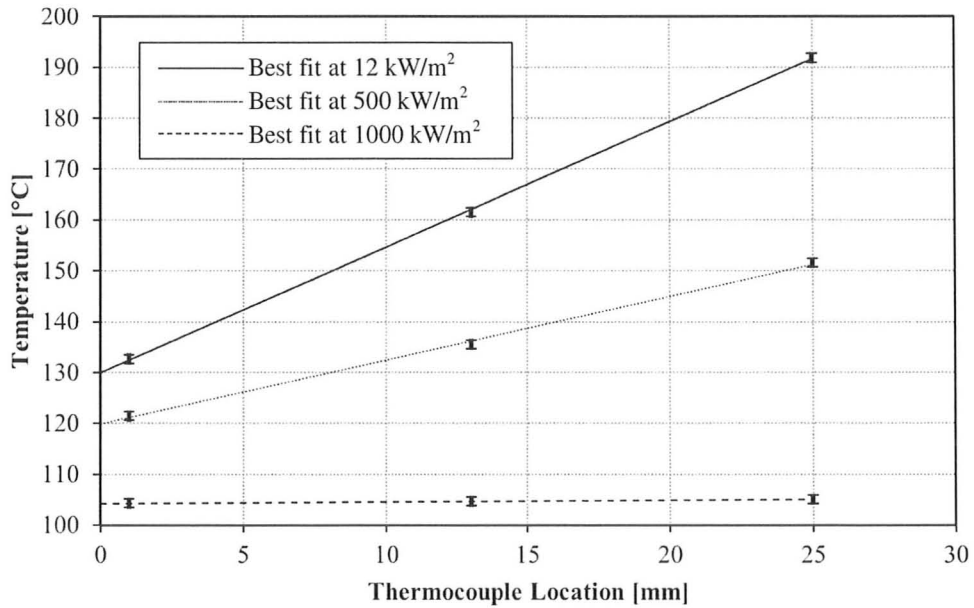


Figure 3.4: Temperature profiles in copper block for Stage 1 experiments at different heat fluxes

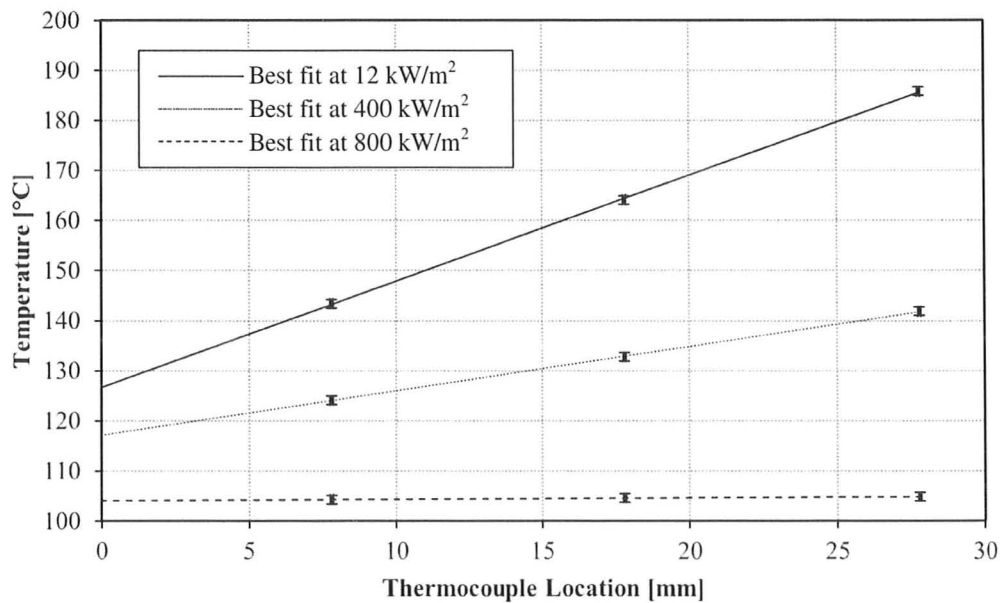


Figure 3.5: Temperature profiles in copper block for Stages 2 & 3 experiments at different heat fluxes

### 3.3.1 Uncertainty in Heat Flux ( $q''$ )

The uncertainty in the calculated heat flux is due to the uncertainty in the temperature gradient in the copper block. Calculating the uncertainty in  $q''$  using Equation (3.3) gives a maximum experimental uncertainty of  $\pm 19.8 \text{ kW/m}^2$  for Stage 1 experiments, and  $\pm 23.7 \text{ kW/m}^2$  for Stages 2 & 3. The intermediate heat flux for Stage 1 and Stages 2 and 3 were  $500$  and  $400 \text{ kW/m}^2$ , respectively. Therefore, the uncertainty in the heat flux at intermediate heat flux values was  $4.0 \%$  and  $5.9 \%$  for Stage 1 and Stages 2 and 3, respectively.

### 3.3.2 Uncertainty in Surface Temperature ( $T_s$ )

The uncertainty in surface temperature was calculated using Equation (3.3), which yields an uncertainty in surface temperature of  $\pm 0.83 \text{ }^\circ\text{C}$  for Stage 1 experiments, and  $\pm 1.17 \text{ }^\circ\text{C}$  for Stages 2 and 3. Using an intermediate surface temperature of  $115 \text{ }^\circ\text{C}$ , the uncertainties in surface temperature are  $0.8 \%$  and  $1.1 \%$  for Stage 1 and Stages 2 and 3, respectively.

### 3.3.3 Uncertainty in Bulk Fluid / Liquid Saturation Temperature ( $T_{sat}$ )

All liquids were boiled at saturation under atmospheric pressure. Due to changes in atmospheric pressure, the saturation temperature would change from one experiment to another. The saturation temperature was recorded by measuring the bulk fluid

temperature during boiling. The minimum recorded saturation temperature was 99.4 °C and the highest was 100.9 °C.

The bulk fluid temperature was recorded using two thermocouples. The average of the two temperatures was calculated and used as the saturation temperature, as shown in Equation (3.4).

$$T_{sat} = (T_1 + T_2)/2 \quad (3.4)$$

The error in each thermocouple was  $\pm 0.85$  °C each, which yields a combined error of  $\pm 0.6$  °C in the liquid saturation temperature. For an average liquid saturation temperature of 100 °C, the uncertainty in bulk fluid temperature is 0.6 %.

The measurement of water saturation temperature was validated against the ambient pressure in the room. The pressure was measured using a barometer during one experiment and was 101.9 kPa, which gives a saturation temperature equal to 100.1 °C. The measured water temperature was 100.5 °C, which is within the uncertainty of the bulk fluid measurement.

#### 3.3.4 Uncertainty in Surface Superheat ( $T_s - T_{sat}$ )

The uncertainty in surface superheat is due to the uncertainty in surface temperature and liquid saturation temperature. Combining the two using Equation (3.3) gives an uncertainty in surface superheat of  $\pm 1.02$  °C for Stage 1 experiments, and  $\pm 1.31$

°C for Stage 2 & 3 experiments. Using an intermediate surface superheat of 15 °C gives an uncertainty in surface superheat of 6.8 % and 8.7 % for Stage 1 and Stages 2 and 3, respectively.

### **3.4 Parameters Investigated and Conditions of Experiments**

#### **3.4.1 Stage 1: Effect of Preparation Method and Stability**

It was suspected that the pH value (or stability), and the method of preparation of the nanofluids will have an effect on pool boiling of nanofluids. The effects of pH value and preparation method were investigated in this stage of the research. The variable parameters were:

- Preparation method: nanofluids prepared from dry particles and ready-made suspensions
- pH value / stability: pH = 5, pH = 6.5

The concentration was kept constant at 0.1 vol. %, as this value was one of the most commonly used in the literature and permits comparison to other research. It is worth mentioning at this point that the boiling experiment time was 45 minutes; the boiling time was changed in Stage 3. The average surface-roughness used in this stage was measured before every experiment and was between 100 and 150 nm. The surface-roughness was measured at five different spots on the boiling surface before and after each experiment to represent the average surface-roughness of the surface. The locations of the measurements of surface-roughness taken on the surface are shown in Figure 3.6.

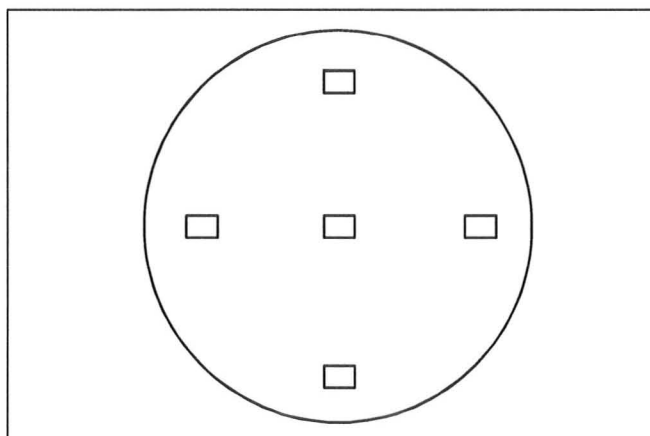


*Figure 3.6: Locations of surface-roughness measurements of the boiling surface taken in Stage 1 experiments*

#### 3.4.2 Stage 2: Effect of Concentration and Stability

Since concentration was investigated in almost all the past works, it was incorporated at this stage. The combined effects of concentration and pH value have not been investigated before, and are studied in this stage of experiments. These concentrations have been considered: 0.01, 0.1 and 0.5 vol. %, and the two pH values used in the previous stage: pH = 5, pH = 6.5. The concentrations were chosen to cover the range used by most previous researchers.

A different surface preparation method was adopted in Stage 2. This method was better at keeping the surface flat and was also safer. As a result, the surface became smoother. This method is explained in section 3.6. The average surface-roughness for Stage 2 was about 50 nm.

### 3.4.3 Stage 3: Effect of Concentration and Prolonged Boiling Duration on Nanoparticle Deposition

A deposition phenomenon of nanoparticles on the surface was observed during Stages 1 and 2. The effect of this deposition pattern is studied in Stage 3 at the three concentrations: 0.01, 0.1 and 0.5 vol. %. During the boiling experiment, each heat flux was kept constant for 15 minutes to allow the nanoparticle deposition to take place. The total boiling time was 105 minutes in Stage 3.

After each nanofluid experiment, water boiling experiments were carried out on the nanoparticle-deposited surfaces. This approach is to study the effect of the changed surface condition using the same fluid. Water was chosen as the common fluid to boil on the nanoparticle-deposited surfaces to allow visual observation of the boiling surface. Nanofluids were found to be opaque and the surface could not be observed visually. High-speed images of the water boiling experiments were taken.

The pH of the nanofluids was kept constant at a neutral pH of 6.5 during this stage. The number of measurements carried out to represent the average surface roughness was doubled. Therefore, ten measurements were taken instead of five. The locations of the surface-roughness measurements are shown in Figure 3.7. The initial average surface-roughness was also kept constant at 50 nm. A summary of the investigated parameters for the different stages is provided in Table 3.1.

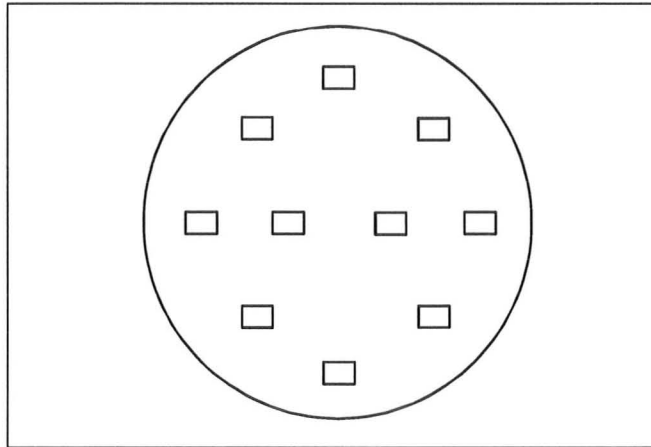


Figure 3.7: Locations of surface-roughness measurements of the boiling surface taken in Stage 3 experiments

Table 3.1: Parameters investigated in this study

Stage	Concentration [vol. %]	pH Value	Preparation Method	Experiment Duration	Average Surface-Roughness $R_a$ [nm]
1	0.1	5	Dry particles	45 minutes	100-150
		6.5	Dry particles		
		5	Suspension		
		6.5	Suspension		
2	0.01	5	Dry particles	45 minutes	50
	0.1				
	0.5				
	0.01	6.5			
	0.1				
	0.5				
3	0.01	6.5	Dry particles	1 hour and 45 minutes	50
	Water		-		0.01 % deposition
	0.1		Dry particles		50
	Water		-		0.1 % deposition
	0.5		Dry particles		50
	Water		-		0.5 % deposition

### 3.5 Nanofluid Preparation

Alumina nanoparticles of 40 - 50 nm nominal particle size were acquired in dry form and ready-made suspensions a concentration of 9 vol. % from Nanophase Technologies Incorporation. Dry nanoparticles had to be measured by weight, therefore, the conversion from mass to volumetric concentrations was carried out using Equation (3.5) [15].

$$\phi_v = \frac{1}{\left(\frac{1 - \phi_m}{\phi_m}\right) \frac{\rho_p}{\rho_f} + 1} \quad (3.5)$$

Dry nanoparticles or ready-made suspension amounts were carefully measured and added to deionised water to obtain the required concentration. Dry nanoparticles had to be handled in a fume hood as they easily suspend in the air and are harmful if breathed in. The nanofluids were then placed in an ultrasonic bath at 40 kHz for five hours prior to each experiment. The ultrasonic vibration was used to break down particle agglomerates as nanoparticles have a high tendency to agglomerate due to strong Van der Waals forces [3].

Two tests were carried out to check the nanoparticle size. The first test was carried out using Scanning Electron Microscope (SEM) imaging of the particles after the ultrasonic vibration. A drop of the nanofluid was left to dry overnight and the SEM was carried out the following morning. The image at 80,000 times magnification is shown in Figure 3.8. It can be seen that the particles size lie in the range of 10 – 100 nm. Therefore, the average size provided by the manufacturer was considered as an accurate estimate.

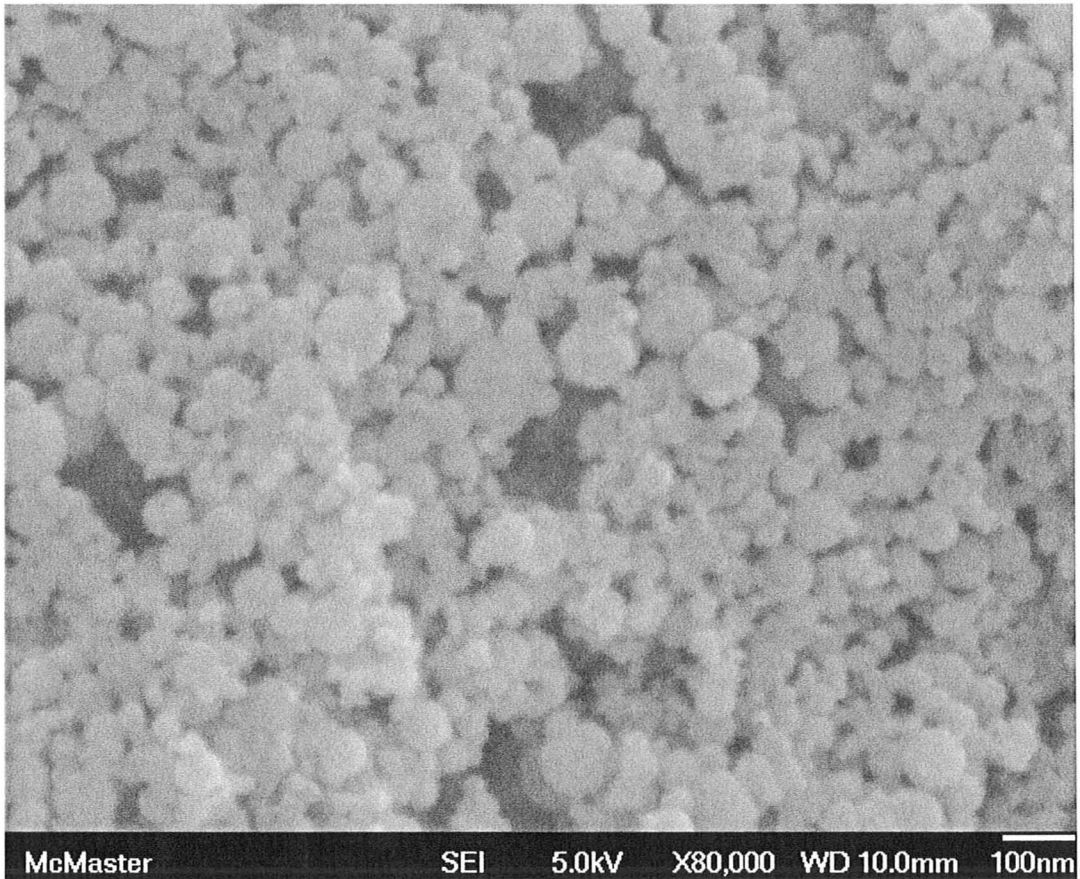


*Figure 3.8: SEM image of the nanoparticles sample*

The second test was carried out using a Dynamic Light Scattering (DLS). This method measures the overall size of the particles in motion. The nanofluid was diluted until it became transparent. A laser beam was exposed directly through the suspensions, where the laser would scatter upon impact with the particles. As the particles move under Brownian motion, the scattering of the laser would constantly change. The scattering of the laser is detected and fed to a correlation which gives the range of the particles size in suspension.

Nanofluid samples were taken at different times from the start of the ultrasonic vibration and the DLS tests was carried out afterwards. The results are shown in Figure 3.9. The particles size is reduced with time from about 300 nm to 200 nm after 5 hours. The effective particle size is about 4 – 6 times larger than the nominal particle size given by the supplier. The particles agglomerate and are very hard to break up into their individual particle size under ultrasonic vibration. All the nanofluids were exposed to ultrasonic vibration for 5 hours before each experiment.

To adjust the pH value of the nanofluids, hydrochloric acid was added. The nanofluids were considered stable at both an acidic and a neutral pH value, as the nanoparticles remained in suspension for days and no sedimentation was observed by the

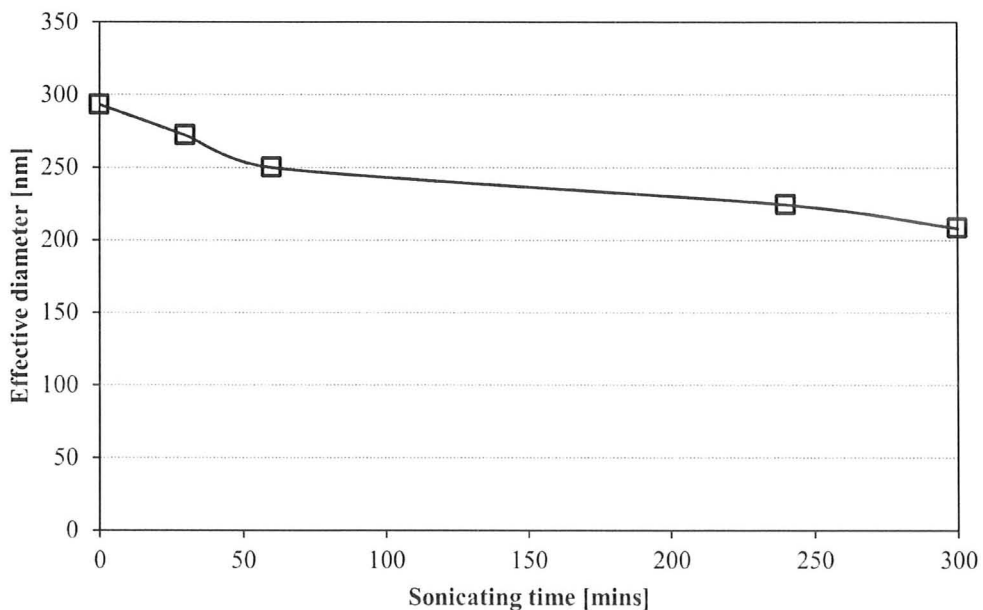


Figure 3.9: Variation of particle size with ultrasonic vibration time using DLS

naked eye. However, the more acidic nanofluids are regarded more stable as their pH value is further away from the iso-electric point.

### **3.6 Surface Preparation**

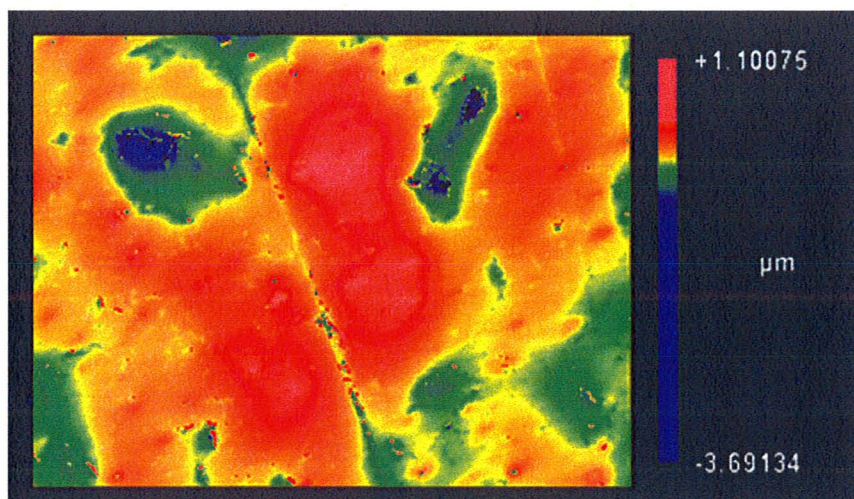
To carry out an experiment the boiling surface was polished before every experiment to ensure that no particles remained on the surface. As aged or oxidised surfaces give different boiling characteristics, the surface was polished before each experiment to a mirror-finish grade using a 1 micron rotating diamond cloth. During Stage 1, the copper block was held and pressed down on the diamond cloth as it rotates by hand. This procedure was difficult as the block would tend to rotate with the diamond cloth due to friction. The surface would be gently wiped using a cotton ball, soap and water after the polishing to clean it. Any excess water would be absorbed using a dry cotton ball. The average surface-roughness would then be measured to ensure consistency of the surface finish before each experiment. If the surface was found to be rougher than the required surface-roughness, it would be polished again and the surface-roughness would be measured again.

During Stages 2 and 3, the polishing procedure was modified. A 2½ inch diameter steel collet was used to hold down the copper block on the polishing cloth. This prevented the copper block from rotating during the polishing process, making the process safer and more consistent. It also helped keep the copper block surface perfectly horizontal on the polishing cloth, producing a perfectly flat surface. As a result, the surface was found to be

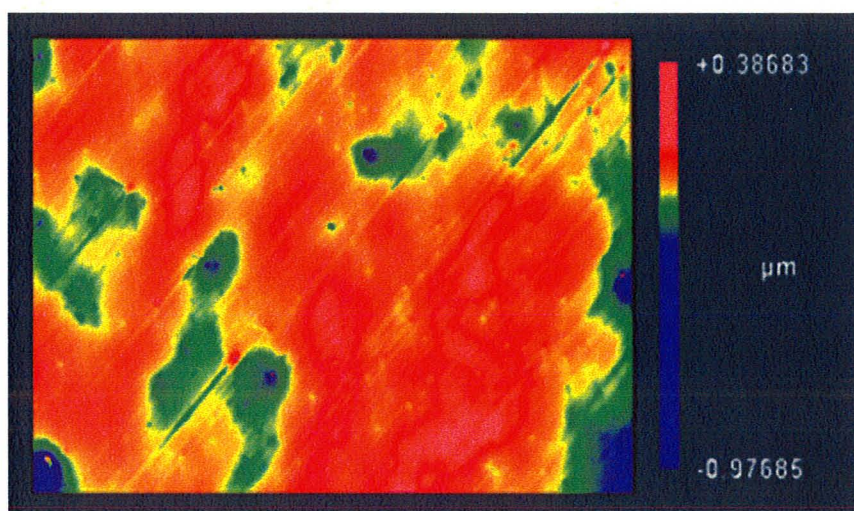
smoother as mentioned earlier in section 3.4.2. A sample of the 3D profiles of the clean surfaces is shown in Figure 3.10. The 3D images of the post-boiling surfaces are shown in Chapter 4.

### 3.7 Test Procedure

The boiling vessel was washed and wiped down from any residual nanoparticles remaining from the previous experiments. The boiling vessel was then assembled together. All heaters and thermocouples would be connected. The vessel was then filled with five litres of nanofluid or pure water. The bulk fluid and air heaters would be switched on. The bulk fluid heater controller was set to a temperature of 104 °C and the air heater controller to 110 °C. The controllers were set to a slightly higher temperature than the required because the final temperature of the liquid or air was found to be always a few degrees lower than the set temperature on the controller. Once the liquid temperature approaches 100 °C, the bulk fluid heater controller would be switched to manual control and set to 50 % of full power. The inlet condensing water valve would also be opened at a flow rate of about 900 cm<sup>3</sup>/min. The heater in the inlet condensing water pipe would also be switched on to raise the temperature of the condensing water. The inlet condensing water temperature was raised to about 35 °C. The fluid in the vessel would be left to boil vigorously for 15 minutes under these settings to remove any non-condensable gases as well as to bring the whole vessel to a temperature close to the saturation temperature of the fluid.



Stage 1:  $Ra = 131 \text{ nm}$



Stages 2 & 3:  $Ra = 54 \text{ nm}$

*Figure 3.10: 3D profiles of the polished surface before Stage 1, 2 and 3 experiments*

After the 15 minutes, the bulk fluid heater controller would be switched back to the automatic temperature control setting and the inlet condensing water flow rate reduced to  $300 \text{ cm}^3/\text{min}$ . The inlet condensing water temperature would be about  $55 \text{ }^\circ\text{C}$ ,

which prevented liquid subcooling during the experiments. The main heaters in the copper block would then be switched on using manual control settings. Once the temperatures of the copper block thermocouples reached steady state, these temperatures were recorded and marked as a steady-state point. Steady state was assumed to be achieved when the copper block temperature would remain within 0.1 °C for 30 seconds. It usually took 2 minutes for the copper block temperature to reach steady-state. After the temperatures were recorded, the input to the main heaters controller is incremented to attain a higher heat flux, and this procedure is repeated.

### **3.8 Post-Experiment Procedure**

After an experiment was carried out, the nanofluid would be cooled down using the subcooling coils and then drained out of the boiling vessel when the nanofluid temperature was safe for removal. The copper block was taken out of the vessel and the surface-roughness would be measured to assess nanoparticle deposition that took place during the experiment. Any change in surface-roughness would be only due to nanoparticle deposition. It was confirmed that water boiling had no effect on the surface-roughness. Surface-roughness measurements of pre- and post- pure water boiling experiments were almost identical; average surface-roughness after water boiling during Stage 2 changed from 54 to 58 nm.

As the nanofluids were drained, a small film of nanofluid would remain on the surface. This film was not allowed to air-dry as the nanoparticles suspended in that film

would settle on the surface and indicate deposition due to nanofluid film evaporation rather than deposition due to boiling. This film was washed away with a weak water jet and the surface was allowed to air-dry afterwards.

### 3.8.1 Experiments to Assess Nanoparticle Deposition not due to Boiling

Two experiments were carried out to assess the degree of deposition due to air-drying of nanofluid on the surface. Nanofluids at 0.1 vol. % and a neutral pH were used. The surface was polished and assembled in the vessel. The nanofluids were brought to saturation temperature using the bulk fluid heaters. The main heaters were not used in these experiments and no boiling took place on the surface. After 15 minutes of the nanofluids being at saturation temperature, they were cooled down and drained out of the vessel. For the first experiment the nanofluid was left to air-dry on the surface. In the second experiment, the nanofluid was washed off the surface with water before it air-dried. The average surface-roughness increased from 75 nm to 173 nm when the nanofluid was left to air-dry, and from 62 nm to 69 nm when the nanofluid was washed away. These experiments confirmed that air-drying of nanofluid resulted in some nanoparticle deposition on the surface not due to boiling.

Another experiment was carried out to assess the effect of gravity on nanoparticle deposition on the surface. A 0.1 vol. % nanofluid at a neutral pH was used. The nanofluid was left on a clean boiling surface for one hour at room temperature. After draining and

washing the surface, the surface-roughness was measured and did not change. This indicated that gravity does not cause the nanoparticle deposition on the surface.

### 3.9 Validation of Water Boiling Curve

To validate the experimental setup, a pure water boiling curve was obtained during Stage 1 and was compared against the Rohsenow correlation [1]. The constants used in this correlation were  $s = 1$ ,  $r = 0.33$  and  $C_{sf} = 0.0128$ , which Rohsenow suggested for boiling water on an emery polished copper surface. The result of the validation experiment is shown in Figure 3.11.

The Rohsenow correlation lies within the experimental error bars. The boiling curve deviated from the correlation at superheat temperatures above about 16 °C. This can be explained due to the heat flux approaching CHF, where *slugs and columns* [1] of vapour start to form due to the vigorousness of boiling. The heat flux is lower than that predicted by the correlation due to the limited liquid access to the surface due to vigorous vapour formation.

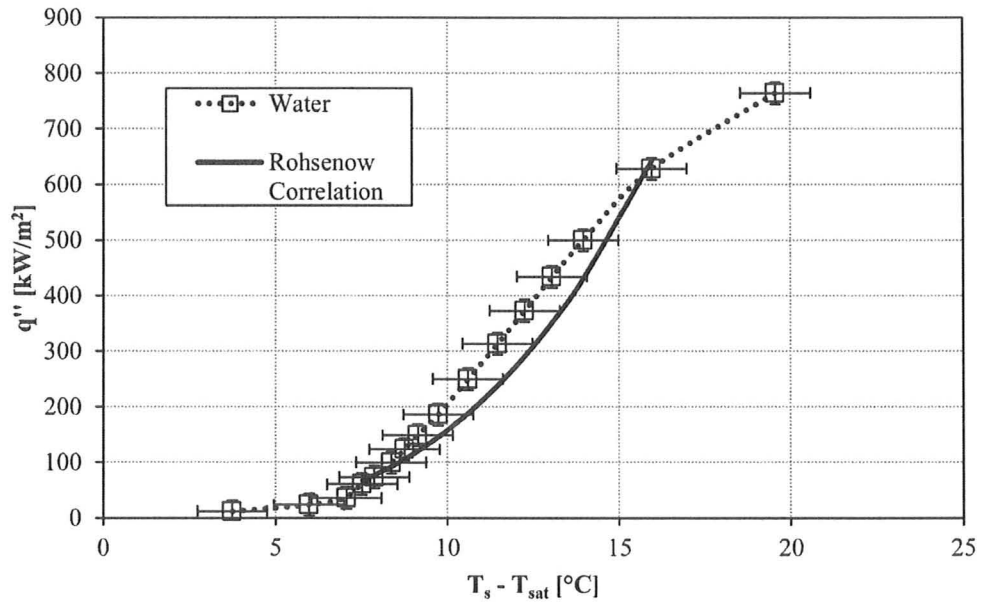


Figure 3.11: Rohsenow correlation validation

## Chapter 4

### Results and Discussion

The results of the experiments carried out in this study are presented and discussed in this chapter. Each stage of experiments is discussed separately. Stage 1 focused on the effects of stability and preparation method on pool boiling of nanofluids. The effects of concentration and stability on pool boiling of nanofluids are examined during Stage 2. Finally, Stage 3 focused on the effects of prolonged boiling duration and concentration on nanoparticle deposition.

#### 4.1 Effects of Stability and Preparation Method (Stage 1)

Four nanofluids have been investigated in experiments of Stage 1. The different nanofluids designations and the results are summarized in Table 4.1. The boiling performance of nanofluids is shown in Figure 4.1. The boiling curves indicate that the HTC of all the nanofluids is lower than that of water. This result is in agreement with those previously found in [7]; *SIP* in these experiments is close to unity which will cause the HTC to be minimum. The average surface-roughness before the experiments was 125 nm. The DLS tests showed effective particle size between 150 and 215 nm for the different nanofluids. Therefore, *SIP* in the experiments is in the range of 0.83 – 0.58.

Table 4.1: Results of experiments carried out during Stage 1

Designation	Preparation method	pH value	HTC % of water @ 15°C	Average post-boiling surface-roughness [nm]	Effective particle size [nm]	SIP
DN	Dry particles	Neutral (6.5)	55	6970	215	0.58
DA	Dry particles	Acidic (5)	70	430	180	0.69
SN	Suspension	Neutral (6.5)	51	3120	170	0.74
SA	Suspension	Acidic (5)	54	360	150	0.83

The nanofluids prepared from dry particles are referred to here as *dry* nanofluids and those prepared from ready-made suspensions are referred to as *suspension* nanofluids. The concentration was kept constant at 0.1 vol. % in the four experiments shown in Table 4.1.

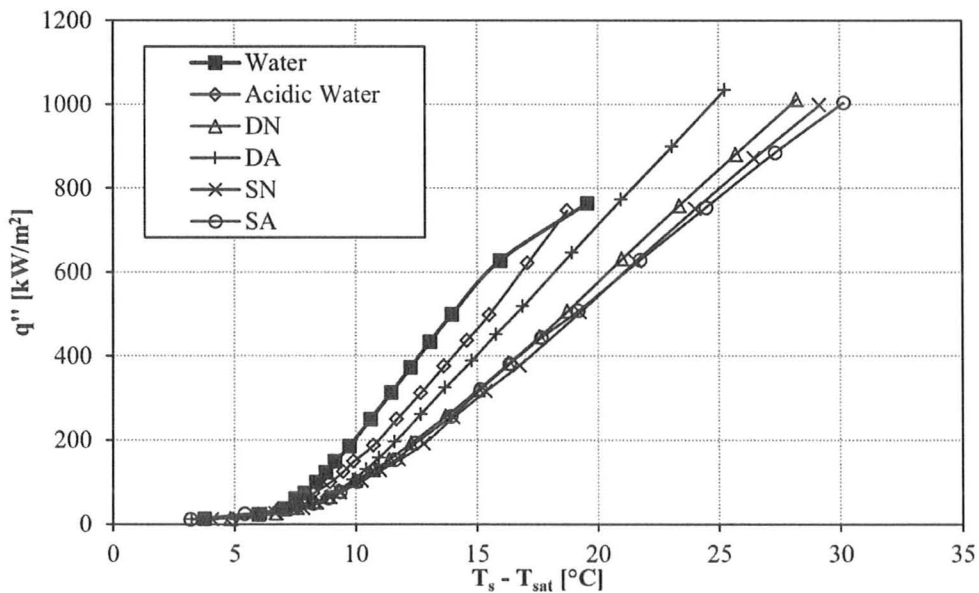


Figure 4.1: Boiling curves obtained during experiments of Stage 1

The curve from the water boiling experiment could be obtained up to a heat flux of about  $800 \text{ kW/m}^2$  only. CHF for water occurred at a higher heat flux. However, for the nanofluids CHF did not occur up to  $1000 \text{ kW/m}^2$ . It can be seen from Figure 4.1 that the heat flux for nanofluids is increasing steadily as well as surface superheat, and there is no indication that the nanofluids curves are approaching CHF. This agrees with previous findings regarding CHF in the literature.

#### 4.1.1 Effect of Stability

In order to quantify the effect of the nanofluids stability on the HTC, the heat flux for the different fluids was evaluated at a superheat of  $15 \text{ }^\circ\text{C}$ . The nucleate boiling regime was established at  $15 \text{ }^\circ\text{C}$  and, for this reason, the enhancement or deterioration was evaluated at this value of surface superheat. The deterioration in HTC was about 50 % for the *suspension* nanofluids at both pH values, and the *dry* nanofluids at a pH of 6.5 (cases SN, SA and DN). The *dry* nanofluid at an acidic pH of 5 (case DA) showed a higher HTC than the other nanofluids; the HTC was deteriorated by 30 %. This shows that the HTC for the DA case was about 25 – 35 % higher than the other nanofluids.

The effect of changing the pH value of pure water was investigated. Acidic water at pH = 5 was boiled in the same manner the nanofluids were. The HTC deteriorated by 20 %. It is suspected that this deterioration is due to a change in surface tension and thermal conductivity. Hydrochloric acid has a surface tension higher and lower thermal

conductivity than water. The change in those two parameters will reduce the HTC, according to the Rohsenow correlation.

The pH value has a significant effect on the HTC of the *dry* nanofluids. Although the pH reduction is shown to reduce the HTC of the base fluid alone, it has an opposite effect on the DA nanofluid. This can be explained by an enhancement in the stability of the nanofluid which overshadows the surface tension change of the base fluid. Stronger charges between the nanoparticles make them suspend better and enhance the thermal conductivity of the nanofluid. It appears that the pH value has no significant effect on the HTC of the *suspension* nanofluid; the SA and SN nanofluids curves are very close to one another.

Visual inspection of the surface after the experiments showed a deposition layer of nanoparticles on the surface which was observed by the naked eye. The layer was not possible to wash away with a water jet. It could only be washed away with scrubbing action under a water jet. It is assumed that the layer of nanoparticles creates an insulation layer on the boiling surface which hinders the liquid from accessing the surface cavities and the nucleation sites. This deposition layer was found to be thicker for the neutral pH nanofluids (DN and SN) than the acidic pH nanofluids (DA and SA). As shown in Table 4.1, the surface-roughness measurements for the neutral pH nanofluids are about an order of magnitude higher than the acidic pH nanofluids. This observation is also clear in 3D profiles in Figure 4.2 which shows the 3D profiles of the surfaces after the nanofluids experiments in this stage; the surface profiles for the acidic pH nanofluids are more uneven. The more acidic, and therefore more stable, nanofluids have stronger charges

- Surface-roughness value of each image is shown below
- Black areas in the 3D profiles indicate missing data points that could not be captured by the interferometer

Legend: S = *Suspension*                      N = Neutral (pH = 6.5)  
 D = *Dry*    A = Acidic (pH = 5)

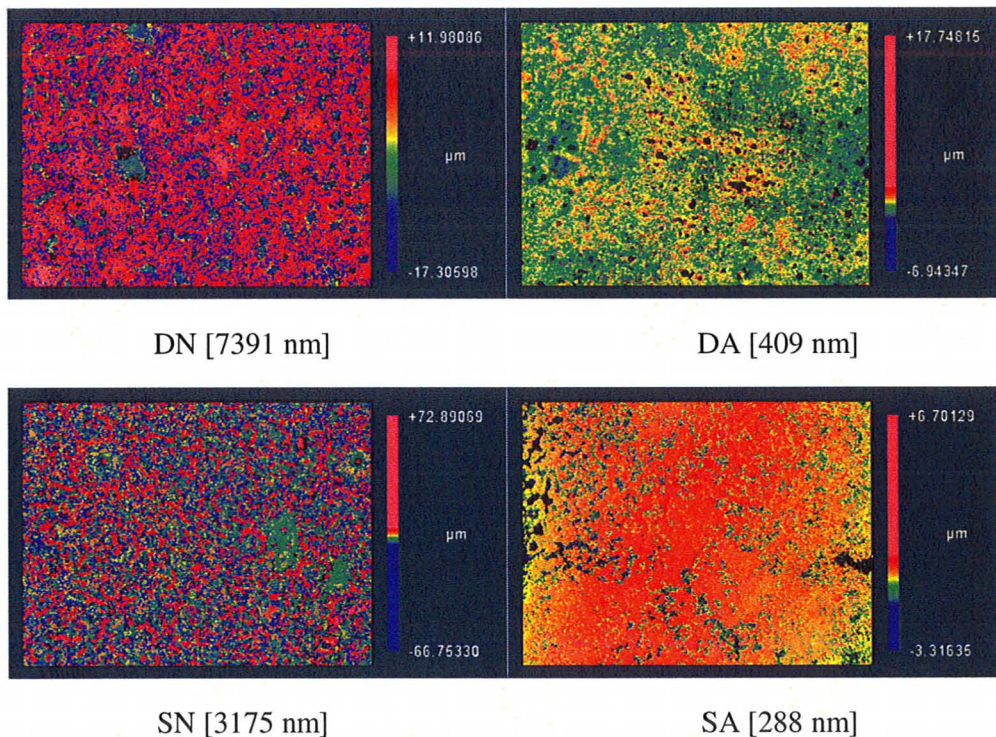


Figure 4.2: 3D images of surfaces after Stage 1 experiments

which keep the particles in suspension and do not settle on the surface as easily as the neutral nanofluids.

DLS measurements were carried out for all the nanofluids used in this stage of experiments. The effective particle size of the nanofluids from the DLS tests is also shown in Table 4.1. The particle size distribution curves of the nanofluids are shown in Figure 4.3. The acidic nanofluids (pH = 5) have a smaller effective particle size than the

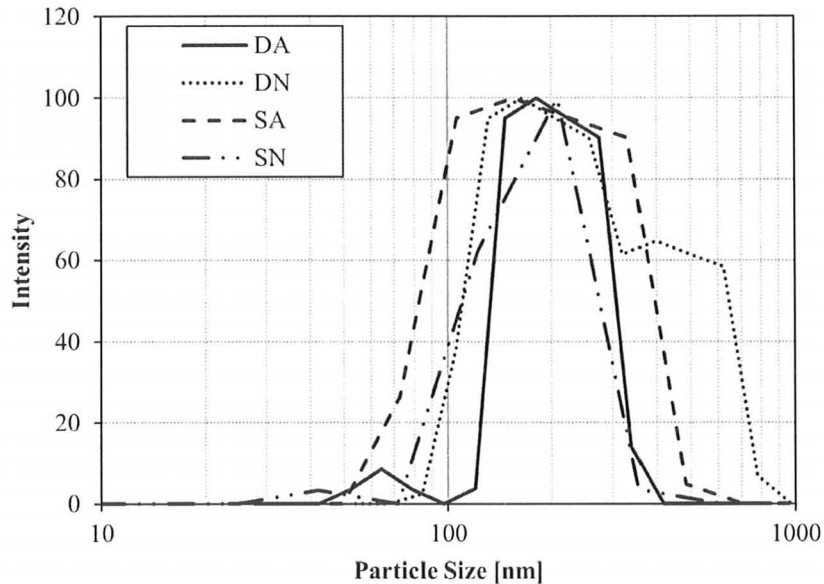


Figure 4.3: Particle size distribution for nanofluids used in Stage 1 experiments

nanofluids neutral ( $\text{pH} = 6.5$ ). The smaller particle size can be attributed to the charges on the particles which reduce the chance for the particles to stick together and form larger agglomerates due to the Van der Waals forces [3].

#### 4.1.2 Effect of Preparation Method

It appears from the measurements of the effective particle size and average surface-roughness that the *suspension* nanofluids are more stable than the *dry* nanofluids. The reduction in surface-roughness due to the reduction in pH is less significant for the *suspension* nanofluids than the *dry* nanofluids. The  $R_a$  was reduced from 6970 to 430 nm for the *dry* nanofluids, which is 6540 nm reduction as the pH is lowered from 6.5 to 5.

The  $Ra$  for the *suspension* nanofluids decreased from 3120 to 360 nm, which is only 2760 nm for the same reduction in pH.

It should be noted here that the post boiling surface-roughness measurement for the DN case was more than double the SN case, however, the HTC of these nanofluids were very similar. The results in Stage 3 experiments will show that surface-roughness measurements alone are insufficient to quantify the change in surface condition. The uniformity of the deposition is a significant factor that will affect the surface condition, which is assessed by visual observation of the overall surface. Assessing the uniformity of the deposition was carried out in Stage 3 experiments only. Therefore, it is speculated that the similarity in HTC between the DN and SN cases is due to similar uniformity in deposition.

The change in particle size also shows that the *suspension* nanofluids appear to be more stable than the *dry* nanofluids; the *suspension* nanofluids had a smaller reduction in effective particle size than the *dry* nanofluids as the pH was lowered from 6.5 to 5. The effective particle size was reduced from 170 to 150 nm (20 nm reduction) for the *suspension* nanofluids, and from 215 to 180 nm (35 nm reduction) for the *dry* nanofluids as the pH was lowered from 6.5 to 5. This shows that the stability has a less significant effect on the particle size for the *suspension* nanofluids than the *dry* nanofluids.

It was expected in this study that using nanofluids prepared from ready-made suspensions would enhance the heat transfer in accordance to results reported in [12]. The experiments showed that preparation method is not the critical parameter that affects the

enhancement or deterioration of HTC of nanofluids. Moreover, the enhancement in HTC found in [12] is in contradiction with the deterioration was found in this study due to the difference in the experimental conditions between the two studies. A 0.4 mm NiCr wire of unknown surface-roughness and silica nanoparticles were used in [12] whereas a flat copper surface of a mirror-finish grade and alumina nanoparticles were used in this study.

#### 4.2 Combined Effects of Concentration and Stability (Stage 2)

As mentioned in section 3.4.2, three concentrations of nanofluids were investigated in this stage. Each concentration was studied at a neutral pH of 6.5 and a more acidic pH of 5. Some scientists who found the HTC of nanofluids to be enhanced have attributed this enhancement to the improved stability of their nanofluids. However, no previous work has been carried out with nanofluids of different pH values using the same experimental setup and conditions. This stage investigates the effect of the enhanced stability at different concentrations. Since stability was found to have a more significant effect on *dry* nanofluids, all the nanofluids in Stage 2 were prepared from dry particles.

The boiling curves for the neutral pH nanofluids are shown in Figure 4.4 and the curves for the acidic pH nanofluids are shown in Figure 4.5. The surface-roughness measurements after each boiling experiment are shown in Figure 4.6. The surface-roughness measurements of these experiments were more scattered than in Stage 1, therefore, the average surface-roughness in Figure 4.6 is expressed in terms of the

average value and the standard deviation. The 3D profiles of the post-boiling surfaces are shown in Figure 4.7. Table 4.2 shows the results of the experiments carried out during Stage 2.

The results from Stage 2 experiments show a mix of results regarding the HTC. Enhancement, deterioration and no change in HTC took place for the nanofluids at different concentrations and pH values. CHF for water occurred at heat flux lower than for the nanofluids, therefore, the nanofluids curves could be obtained at higher heat fluxes.

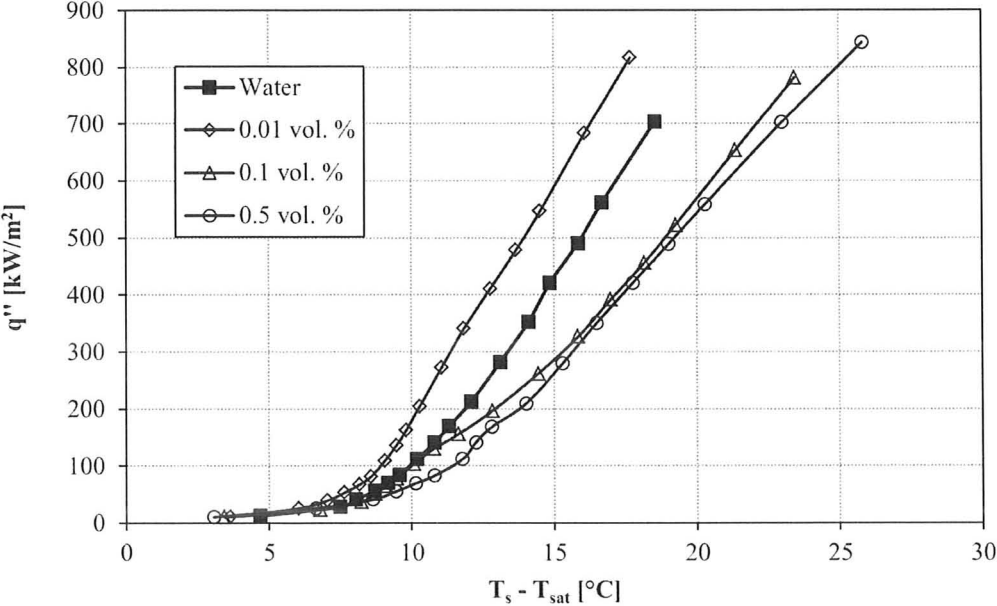


Figure 4.4: Boiling curves for neutral nanofluids (pH = 6.5)

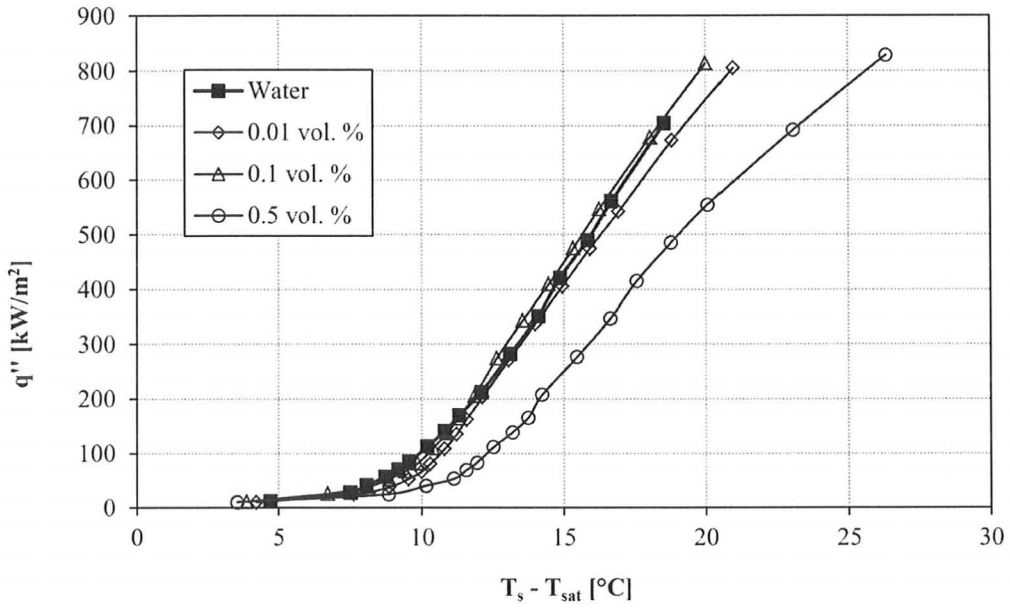


Figure 4.5: Boiling curves for acidic nanofluids (pH = 5)

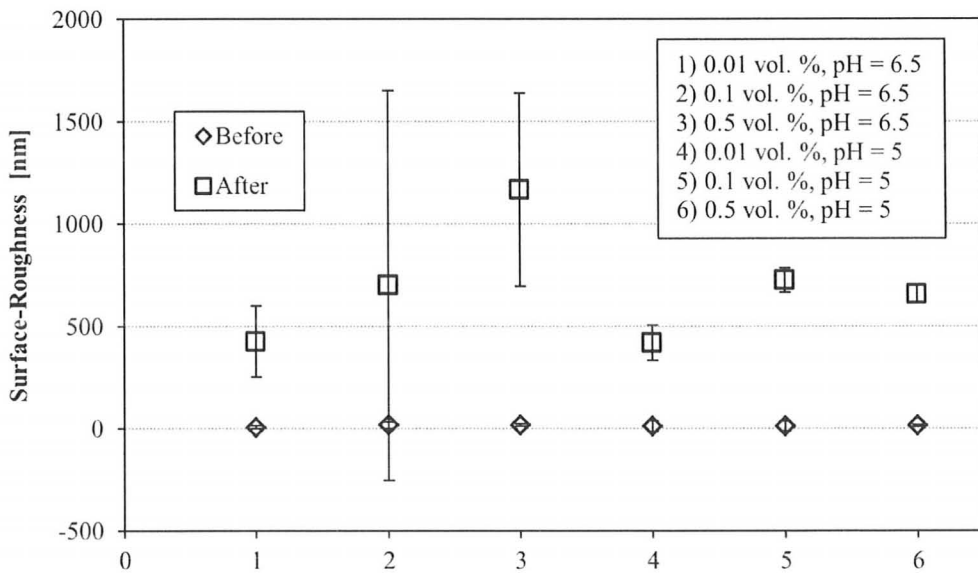


Figure 4.6: Surface-roughness measurements for Stage 2 experiments

- Surface-roughness value of each image is shown below
- Black areas in the 3D profiles indicate missing data points that could not be captured by the interferometer

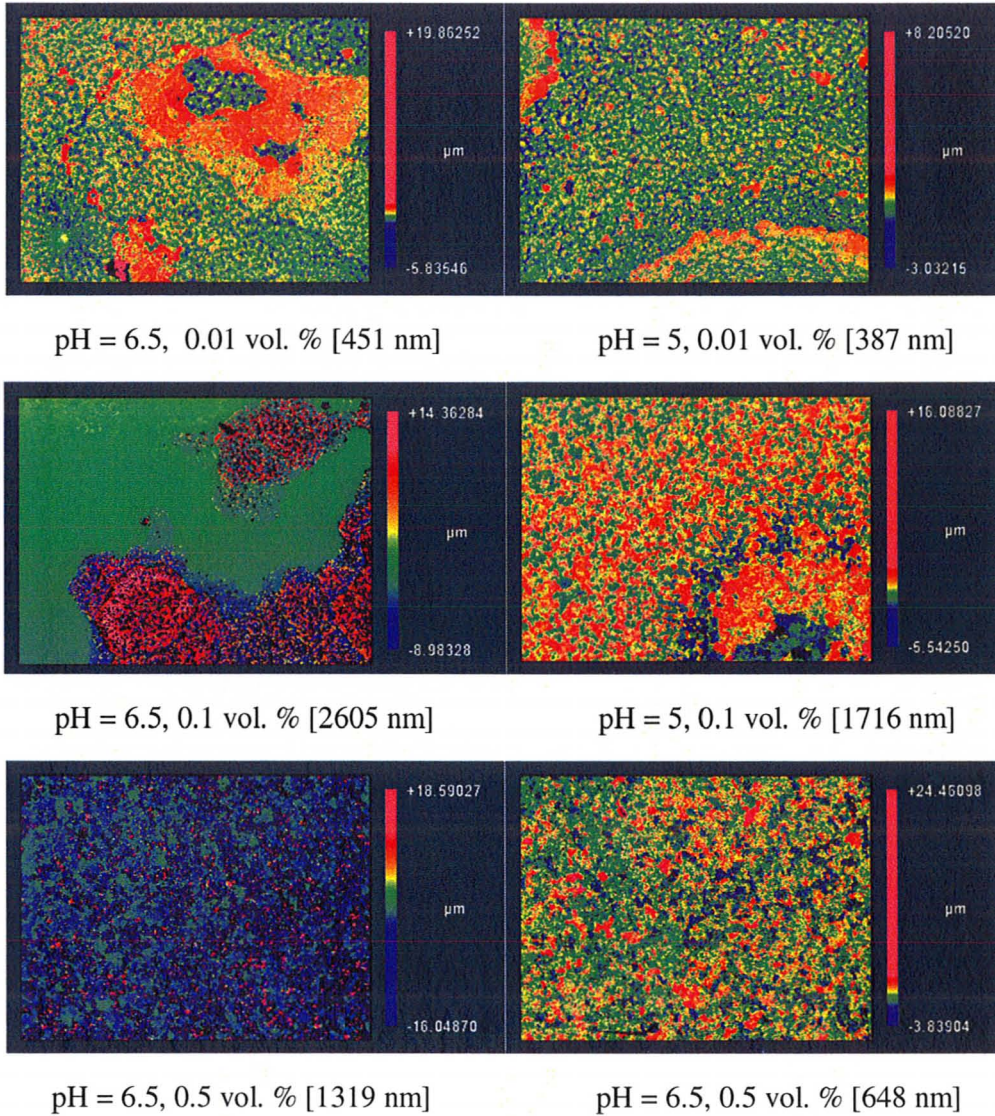


Figure 4.7: 3D images of surfaces after Stage 2 experiments

Table 4.2: Results of experiments carried out during Stage 2

Concentration	pH Value	HTC % of water @ 15°C	Average post-boiling surface-roughness [nm]
0.01	Neutral (6.5)	141	426
0.1	Neutral (6.5)	71	700
0.5	Neutral (6.5)	63	1166
0.01	Acidic (5)	98	420
0.1	Acidic (5)	106	724
0.5	Acidic (5)	59	656

#### 4.2.1 Effect of Concentration

An enhancement in HTC occurred with 0.01 vol. % nanofluid at a neutral pH of 6.5. About 40 % enhancement in HTC was recorded at 15 °C superheat. Deterioration in HTC occurred when increasing the concentration to 0.1 and 0.5 vol. %. The deterioration for the 0.1 and 0.5 vol. % nanofluids was very similar and was about 30 – 40 % at 15 °C superheat. The enhancement at the low concentration of 0.01 vol. % can be attributed to the fact that less deposition took place on the surface compared to the higher concentrations. The  $Ra$  measurement was about 425 nm for the 0.01 vol. % nanofluid, whereas a much larger deposition resulting in  $Ra$  of 700 and 1150 nm recorded for the 0.1 and 0.5 vol. %, respectively.

The results for the acidic nanofluids at pH = 5 show that the 0.01 and 0.1 vol. % concentrations had a very similar HTC to that of pure water. The HTC of the 0.5 vol. % concentration deteriorated by about 40 % at 15 °C superheat. The results from the experiments carried out in this stage are discussed further in section 4.2.2. However, a

general statement can be made regarding the effect of concentration for the nanofluids at both pH values; increasing the concentration either decreased the HTC or had a little effect. This behaviour of HTC with concentration agrees with [4, 7-8, 14-15], but disagrees with [3, 13, 19].

#### 4.2.2 Effect of Stability

To isolate the effect of stability from the effect of concentration, results shown in Figures 4.4 and 4.5 have been reconstructed into Figures 4.8 – 4.10. Figure 4.8 shows that reducing the pH of the 0.01 vol. % nanofluid resulted in a decrease in the HTC. This effect opposes expectations where the stability is expected to increase the HTC of the nanofluid. This effect can be explained as reducing the pH was found to deteriorate the HTC of pure water due to surface tension change, as previously explained in the findings of Stage 1. An acidic water experiment at a pH of 5 was carried out in this stage and the boiling curve is also shown in Figure 4.8. The HTC for the acidic water experiment deteriorated by about 40 % at 15 °C superheat. At a low concentration, the effect of the pH on the base fluid properties is more dominant than the effect of the nanoparticles. Both pH values of the 0.01 vol. % concentration resulted in very similar average surface-roughness after the experiments; 425 and 420 nm. This shows that the stability of the nanofluid was not affected due to the pH change, and the change in HTC is due to the change in the base fluid properties.

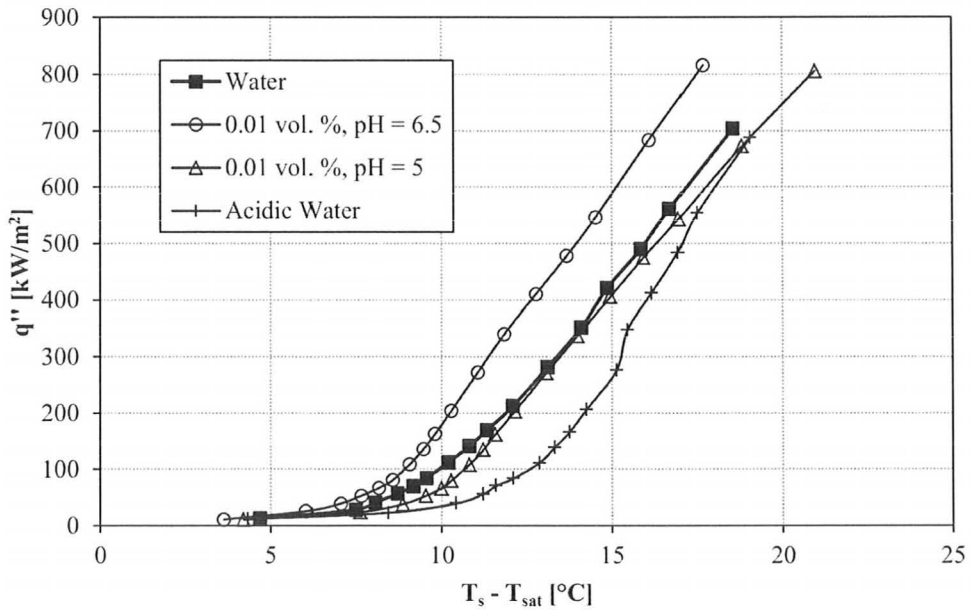


Figure 4.8: Boiling curves for Stage 2 experiments at 0.01 vol. % concentration

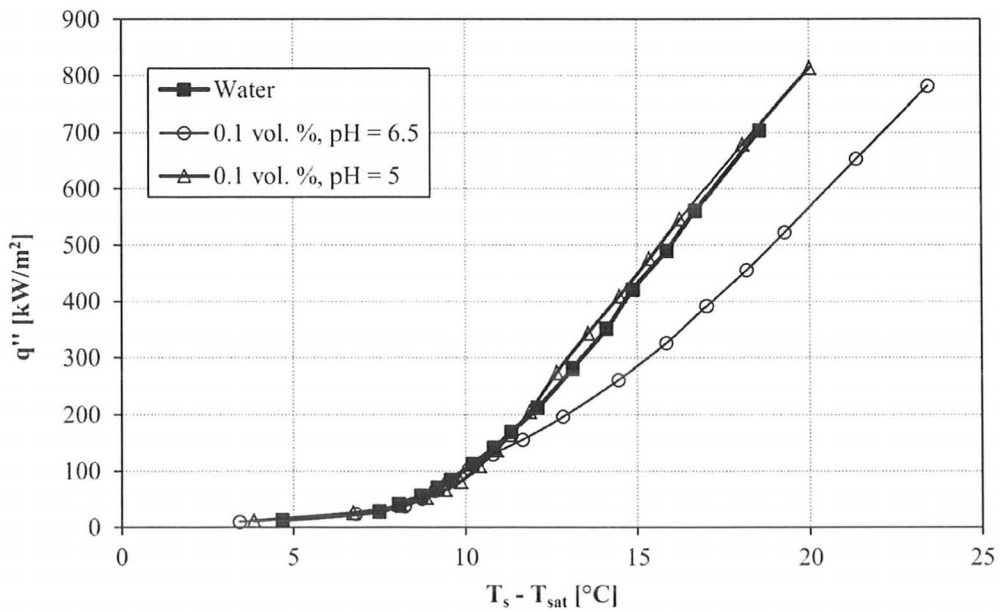


Figure 4.9: Boiling curves for Stage 2 experiments at 0.1 vol. % concentration

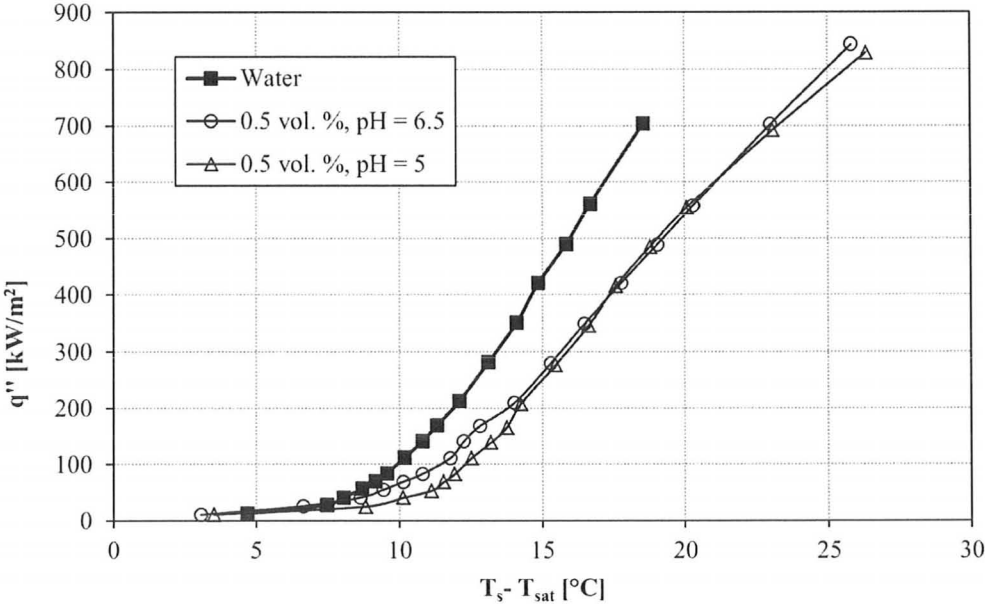


Figure 4.10: Boiling curves for Stage 2 experiments at 0.5 vol. % concentration

The results for the 0.1 vol. % nanofluid are similar to those found in Stage 1 experiments. The HTC for the 0.1 vol. % nanofluid increased from a 30 % deterioration to being almost the same as water when the pH was reduced from 6.5 to 5. The pH reduction enhanced the stability of the nanofluid which has caused less deposition to take place on the surface. Although the average surface-roughness measurements are very similar, the standard deviation for the neutral nanofluid is higher, which indicates that the deposition was heavier at certain locations on the surface. This result shows that the effect of nanoparticles stability due to the pH reduction at 0.1 vol. % is more dominant than the effect of the acid on the base fluid properties. The increase in HTC at 0.1 vol. % with pH reduction is attributed to the less deposition of nanoparticles on the surface, as well as the enhanced thermal conductivity of the nanofluid at the lower pH.

The 0.5 vol. % nanofluid experienced almost no change in HTC with pH change. Both pH = 6.5 and pH = 5 nanofluids had an almost equal deterioration in HTC of about 40 %. The pH = 5 nanofluid has better stability as reflected in the surface-roughness measurements. The pH = 6.5 nanofluid resulted in an average surface-roughness measurement of about 1150 nm, whereas the pH = 5 nanofluid resulted in about 650 nm. The enhanced stability of the nanofluid and the change in base fluid properties due to the pH change did not affect HTC at 0.5 vol. % concentration. The deposition of nanoparticles on the surface at 0.5 vol. % concentration was the dominant factor that governed the HTC.

#### 4.2.3 Nanoparticle Deposition Pattern

The nanoparticle deposition pattern after the boiling experiment of the 0.01 vol. % concentration at pH = 6.5 was examined closely with the naked eye. Unfortunately at this stage of the research photographs of the surface after the experiments were not taken. The observed pattern could be described as a white layer covering the entire surface with some heavier deposition spots than the rest of the surface. These spots were round and are estimated to be 1 – 2 mm in diameter. It is suspected that these spots are locations of active nucleation sites. One of these spots was scanned using the Zygo interferometer. The pattern is shown in Figure 4.11 in black and white. Printing the pattern in color does not show the precise details of the figure.

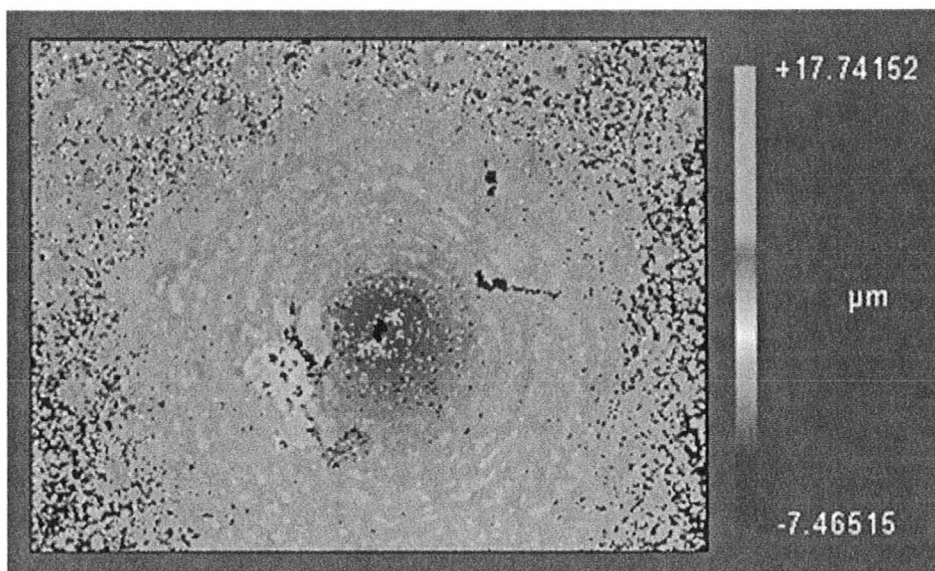


*Figure 4.11: Nanoparticle deposition pattern at a heavy deposition spot on the surface after 0.01 vol. %, pH = 6.5 nanofluid ( $R_a = 1332$  nm)*

Figure 4.11 shows a concentric deposition pattern of nanoparticles. This shows that the deposition of nanoparticles took place during bubble generation. The pattern indicates that the nanoparticles deposit as the vapour bubble grows from its nucleation site in a spherical manner. Microlayer evaporation during bubble growth and departure is the mechanism responsible for the deposition of nanoparticles on the surface. The nanoparticles come out of suspension as the microlayer evaporates, and adhere to the surface as they are in a temporarily dry atmosphere before the bubble departs. The average surface-roughness measurement of that spot was 1132 nm, which is much higher than the average 420 nm recorded for the surface after boiling the 0.01 vol. % nanofluid at a pH of 6.5. The pattern also shows that the deposition occurs at different diameters

from the centre of the nucleation site. This may be due to the bubble becoming smaller in diameter as the deposition of nanoparticles makes the nucleation site smaller.

### **4.3 Effect of Concentration and Prolonged Boiling Duration on Nanoparticle Deposition (Stage 3)**

The past two stages of experiments revealed that nanoparticle deposition is an important phenomenon that occurs when boiling nanofluids. The extent of the deposition depends on the method of nanofluid preparation, concentration and stability. The boiling HTC of any fluid is dependent on the fluid property as well as the surface condition of the boiling surface. In past experiments, fluid properties were changed by changing the nanofluid concentration used, and the deposition changed subsequently. The experiments carried out in Stage 3 aims at isolating the effect of nanoparticle deposition from that of the fluid property.

Three nanofluids of different concentrations 0.01, 0.1 and 0.5 vol. % were boiled. Pure water was boiled after the nanofluid boiling experiments. The objective was to keep fluid property known and constant while examining the effect of surface condition changes due to nanoparticle deposition. High speed videos were taken at this stage of experiments. The duration of the nanofluids boiling experiments was extended to study the effect of experiment duration on nanoparticle deposition and on the surface temperature. The duration of Stage 3 experiments was increased from 45 minutes in the case of Stage 1 and 2 to 105 minutes. The initial average surface-roughness for Stage 3 remained the same as Stage 2 and was about 50 nm. The nanofluids used in Stage 3 were

prepared from dry particles and were at a neutral pH of 6.5. The nanofluid boiling curves obtained from Stage 3 experiments are shown in Figure 4.12. The results of the experiments carried out in Stage 3 are shown in Table 4.3.

The general trend of the nanofluid boiling curves obtained in Stage 3 is similar to that found in Stage 2 experiments for the neutral pH nanofluids. The 0.01 vol. % nanofluid showed an enhancement in HTC of 35 % at 15 °C superheat. The 0.1 vol. % had a very similar HTC to water and the 0.5 vol. % had deteriorated HTC by 45 %. The decrease in HTC with increasing concentration is consistent with results of Stage 2 experiments.

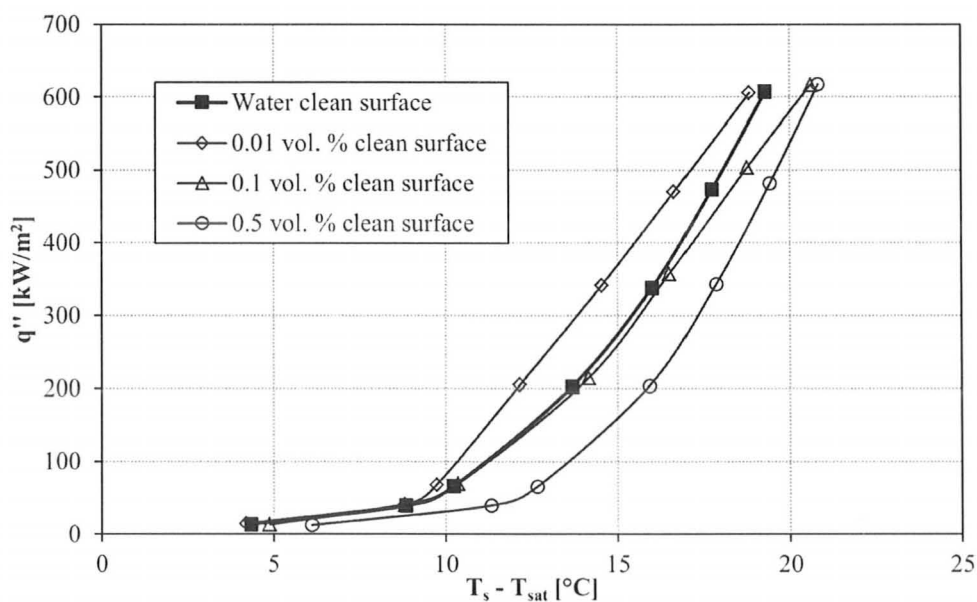


Figure 4.12: Nanofluids boiling curves for a clean surface in Stage 3 experiments

Table 4.3: Results of experiments carried out during Stage 3

Fluid	Surface Condition	HTC % of water	HTC evaluated at [°C]
Nanofluid 0.01 vol. %	Clean	135	15
Nanofluid 0.1 vol. %	Clean	95	15
Nanofluid 0.5 vol. %	Clean	55	15
Water	NPD 0.01 vol. %	19	18
Water	NPD 0.1 vol. %	18	18
Water	NPD 0.5 vol. %	20	18

The water boiling curves on a nanoparticle-deposited (NPD) surface are shown in Figure 4.13. It can be seen from the figure that the HTC of boiling water has severely deteriorated due to nanoparticle deposition. There is also a significant shift in the temperature at which the onset of nucleate boiling (ONB) takes place. ONB took place at

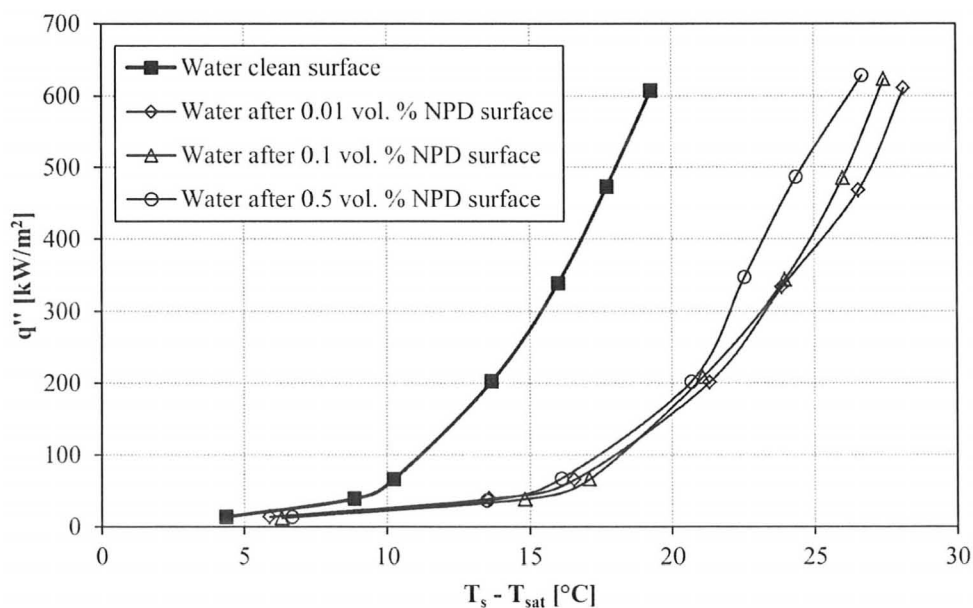


Figure 4.13: Water boiling curves for a nanoparticle-deposited (NPD) surface in Stage 3 experiments

about 9 °C superheat for the clean surface and about 16 °C for the NPD surfaces. The HTC has deteriorated by about 80 % at 18 °C superheat. Figure 4.14 shows the boiling curve for the 0.5 vol. % nanofluid on a clean surface, water on a 0.5 vol. % NPD surface as well as water on a clean surface. The drop in heat transfer of boiling water on the 0.5 vol. % NPD surface from the 0.5 vol. % nanofluid on a clean surface is expected as water has a lower thermal conductivity and higher surface tension than the nanofluids, which will result in a lower HTC.

Wettability has been reported to be enhanced for NPD surfaces using a water droplet in [18]. Therefore, water is going to wet the surface better for the 0.5 vol. % NPD surface than the clean surface. With a wetted surface the nucleation sites are more likely

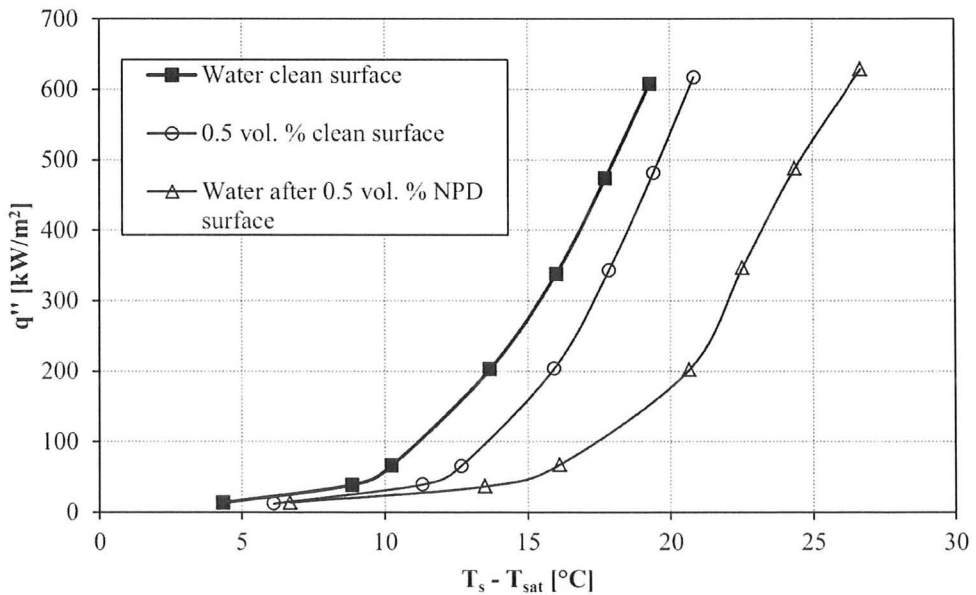


Figure 4.14: Comparison between boiling water on a clean surface, 0.5 vol. % nanofluid on a clean surface and water on a 0.5 vol. % NPD surface in Stage 3 experiments

to be flooded and become deactivated, which may be another mechanism that deteriorates the HTC for the NPD surfaces.

Moreover, the nanoparticle layer on the surface will hinder liquid access to the surface and reduce the number of active nucleation sites. This reduction in the number of active nucleation sites will cause the deterioration in HTC, as well as the higher temperature required for ONB to take place. Figure 4.13 shows that the HTC for the water boiling curve for the 0.5 vol. % NPD surface was higher than the NPD surfaces at other concentrations at a surface superheat higher than 21 °C. This is contrary to expectations as higher concentration nanofluids are expected to deposit more nanoparticles on the surface and result in more deterioration in HTC. This result is discussed in more detail in section 4.3.2.

Deterioration in HTC shown in Figure 4.13 might be due to deactivation of nucleation sites due to flooding. An experiment was carried out to quantify this effect. Nucleation sites are cavities on the boiling surface with entrapped gases or vapour. The gases in the cavities will slowly dissolve and get carried away with each bubble during boiling. Over a few minutes or hours, the cavities will be free of gas and become filled with vapour. When the boiling is stopped and the surface cools down, the entrapped vapour will condense and flood the nucleation site and the site becomes deactivated [1]. The deterioration in HTC in the water boiling experiments on nanoparticle-deposited surfaces may be partly attributed to nanoparticle deposition and partly due to the flooding of nucleation sites.

A water boiling experiment was carried out in a similar manner to the nanofluid boiling experiment to investigate the effect of flooding the nucleation sites. The water was drained out and fresh cold water was used in the vessel. Water was chosen as opposed to a nanofluid as boiling a nanofluid would deposit nanoparticles on the surface. The surface would not be exposed to air and was covered with water at all times. The results are shown in Figure 4.15.

*Water 1* refers to the first water boiling experiment, and *Water 2* refers to the second boiling experiment. The series *Water* represents the original water boiling curve used to compare against the nanofluid curves. It is clear that there is an insignificant change in the heat transfer between the first and second boiling experiments. This indicates that the flooding of nucleation sites has little effect on the HTC. Therefore, the

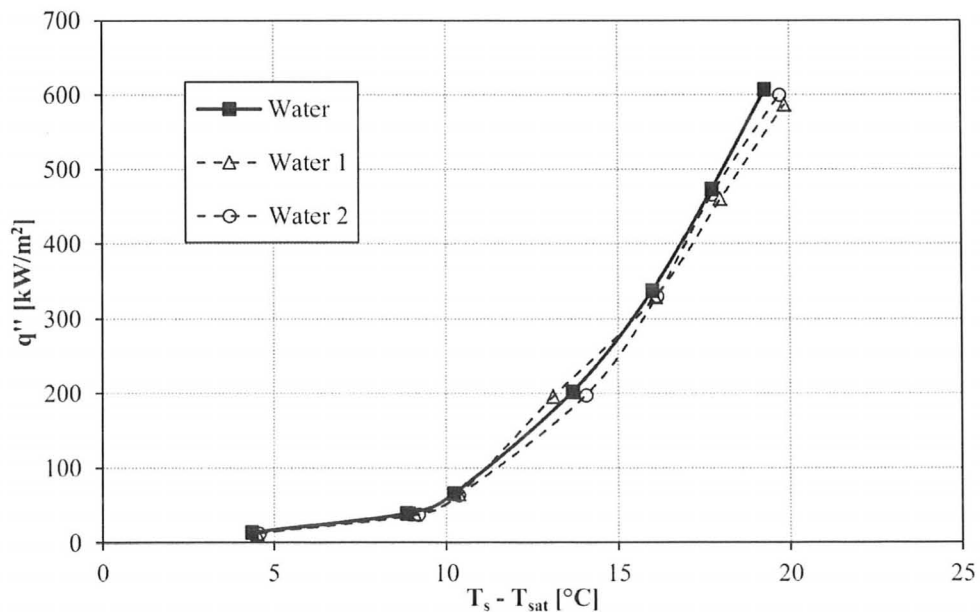
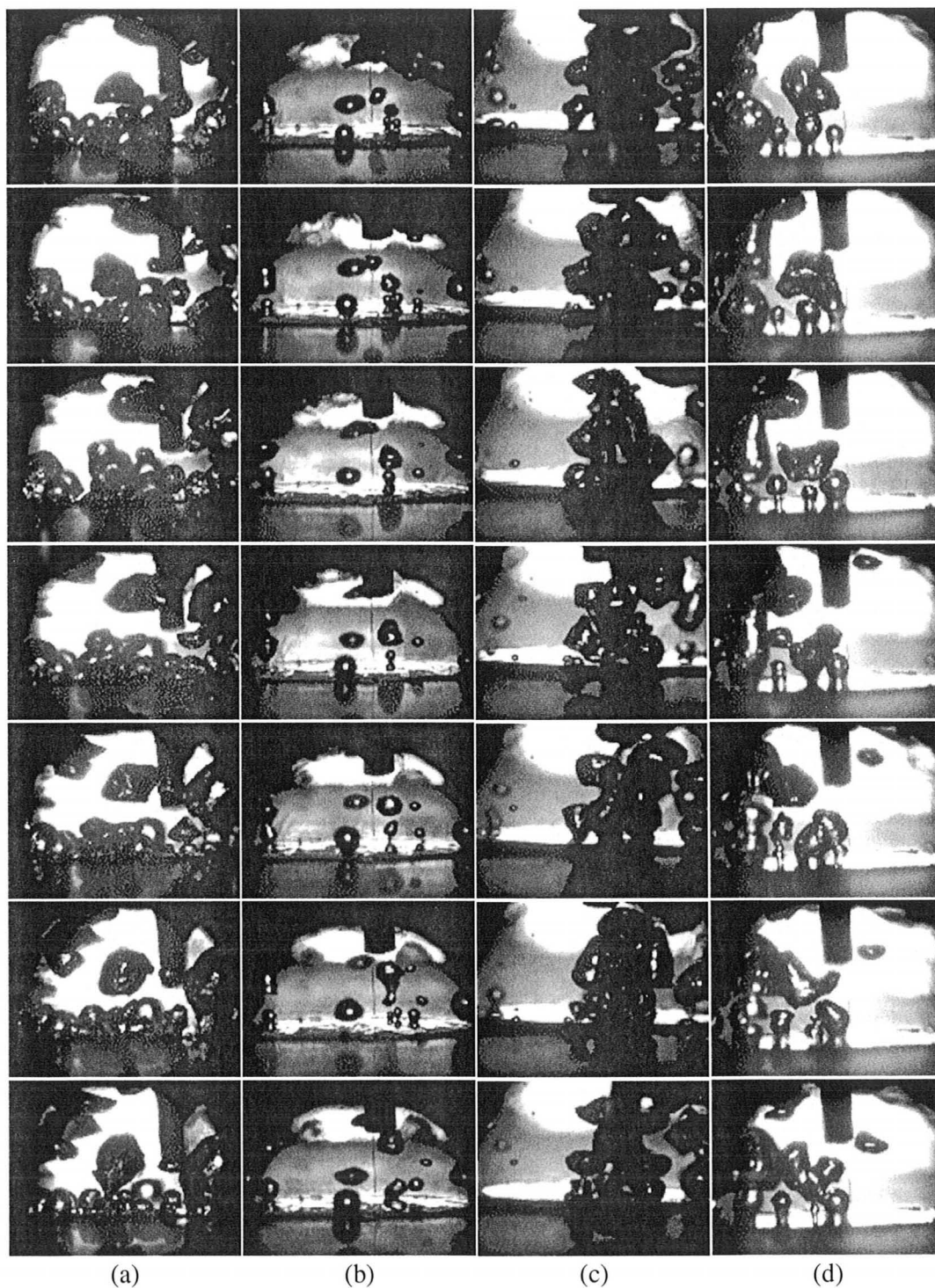


Figure 4.15: Results of repeated water boiling experiments on a clean surface

deterioration in HTC for the water boiling experiments shown in Figure 4.13 on the nanoparticle-deposited surface cannot be attributed to flooding of nucleation sites; it is rather due to the effect of the nanoparticle layer deposited on the surface. It can also be seen in Figure 4.15 that there is good repeatability from one experiment to another.

Images captured during water boiling experiments on the clean and nanoparticle-deposited surfaces are shown in Figure 4.16. The images were captured at a rate of 1000 frames per second. The images for the clean surface in Figure 4.16 (a) show that the surface is not visible due to bubbles formed over its entire area. There are enough active nucleation sites to form bubbles covering the entire surface. The bubble formation for the nanoparticle-deposited surface took place at a fraction of the surface area. The images in Figure 4.16 (b), (c) and (d) show that the number of nucleation sites for the nanoparticle deposited surfaces is reduced. There are areas on the surface that have no bubble generation activity. Viewing the surface from the side did not permit the assessment of the difference in the number of nucleation sites for the nanoparticle deposited-surfaces. Also, bubble coalescence made it difficult to count individual nucleation sites. Therefore, nucleation site analysis could not be carried out.



*Figure 4.16: Images 1 ms apart of water boiling from (a) clean surface (b) 0.01 vol. % (c) 0.1 vol. % and (d) 0.5 vol. % nanoparticle-deposited surface*

#### 4.3.1 Assessment of Surface Factor Change and Nanofluid Properties using the Rohsenow Correlation

The Rohsenow correlation [1] has been used to predict the boiling heat transfer for nanofluids. The correlation uses fluid properties and a surface factor to predict the heat flux at a specific surface temperature. An analysis and discussion of the effect of surface factor and the fluid properties on the pool boiling of nanofluids has been carried in this section out using the Rohsenow correlation. The Rohsenow correlation is shown again here in Equation (4.1).

$$q'' = \mu h_{lv} \left[ \frac{\sigma}{g(\rho_l - \rho_v)} \right]^{-1/2} Pr^{-s/r} \left[ \frac{C_p}{h_{lv} C_{sf}} (T_s - T_{sat}) \right]^{1/r} \quad (4.1)$$

The surface factor  $C_{sf}$  in the Rohsenow correlation represents the surface condition. This factor changes with changing surface-roughness and liquid/surface combination. The fluid properties that affect the heat transfer in the Rohsenow correlation are: latent heat of vaporisation ( $h_{lv}$ ), density ( $\rho$ ), specific heat capacity ( $C_{pl}$ ), viscosity ( $\mu$ ), surface tension ( $\sigma$ ) and thermal conductivity ( $k$ ).  $h_{lv}$  of nanofluids is assumed to be equal to that of water since the nanoparticles do not evaporate during boiling. At 0.5 vol. % concentration,  $\rho$  is 1.3 % higher than water, and  $C_{pl}$  is lower by 1.5 % [15]. Change in  $\mu$  was found minimal in [4, 7-8]. Therefore  $\rho$ ,  $C_{pl}$  and  $\mu$  in the Rohsenow correlation are assumed to be equal to water.

Fluid properties that have been found change significantly are  $k$  and  $\sigma$ . Measurements in [18] revealed a 15 % reduction in  $\sigma$  when adding 0.5 vol. %

nanoparticles to water. Measurements of  $k$  reported in [21] showed a 22 – 28 % enhancement for the 0.5 vol. % nanofluids. Therefore, the heat flux predicted by the Rohsenow correlation is expected to vary according to Equation (4.2).

$$\left. \frac{q''_{NF}}{q''_W} \right)_{T_s - T_{sat} = const.} = \frac{\Delta k^{s/r}}{\sqrt{\Delta \sigma}} \cdot \frac{1}{\Delta C_{sf}^{1/r}} \quad (4.2)$$

It is assumed that the constants  $r$  and  $s$  remain unchanged ( $r = 0.33$  and  $s = 1$ ).  $C_{sf}$  can be determined using curve fitting of the water boiling curves on the nanoparticle-deposited surfaces. The curve fitting tool in MATLAB was used to determine  $C_{sf}$ . Once  $C_{sf}$  is determined, its value is used to fit the nanofluid boiling curves and determine the change in fluid properties. The change in thermal conductivity and surface tension reported in the literature are expected to cause an increase in the HTC of nanofluids. Therefore, the parameter  $k^{s/r}/\sqrt{\sigma}$  has been treated as a single parameter.

The surface factor, fluid property parameter and the  $R^2$  values for the fits are shown in Table 4.4. In order to check that this analysis to predict the change in fluid properties is valid, it was carried out on results of the pure water boiling experiment on a clean surface. At atmospheric pressure water has  $k = 0.679$  W/m°C and  $\sigma = 58.91 \times 10^{-3}$  N/m, therefore, the theoretical value of  $k^{s/r}/\sqrt{\sigma}$  for water should be 1.27 and the fitted value was 1.35, which is within 6 %.

The results in Table 4.4 show that the values of  $C_{sf}$  for the nanoparticle-deposited surfaces are higher than the clean surface, which give a lower HTC, and meets

Table 4.4: Surface factor and fluid properties analysis using the Rohsenow correlation

Concentration	$C_{sf}$	$R^2$	$k^{s/r}/\sqrt{\sigma}$	$R^2$
Water (Clean surface)	0.01593	0.9964	1.35	0.9964
0.01 vol. %	0.02372	0.967	5.219	0.9671
0.1 vol. %	0.02314	0.9435	3.664	0.9888
0.5 vol. %	0.02211	0.9431	2.771	0.9543

expectations. However, the surface factor is shown to decrease with higher concentrations, which is contrary to expectations. It is expected that the higher concentration nanofluids will result in a stronger deposition and give a higher surface factor. As a result, the parameter  $k^{s/r}/\sqrt{\sigma}$  decreased for higher concentrations of nanofluids. The parameter  $k^{s/r}/\sqrt{\sigma}$  should increase with higher concentrations;  $k$  increases while  $\sigma$  decreases with higher concentrations. Although the parameter  $k^{s/r}/\sqrt{\sigma}$  for the nanofluids is higher than water, its decrease with increasing concentration is disagrees with measurements reported in [18, 21]. The discussion in the following section (section 4.3.2) provides an explanation to this contradiction.

#### 4.3.2 Examination of Nanoparticle Deposition

The nanoparticle deposition phenomenon was examined in order to explain the controversy in the surface factor determined and discussed in the previous section. Surface-roughness measurements have been carried out for the nanoparticle-deposited surfaces. Results are shown in Figure 4.17. The surface-roughness for the 0.1 vol. % nanofluid was much higher than for the 0.01 vol. %. However, the highest concentration

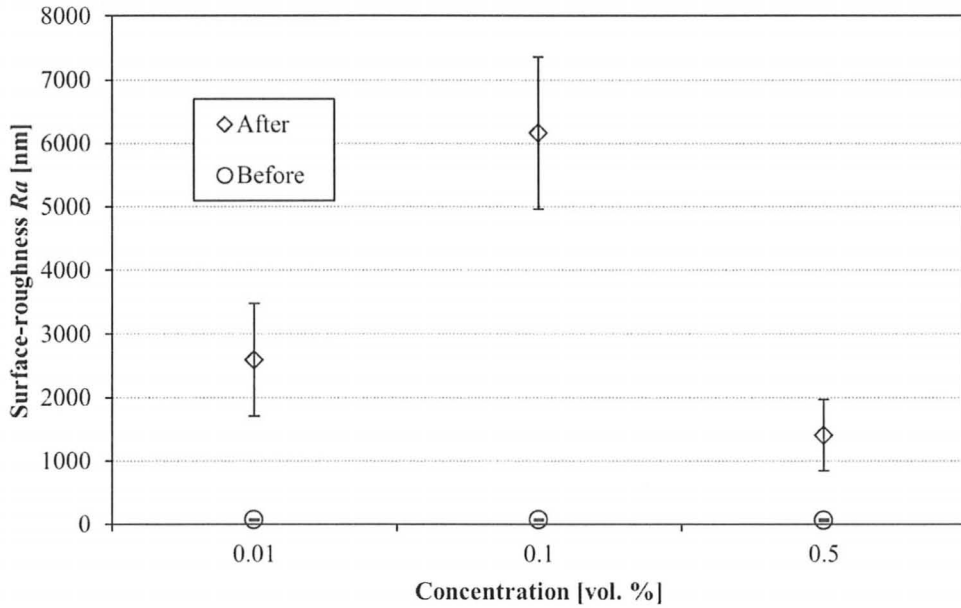


Figure 4.17: Surface-roughness measurements for Stage 3 experiments

nanofluid gave the lowest surface-roughness. This low surface-roughness measurement for the high concentrations may explain why the water boiling on the 0.5 vol. % NPD surface gave a higher HTC at a surface superheat higher than 21 °C. However, the overall trend of the surface-roughness findings does not explain the controversy found in  $C_{sf}$  shown in Table 4.4.

Photographs of the boiling surfaces were taken after the experiments to visually observe the deposition pattern and are shown in Figure 4.18. The photographs show that the deposition becomes less uniform with increasing the concentration. The 0.01 vol. % nanofluid resulted in a very uniform deposition pattern covering the entire surface. The deposition after the 0.1 vol. % nanofluid was less uniform leaving some areas of the surface with very little deposition. The deposition pattern on the surface after the 0.5 vol.



(a)



(b)



(c)



(d)

*Figure 4.18: Photographs of the boiling surface for Stage 3 experiments:  
(a) clean surface (b) after 0.01 vol. % (c) after 0.1 vol. % and (d) after 0.5 vol. %  
nanofluids boiling experiments*

% nanofluid is even less uniform and more areas of the surface have little deposition. Such non-uniformity rendered local surface-roughness measurements inappropriate in assessing the effect of concentration on deposition of nanoparticles on the surface. It is the uniformity of the nanoparticle deposition that explains the trend found regarding  $C_{sf}$  in the previous section. The more uniform deposition which covers more portions of the surface deteriorates the HTC more than a less uniform deposition.

The 3D profiles of the surfaces after the experiments carried out in Stage 3 are shown in Figure 4.19. It can be seen in the 3D profiles that there are more missing data points with the less uniform deposition patterns, which is what makes the surface-roughness measurements inappropriate to quantify nanoparticle deposition.

#### 4.3.3 Effect of Prolonged Boiling Duration on Nanoparticle Deposition and Surface Temperature

To further investigate nanoparticle deposition, the effect of the time on the deposition phenomenon was studied by plotting the change in surface superheat and heat flux for every experiment against time. The plots are shown in Figures 4.20 – 4.23. The surface heat flux was increased every 15 minutes. It took about 2 minutes for the surface temperature and heat flux to reach steady-state. During this steady-state period the heat flux remained constant. However, the surface temperature varied from one experiment to another.

- Surface-roughness value of each image is shown below
- Black areas in the 3D profiles indicate missing data points that could not be captured by the interferometer

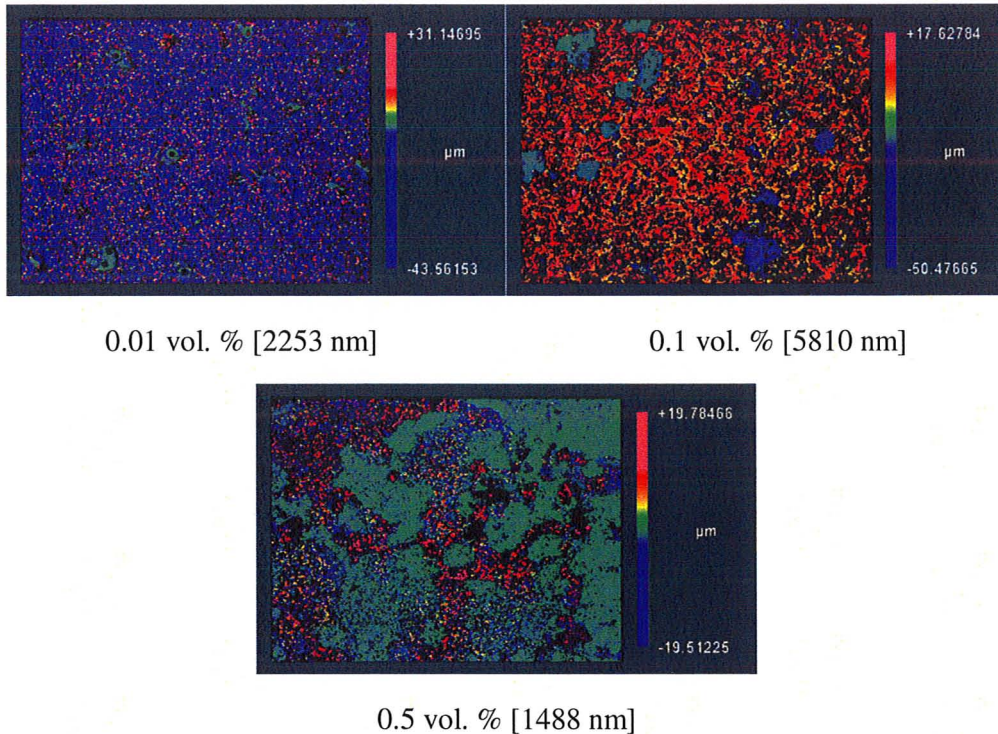


*Figure 4.19: 3D images of surfaces after Stage 3 experiments*

For the water boiling experiments the surface temperature fluctuated by about 0.4 °C during the steady-state periods. During the nanofluids experiments surface temperature did not fluctuate, however, it slowly and consistently rose during the steady-state periods. The surface temperature rise during the steady-state periods is very noticeable in Figure 4.21, for the 0.01 vol. % boiling experiment.

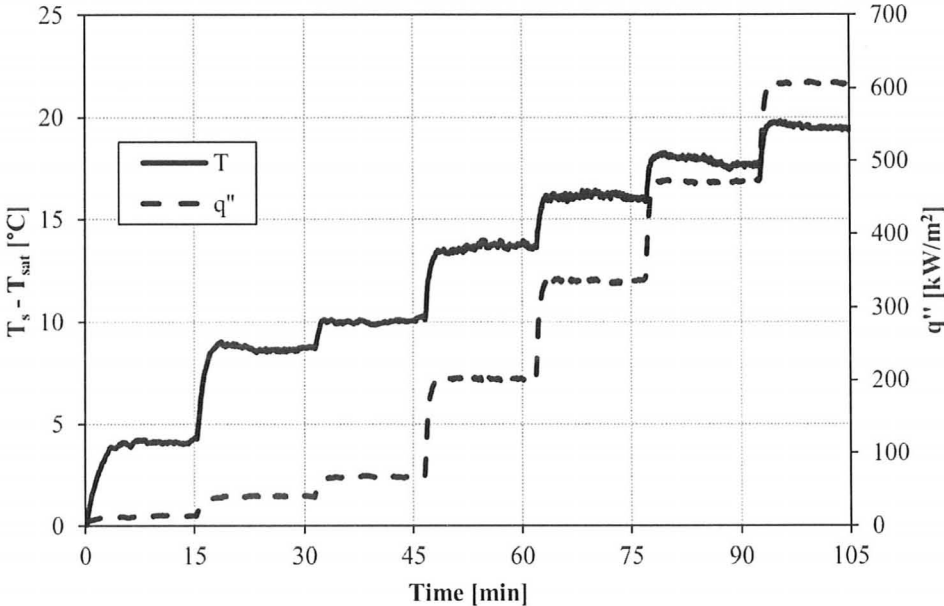


Figure 4.20: Surface superheat and heat flux vs. time during water boiling experiment

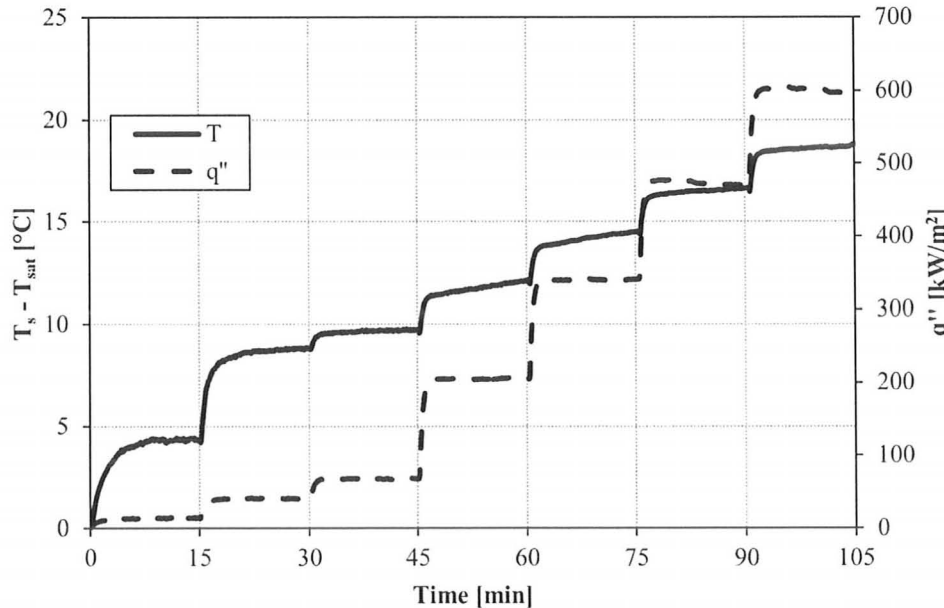


Figure 4.21: Surface superheat and heat flux vs. time during 0.01 vol. % nanofluid boiling experiment

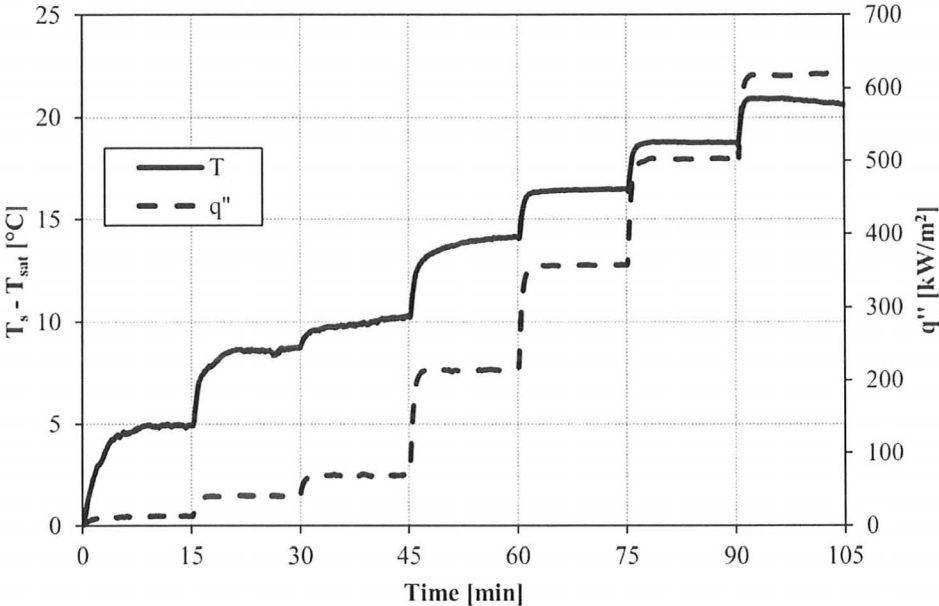


Figure 4.22: Surface superheat and heat flux vs. time during 0.1 vol. % nanofluid boiling experiment

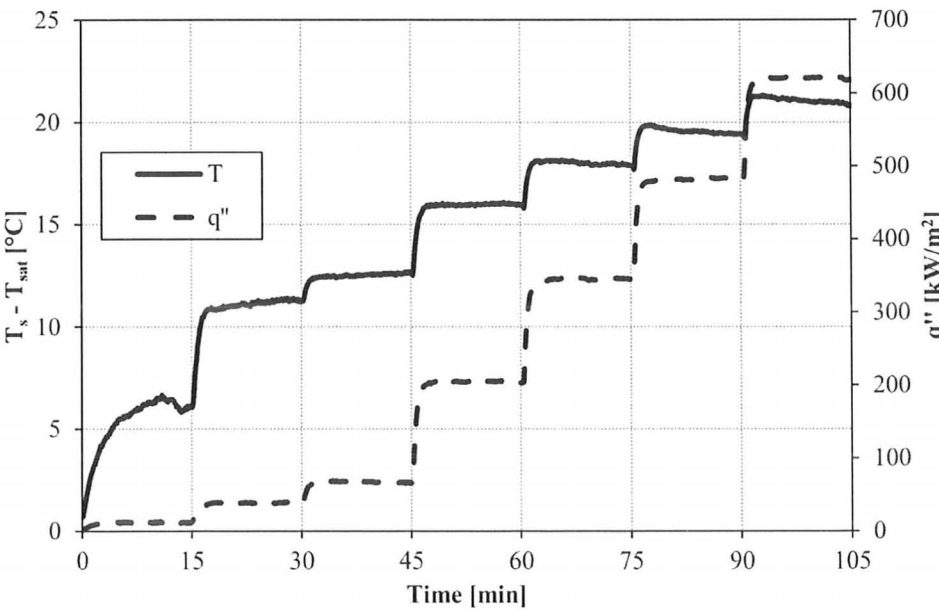


Figure 4.23: Surface superheat and heat flux vs. time during 0.5 vol. % nanofluid boiling experiment

The surface temperature change for the steady-state periods during nucleate boiling are plotted in Figure 4.24. The surface temperature for the 0.01 vol. % nanofluid has consistently risen during all periods. This temperature rise is attributed to the deposition of nanoparticles on the surface. For the 0.1 vol. % nanofluid the temperature rise reached its highest value during the first two steady-state periods and became much smaller during the remaining steady-state periods. The 0.5 vol. % nanofluid showed minimal temperature change for the first three steady-state periods and a small drop in temperature for the last two periods.

The results suggest that the deposition for the 0.01 vol. % nanofluid occurred throughout the whole duration of the experiment. Due to the low concentration, the deposition occurred slowly. For the higher concentration of 0.1 vol. %, the deposition

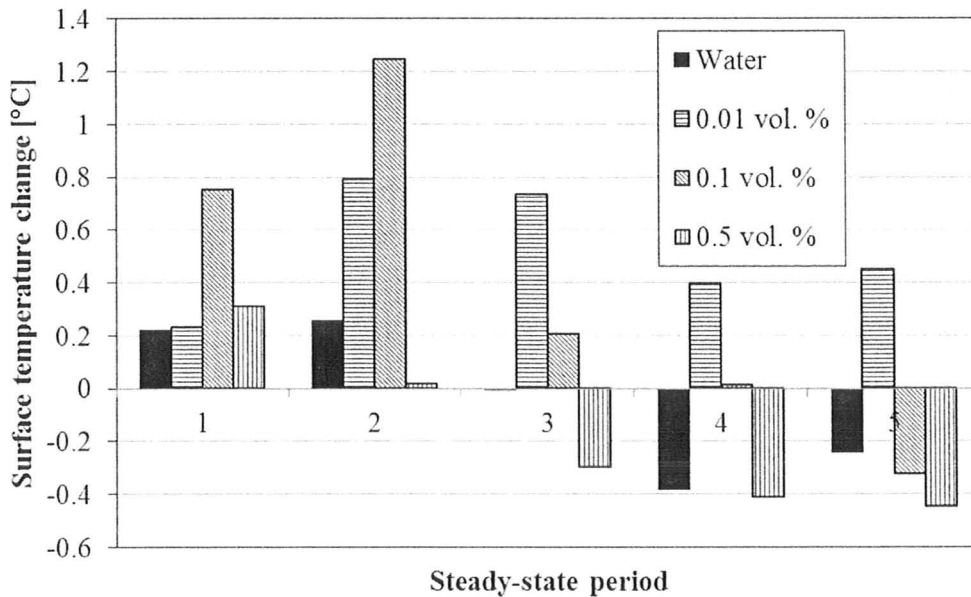


Figure 4.24: Surface temperature change during steady-state periods

occurred much faster and lasted for the first two steady-state periods, until the surface becomes saturated with nanoparticles. Also it seems that the speed of deposition plays a role in the nature of the deposition pattern. The slow deposition for the 0.01 vol. % nanofluid created the uniform deposition pattern shown in Figure 4.18 (b). In the case of the 0.1 vol. % nanofluid, the deposition took place faster and the particles did not have the chance to form a layer as uniform as it was with the 0.01 vol. % nanofluid. Such faster deposition caused the non-uniform deposition pattern shown in Figure 4.18 (c).

For the 0.5 vol. % nanofluid the nanoparticle deposition was formed much faster and resulted in the most non-uniform layer, which is reflected in the surface-roughness measurements and the boiling surface photographs. The temperature rise for the 0.5 vol. % nanofluid was not as significant.

#### 4.3.4 Transient Surface-Factor

Results discussed in the previous section indicated that the deposition of nanoparticles on the boiling surface is a transient phenomenon. The fact that the deposition took place during boiling resulted in a continuously changing boiling surface property. Therefore, it is reasonable to consider that  $C_{sf}$  in the Rohsenow correlation will have different values within the same boiling curve. In the following analysis, the Rohsenow correlation was used to fit the boiling curves exactly by changing  $C_{sf}$  at each data point along the boiling curve. It is hypothesized that  $C_{sf}$  would increase throughout the nanofluid boiling experiment to account for the deposition of nanoparticles taking

place on the surface. An increase in  $C_{sf}$  means that the surface requires a higher superheat to transfer the same heat flux

The liquid properties of the nanofluids were assumed to be the same as water in this analysis. The database of nanofluid properties available from the literature does not cover the exact particle size and concentrations used in this investigation, therefore, prediction of the nanofluid properties used in this investigation from literature is problematic. Also the focus in this analysis was on the change in  $C_{sf}$  within each experiment, rather than the absolute value of  $C_{sf}$ . If the nanofluid properties are accounted for, the values of the surface factor for each experiment will shift but the change within each experiment will remain the same. The change in surface factor for the water and nanofluid boiling experiments in Stage 3 is plotted in Figure 4.25.

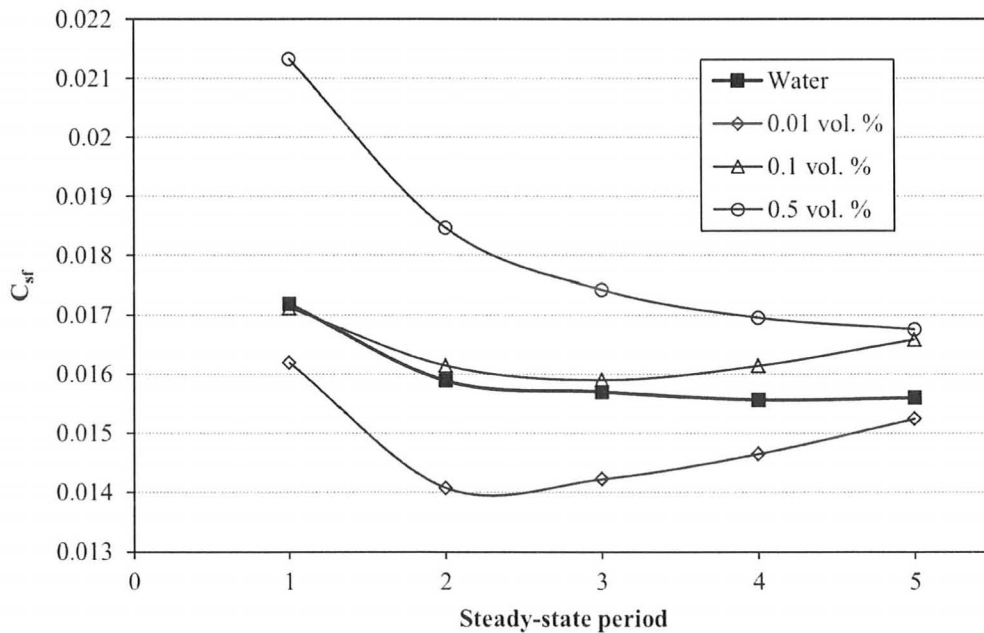


Figure 4.25: Change in  $C_{sf}$  for the water and nanofluid boiling experiments

This hypothesis is true for the 0.01 vol. % nanofluid excluding the first steady-state period. Figure 4.24 shows that nanoparticle deposition occurred during all the steady-state periods for the 0.01 vol. % nanofluid and hence,  $C_{sf}$  would increase from one period to another, as shown in Figure 4.25, with the exception of the first period. The reduction in  $C_{sf}$  after the first period may be attributed to the nature of the boiling behaviour, which is similar to the change in  $C_{sf}$  for pure water boiling after the first period as well.

The hypothesis is not satisfied for the 0.1 vol. % nanofluid. A sharp increase in  $C_{sf}$  is expected after the first and the second steady-state periods due to a larger increase in surface temperature during those periods.  $C_{sf}$  was reduced after the first period and almost no change is observed after the second period.  $C_{sf}$  then increases slightly for the remaining periods, where very little deposition is occurring.

For the 0.5 vol. % nanofluid the hypothesis is true for the last three steady-state periods. A small drop in surface temperature occurs during the last three steady-state period for the 0.5 vol. % nanofluid, which indicates nanoparticles departing from the surface. A reduction in  $C_{sf}$  would be expected for these steady-state periods.  $C_{sf}$  is reduced for the last three periods which supports the hypothesis if nanoparticles are departing from the surface during those periods.

The calculation of  $C_{sf}$  from the Rohsenow correlation had a large error bar associated with its calculation. The change in  $C_{sf}$  is shown again in Figure 4.26 and the errors bars for the calculation of  $C_{sf}$  for water are added. It is clear that the error bars are

large with respect to the change from one value to another for each experiment. The error in the calculation of  $C_{sf}$  is of the same order of magnitude as the change in  $C_{sf}$  within each curve.

The high error associated with the calculation of  $C_{sf}$  explains why the hypothesis is not true in all the cases. This analysis has not been carried out before by other researchers. Therefore, it sheds light on a methodology that may be used to predict the heat transfer of nanofluids using the Rohsenow correlation.

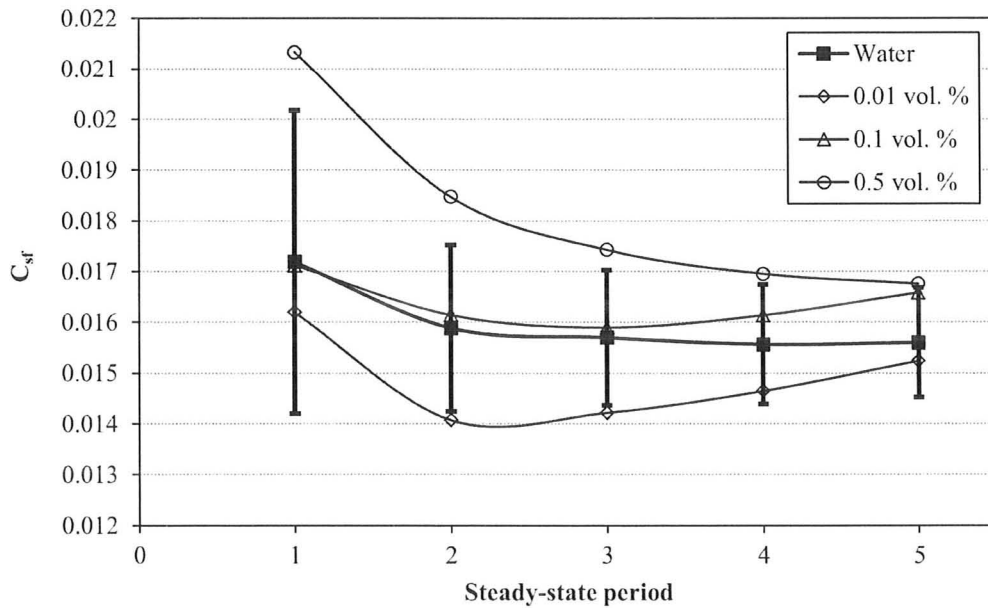


Figure 4.26:  $C_{sf}$  for water and nanofluid experiments showing associated errors

#### 4.4 Comparison of HTC Ratio with Literature

Figure 4.27 shows the HTC ratio found in the literature at the concentrations covered by experiments in this study. The HTC ratios of the experiments carried out in this study are also shown on the figure. The most comparable experimental setup in the literature to that used in this investigation is the one used by Bang and Chang in [15]. Although they did not report the material of the heater used in their investigation, all the other characteristics of their heater are very close to the heater used in this investigation. Bang and Chang's heater was a horizontal flat surface with average surface-roughness of 37 nm. The HTC ratios in this investigation and in Bang and Chang's at 0.5 vol. % are very close. This is an interesting result as it shows that similar results can be obtained when using similar experimental setups, and that contradicting findings among the different researchers is indeed because different experimental conditions have been used.

Another similarity in HTC ratio was found between the results from Das et al. [4] at 0.1 vol. % concentration and results from Stage 1 and 2 experiments. The heater used in [4] is a stainless steel tube with  $Ra = 400 - 1100$  nm. Clearly the characteristics of their heater are different from the heater used in the present study and different results are expected. The fact that the results are similar is possibly due to several heater properties being changed that cancel the effect of one another and give a similar result.

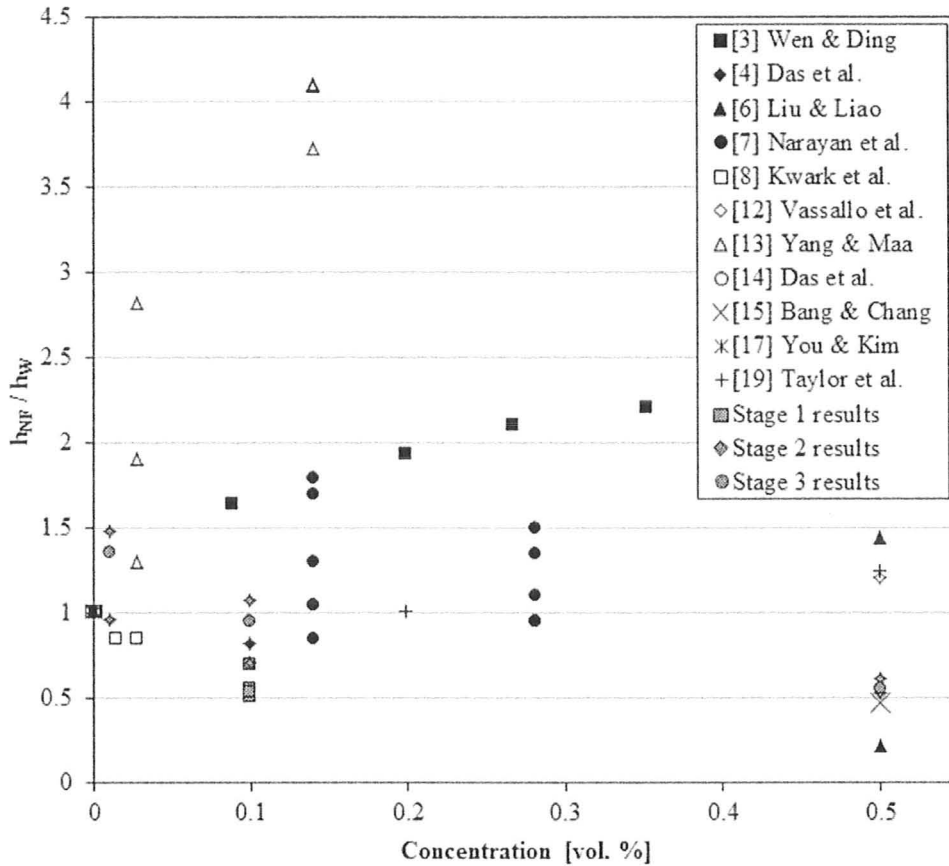


Figure 4.27: HTC ratio found in literature and determined in this investigation

The closest concentration to 0.01 vol. % used in the literature is that used by Kwark et al. in [8], which was 0.014 vol. %. The result of Kwark et al. at that concentration is comparable to the result from Stage 2 experiments. The heater used by Kwark et al. is similar to the one used in this study, but the heater surface-roughness has not been reported. However, their nanofluids were at pH = 6.3, and the closest result from the present investigation was at pH = 5. Therefore, there is a drift in the result, possibly due to differences in heater surface-roughness. Another source for the drift could be the duration of the experiments carried out, which was also not reported in [8].

## Chapter 5

### Summary and Conclusions

An experimental study has been carried out to study the effect of parameters suspected to explain contradictions in HTC results found in previous studies on pool boiling of nanofluids. The effects of nanofluid preparation method, pH value and duration of boiling experiment were suspected and studied. Nanofluid concentration was also incorporated in the investigation due to its popularity as a studied parameter in the literature.

Nanofluids prepared from dry particles and ready-made suspensions have been used, and pH values of 6.5 (neutral) and 5 (acidic) have also been used. The concentrations used were 0.01, 0.1 and 0.5 vol. %. The experiments were carried out in three stages. The effect of preparation method and pH value, or stability, were studied in the first stage, concentration and stability were studied in the second stage. The effects of prolonging the boiling duration and concentration on nanoparticle deposition were studied in Stage 3.

The Rohsenow correlation was used to predict changes in surface condition due to nanoparticle deposition, and the change in nanofluid properties. The Rohsenow correlation was also used to predict the transient change in surface condition due to the continuous deposition of nanoparticles.

The preparation method of nanofluids has been found not to be a critical parameter that explains one of the contradictions in the results in the literature. It was suspected that preparing the nanofluids from a ready-made suspension would result in an enhanced HTC as reported in [12], however, this was not the case. The HTC of the *suspension* nanofluids deteriorated. The following conclusions refer to nanofluids prepared from dry nanoparticles.

Changing the pH value of the nanofluids showed to affect the nanofluids in different ways. The reduction in pH value enhances the electrostatic stability of the nanofluid which makes the nanoparticles suspend better and deposit less particles on the surface. The reduction in pH value also increases the surface tension of the base fluid within the nanofluid, and causes a reduction in the HTC. Finally, the pH value also has an effect on the thermal conductivity of the nanofluid [10]. The reduction in pH value increases the thermal conductivity of the nanofluid which has a positive effect on the HTC.

The increased surface tension of the base fluid due to pH reduction is more dominant at the lowest concentration (0.01 vol. %), and caused a reduction in the HTC. At 0.1 vol. %, the enhanced thermal conductivity and/or stability are more dominant when the pH value is reduced and the HTC is increased. At the highest concentration (0.5 vol. %), the deposition of nanoparticles on the surface became the dominant effect and the reduced pH of the nanofluid did not have an effect on the HTC.

Studying the deposition phenomenon that took place on the surface showed that nanoparticles deposit during bubble generation and release during boiling. The rate of deposition of nanoparticles is faster at higher concentrations; therefore, the HTC is reduced at higher concentrations. Nanoparticle deposition reduces the HTC due to the reduction in the number of active nucleation sites.

Using the Rohsenow correlation to predict the change in surface condition due to nanoparticle deposition and the change in nanofluid properties gives results which contradict the trends of nanofluid properties reported in the literature. Fitting the Rohsenow correlation to a water boiling curve for a NPD surface is not an appropriate method of quantifying the nanoparticle deposition that takes place on the surface during nanofluid boiling. The change in the condition of the heater surface due to nanoparticle deposition is not only dependent on the intensity of the deposition, but the uniformity as well.

Using a transient surface factor in the Rohsenow correlation is a new approach to predicting the pool boiling heat transfer of nanofluids using the Rohsenow correlation. This approach may be used to quantify the change in surface condition due to nanoparticle deposition throughout the duration of the boiling experiment.

Finally, contradictions among researchers regarding findings in HTC are due to differences in experimental conditions.

## Chapter 6

### Recommendations for Future Work

To better understand the behaviour of nanofluids under pool boiling in future work, the physical properties of the nanofluids used in the experiments should be measured. Quantifying the change of each property of the nanofluids will make it possible to better attribute the change in HTC to which property. Particular attention should be given to thermal conductivity and surface tension.

Nanofluids prepared from different nanoparticle materials should be investigated in the future. In particular, a nanoparticle material of a thermal conductivity close to that of the heater surface should be investigated. The deposition layer on the surface may act as an insulation layer if the thermal conductivity of the nanoparticles is lower than that of the heater [22]. However, if the thermal conductivity of the nanoparticles is close to that of the heater, the deposition layer will conduct the heat from the surface and not act as an insulation layer between the surface and the nanofluid. Another type of nanofluid that should be interesting to study is carbon nanotube nanofluids. Carbon nanotubes have a high thermal conductivity, high aspect ratio, high specific surface area and low density which are all favourable properties of nanoparticles to prepare nanofluids [23].

Experiments using a different particle size as well as heater average surface-roughness should also be carried out in the future. As outlined in [7], *SIP* is a parameter that influences the enhancement/deterioration of pool boiling of nanofluids. Experiments

with *SIP* far from unity should be carried out in order to achieve higher enhancements in HTC.

Since nanoparticle deposition has been found to reduce the number of active nucleation sites and cause deterioration in HTC, there should be efforts made to reduce the deposition of nanoparticles. The nanoparticles not only deposit on the surface, but also adhere to the surface and are not washable with a water jet. This adhesion is possibly due to electrophoresis and/or thermophoresis taking place. If the particles do not adhere to the surface as they come out of suspension during microlayer evaporation, the particles will be swept away from the surface by fluid motion after the bubble has departed. It is shown in [24] that exhaust soot particles from internal combustion engines adhere to an electrostatically charged surface due to oppositely charged particles being attracted to the surface due to electrophoresis. Nanoparticles in suspension have a positive ( $H^+$ ) charge on their surface at pH values below 9.1 [7]. If the boiling surface has a positive electrostatic charge, the particles may be repelled and not adhere to the surface. Thermophoresis should also be considered as there is a temperature gradient between the heater surface and the nanofluid, which will cause migration of nanoparticles from the surface [19]. The effects of electrophoresis and thermophoresis should be considered when carrying out future work, as they will promote or diminish nanoparticle deposition during pool boiling.

A closer examination of the surface should be carried out to assess the change in surface condition. The number of nucleation sites should be quantified rather than rely on surface-roughness measurements to evaluate the change in surface condition due to nanoparticle deposition. An analysis of the nucleation site size should be carried out to

relate it to the particle size and gain a better understanding of the interaction between the nanoparticles and the nucleation sites.

Finally, there is safety concern regarding the possibility of nanoparticles being released into the air during boiling of nanofluids. It is not known how likely the nanoparticles can be released into the air. It is recommended that this matter be addressed by finding out whether the nanoparticles do come out of suspension and are released into the air, and using appropriate personal protective equipment (PPE) if this is the case.

## **Appendix A**

### **Repeatability**

Two experiments were repeated to examine the repeatability of the boiling curves. These experiments were carried out in Stage 2 experiments. Experiments using water and the 0.01 vol. % nanofluid at an acidic pH of 5 were chosen to be repeated. The acidic nanofluid was chosen as opposed to the neutral to test the repeatability of the preparation of the concentration as well as acidity.

Results of the water boiling experiment is shown in Figure A.1, and the nanofluid in Figure A.2. The boiling curves lie within the experimental error showing that good repeatability is established for water and nanofluids.

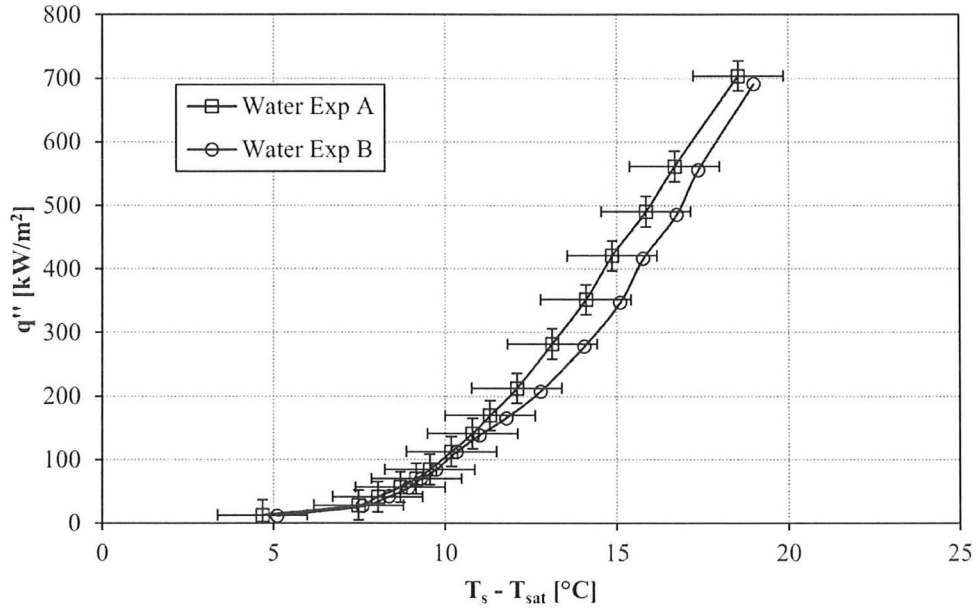


Figure A.1: Repeatability of water boiling in Stage 2 experiments

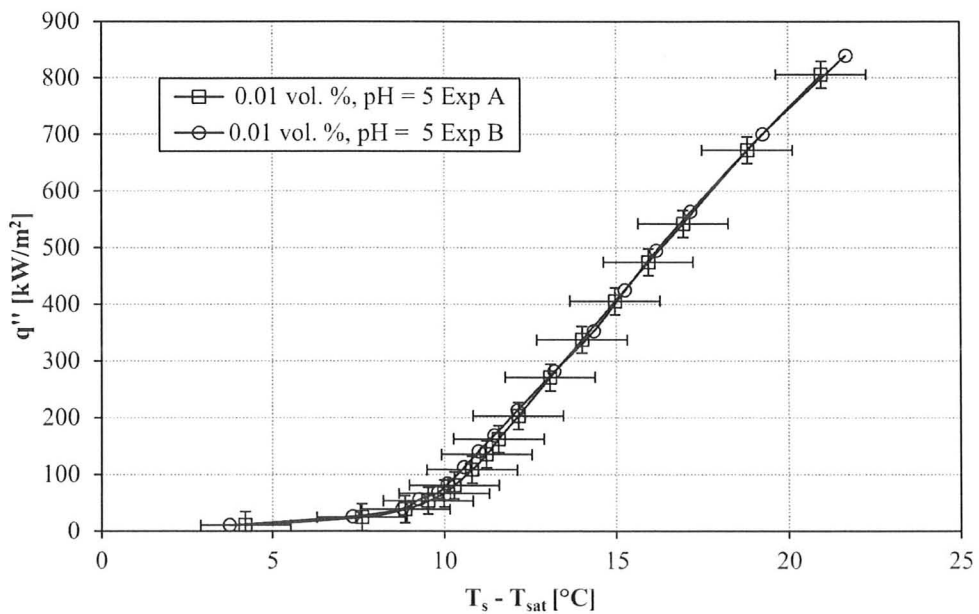


Figure A.2: Repeatability of 0.01 vol. % nanofluid boiling at pH = 5 from Stage 2 experiments

## References

- [1] Van P. Carey, *Liquid Vapor Phase-Change Phenomena*, Second Edition, Taylor & Francis Group, 2008.
- [2] Sarit Kumar Das, Stephen U.S. Choi, Wenhua Yu, and T. Pradeep, *Nanofluids: Science and Technology*, John Wiley & Sons Inc., 2008.
- [3] Dongsheng Wen and Yulong Ding, "Experimental investigation into the pool boiling heat transfer of aqueous based alumina nanofluids", *Journal of Nanoparticle Research*, vol. 7, pp. 265-274, 2005.
- [4] Sarit Kumar Das, Nandy Putra, and Wilfried Roetzel, "Pool boiling characteristics of nano-fluids", *International Journal of Heat and Mass Transfer*, vol. 46, pp. 851-862, 2003.
- [5] Yimin Xuan and Qiang Li, "Heat transfer enhancement of nanofluids", *International Journal of Heat and Fluid Flow*, vol. 21, pp. 58-64, 2000.
- [6] Zhen-Hua Liu and Liang Liao, "Sorption and agglutination phenomenon of nanofluids on a plain heating surface during pool boiling", *International Journal of Heat and Mass Transfer*, vol. 51, pp. 2593-2602, 2008.
- [7] G. Prakash Narayan, K. B. Anoop, and Sarit Kumar Das, "Mechanism of enhancement/deterioration of boiling heat transfer using stable nanoparticle suspensions over vertical tubes", *Journal of Applied Physics*, vol. 102, p. 074317, 2007.
- [8] Sang M. Kwark, Ratan Kumar, Gilberto Moreno, Jaisuk Yoo, and Seung M. You,

- "Pool boiling characteristics of low concentration nanofluids", *International Journal of Heat and Mass Transfer*, vol. 53, pp. 972-981, 2010.
- [9] Sarit Kumar Das, Nandy Putra, Peter Thiesen, and Wilfried Roetzel, "Temperature dependence of thermal conductivity enhancement for nanofluids", *Journal of Heat Transfer*, vol. 125, p. 567, 2003.
- [10] Huaqing Xie, Jinchang Wang, Tonggeng Xi, Yan Liu, and Fei Ai, "Thermal conductivity enhancement of suspensions containing nanosized alumina particles", *Journal of Applied Physics*, vol. 91, no. 7, pp. 4568 - 4572, 2002.
- [11] Seok Pil Jang and Stephen U. S. Choi, "Role of Brownian in the enhanced thermal conductivity of nanofluids", *Applied Physics Letters*, vol. 84, no. 21, pp. 4316-4318, 2004.
- [12] Peter Vassallo, Ranganathan Kumar, and Stephen D'Amico, "Pool boiling heat transfer experiments in silica-water nanofluids", *International Journal of Heat and Mass Transfer*, vol. 47, pp. 407-411, 2004.
- [13] Yu Min Yang and Jer Ru Maa, "Boiling of suspension of solid particles in water", *International Journal of Heat and Mass Transfer*, vol. 27, pp. 145-147, 1984.
- [14] Sarit Kumar Das, Nandy Putra, and Wilfried Roetzel, "Pool boiling of nano-fluids on horizontal narrow tubes", *International Journal of Multiphase Flow*, vol. 29, pp. 1237-1247, 2003.
- [15] In Cheol Bang and Soon Heung Chang, "Boiling heat transfer performance and phenomena of Al<sub>2</sub>O<sub>3</sub>-water nano-fluids from a plain surface in a pool", *International*

- Journal of Heat and Mass Transfer*, vol. 48, pp. 2407 - 2419, 2005.
- [16] Hyungdae Kim, Jeongbae Kim, and Moo Hwan Kim, "Effect of nanoparticles on CHF enhancement in pool boiling of nano-fluids", *International Journal of Heat and Mass Transfer*, vol. 49, pp. 5070-5074, 2006.
- [17] S. M. You and J. H. Kim, "Effect of nanoparticles on critical heat flux of water in pool boiling heat transfer", *Applied Physics Letters*, vol. 83, no. 16, pp. 3374 - 3376, 2003.
- [18] Yong Hoon Jeong, Won Joon Chang, and Soon Heung Chang, "Wettability of heated surfaces under pool boiling using surfactant solutions and nano-fluids", *International Journal of Heat and Mass Transfer*, vol. 51, pp. 3025-3031, 2008.
- [19] Robert A. Taylor and Patrick E. Phelan, "Pool boiling of nanofluids: Comprehensive review of existing data and limited new data", *International Journal of Heat and Mass Transfer*, vol. 52, pp. 5339–5347, 2009.
- [20] G. Prakash Narayan, K. B. Anoop, G. Sateesh, and Sarit K. Das, "Effect of surface orientation on pool boiling heat transfer of nanoparticle suspensions", *International Journal of Multiphase Flow*, vol. 34, pp. 145–160, 2008.
- [21] Xiang-Qi Wang and Arun S. Mujumdar, "Heat transfer characteristics of nanofluids: a review", *International Journal of Thermal Sciences*, vol. 46, pp. 1-19, 2007.
- [22] Sarit K. Das, G. Prakash Narayan, and Anoop K. Baby, "Survey on nucleate pool boiling of nanofluids: the effect of particle size relative to roughness", *Journal of Nanoparticle Research*, vol. 10, pp. 1099–1108, 2008.

- [23] Sven Kobelt, Rahmatollah Khodabandeh, Lothar R. Oellrich, and Bjorn Palm, "Heat transfer characteristics of nanofluids in two-phase flow boiling", in *ECI International Conference on Boiling Heat Transfer*, Florianopolis-SC-Brazil, May 2009.
- [24] E. dela Cruz et al., "Electrical effect of soot depositions in a co-axial wire pipe flow", *Journal of Electrostatics*, vol. 67, pp. 128-132, 2009.
- [25] Mamdooh Shoukri, *M. Sc. Thesis: Nucleation Site Activation in Saturated Boiling*. Hamilton, McMaster University, 1974.
- [26] Anthony James Robinson, *M. Sc. Thesis: A Study of the Effect of Subcooling on Bubble Formation in Nucleate Pool Boiling*. Hamilton, McMaster University, 1997.
- [27] O. Ahmed and M. S. Hamed, "On Pool Boiling of Nanofluids", in *The 7th International Conference on Heat Transfer, Fluid Mechanics and Thermodynamics (HEFAT)*, Antalya, Turkey, 2010.
- [28] O. Ahmed and M. S. Hamed, "The Effect of Experimental Techniques on the Pool Boiling of Nanofluids", in *The 7th International Conference on Multiphase Flow (ICMF)*, Tampa, FL, USA, 2010.

## Curriculum Vitae

Name: Osama Ahmed Hassan Ahmed

Date of Birth; 29 October 1984

Contacts numbers: +1-905-962-2995 (Canada), +20-10-526-3995 (Egypt)

Email: osama.ah@gmail.com

### EDUCATION:

- Master of Applied Sciences, Mechanical Engineering, McMaster University, Canada. Expected graduation: November 2010
- Bachelor of Engineering, Mechanical Power Engineering, Ain Shams University, Egypt.
- Class of July 2007
- IGCSE, Modern English School, Cairo. Class of 2002

### PUBLICATIONS:

- O. Ahmed and M. S. Hamed, "On Pool Boiling of Nanofluids," in 7th The International Conference on Heat Transfer, Fluid Mechanics and Thermodynamics (HEFAT), Antalya, Turkey, 2010.
- O. Ahmed and M. S. Hamed, "The Effect of Experimental Techniques on the Pool Boiling of Nanofluids," in The 7th International Conference on Multiphase Flow (ICMF), Tampa, FL, USA, 2010.
- O. Ahmed and M. S. Hamed, "Effect of Nanoparticle Deposition on Pool Boiling of Nanofluids," Special Issue of the Nanoscale Research Letters on Nanofluids, to be submitted for publication, 2010

### WORK EXPERIENCE:

El Galla Gold (Family Business), 2000 - 2007 Part time, 2007 - 2008 Full time

- Planned and organized production of silver and gold products
- Supervised the gold manufacturing process to ensure on-time deliveries
- Received orders from clients and discussed prices and delivery times
- Worked as a liaison between the company and business partners and customers

General Motors Egypt, Summer Internship 2006

- Produced standardized documents for the vehicle assembly processes
- Completed a time-study of the production line and reassigned the workers' workload to increase the production line's productivity

GlaxoSmithKline Egypt, Summer Internship 2002 & 2003

- Learned and used the principles of Lean Manufacturing
- Supervised LeanSigma Advocate training course
- Participated directly in several improvement projects throughout the different production lines

### COMPETENCIES:

- Fluent in English and Arabic
- Extensive use of Microsoft Office
- Intermediate knowledge of AutoCAD, MATLAB, and FORTRAN
- Class G driver's license

### OTHER ACTIVITIES:

- Represented my high school at four international football and basketball tournaments
- Experience in several hiking, camping and mountain climbing trips